TARGETING ESTROGEN RECEPTOR AS A STRATEGY FOR PERSONALIZED MEDICINE IN OVARIAN CANCER

by

Courtney Lynn Andersen

A.A., Liberal Arts & Sciences, Middlesex Community College, 2008

B.S., Biological Sciences, University of Massachusetts Lowell, 2011

Submitted to the Graduate Faculty of

the School of Medicine in partial fulfillment

of the requirements for the degree of

PhD in Molecular Pharmacology

University of Pittsburgh

2016

UNIVERSITY OF PITTSBURGH

SCHOOL OF MEDICINE

This dissertation was presented

by

Courtney L. Andersen

It was defended on

February 16, 2016

and approved by

Don DeFranco, PhD, Professor, Pharmacology & Chemical Biology

Adrian Lee, PhD, Professor, Pharmacology & Chemical Biology,

Anda Vlad, MD, PhD, Professor, Obstetrics, Gynecology, & Reproductive Sciences

Robert Edwards, MD, Chair, Obstetrics and Gynecology, Magee-Womens Hospital of UPMC

Dissertation Advisor: Steffi Oesterreich, PhD, Professor, Pharmacology & Chemical Biology

TARGETING ESTROGEN RECEPTOR AS A STRATEGY FOR PERSONALIZED MEDICINE IN OVARIAN CANCER

Courtney L. Andersen, PhD

University of Pittsburgh, 2016

Ovarian cancer comprises a diverse set of diseases that are difficult to detect and treat successfully. Improving outcomes for ovarian cancer patients is contingent upon identifying targeted, individualized therapeutic strategies. One promising but under-utilized target is estrogen receptor-alpha (ER). ER is expressed in ~70% of epithelial ovarian cancers and epidemiologic studies implicate a role for estrogen in ovarian tumorigenesis. Further, clinical data suggest that a subset of ovarian cancer patients benefit from endocrine therapy. We hypothesized that ER drives development and progression of a subset of ovarian tumors and that outputs of ER function would identify patients who respond to endocrine therapy. We assessed endocrine response and mechanisms of ER signaling in models and clinical samples of high-grade serous ovarian cancer (HGSOC). These studies suggested that expression of ER target genes (ERTGs) reflect active ER in HGSOC and correspond with endocrine responsiveness. In light of this, we profiled ERTG expression to evaluate changes in ER signaling during the progression from benign endometriosis to endometriosis-associated cancer (EAOC). This analysis suggested that canonical ER signaling becomes largely inactivated during this transformation and that de-repressed genes (e.g. FGF18, ESR2) may contribute to the evolution of EAOC. Finally, we compared ER and ERTG expression between serous and mucinous low malignant potential (LMP) tumors. Serous LMP tumors have high expression of ER and several ERTGs (e.g. GREB1). Taken together, our findings describe biomarkers that could identify

ovarian cancer patients across multiple disease subtypes who would benefit clinically from endocrine therapy.

TABLE OF CONTENTS

LIST OF TABLES

LIST OF FIGURES

PREFACE

Education is the most powerful weapon which you can use to change the world.

- Nelson Mandela

Non nobis solum nati sumus.

- Marcus Cicero

First and foremost, I would like to thank my phenomenal advisor Dr. Steffi Oesterreich. Steffi's mentorship allowed me to challenge myself scientifically and professionally while still maintaining my happiness and sanity. She sets an excellent example of how to be successful in one's career but also make time for friends, family, and hobbies away from the lab. I am honored to be her first Pitt graduate student and look forward to continuing our professional and personal relationships.

I also would like to thank Dr. Matt Sikora. Matt took me under his wing from the start of my rotation in the Oesterreich lab and his guidance has been paramount to my development as a scientist. Over the last several years he has been both a wonderful mentor and great friend.

I thank my thesis committee members Dr. Don DeFranco, Dr. Anda Vlad, Dr. Robert Edwards, and Dr. Adrian Lee, for their invaluable guidance on my project. I would like to acknowledge the entire Women's Cancer Research Center for their support. I cannot imagine a

greater setting than the WCRC and the Molecular Pharmacology program in which to have done my graduate training; I am indebted to Dr. Patrick Pagano and Dr. Bruce Freeman for their continued support throughout my studies.

Thank you to my parents, Lance and Tonya, and my sister, Brittany, for their love and support. I thank my friends and colleagues (in no particular order): Becky, Kris, Ali, Emily, Kenny, Chris, Kevin, Nolan, Atif, Bart, Shweta, Mel, Ryan, Dave, Amir, and Tiffany. I also thank Dr. Ed Jahngen, who first recognized the researcher in me. Thank you to Millie and Gary Ryan as well as Lise Woodard and Dr. John Reilly for their support through ARCS and through our wonderful dinner conversations.

One of the first things I learned in graduate school was that science, particularly translational research, is very much a team effort. The work described herein would not have been possible without the help of numerous collaborators. Dr. Gina Mantia-Smaldone, Dr. Kunle Odunsi, and Dr. Karen McLean provided clinical samples that were critical to the studies in Chapter 2. Tianzhou (Charles) Ma performed the statistical analysis of clinical data in Chapters 2 and 4 with guidance from Dr. George Tseng. Dr. Paul Haluska provided the patient-derived xenograft models and Dr. Marc Becker provided guidance on the technical details of working with the PDXs. Dr. Sarah Taylor provided the LMP samples in chapter 5 and really helped drive the project; she is first author on the associated manuscript. Ravi Patel contributed technical assistance to the experiments described in Chapter 3, particularly the validation of the NanoString experiment and assessment of ER mRNA in 2-D versus ULA. Tanya Minteer helped with the patient-derived xenografts. Dr. Michelle Boisen provided clinical insight and technical assistance during her tenure in the lab. She contributed as much as I did to the EAOC

studies (and shares first-authorship of the associated manuscript). She was a pleasure to work with and to mentor; I hope she learned as much from me as I did from her.

This work has been supported financially by NIH Ruth L. Kirschstein National Research Service Award F31 CA186736, NIH Predoctoral Training Grant in Pharmacological Sciences T32 GM008424, the ARCS Foundation Woodard-Ryan Award, the Magee-Womens Research Foundation, and the University of Pittsburgh Cancer Institute.

LIST OF ABBREVIATIONS

4OHT	4-hydroxytamoxifen
AI	Aromatase inhibitor
BSA	Bovine serum albumin
CSS	Charcoal-stripped serum
DMEM	Dulbecco’s Modified Eagle Medium
DMSO	Dimethyl sulfoxide
DNA	Deoxyribonucleic acid
E2	17beta-estradiol
EAOC	Endometriosis-associated ovarian cancer
ENOC	Endometrioid ovarian cancer
ER	Estrogen receptor-alpha
ERTG	Estrogen receptor target gene
FBS	Fetal bovine serum
FC	Fold change
FCCC	Fox Chase Cancer Center
FFPE	Formalin-fixed, paraffin-embedded
GSEA	Gene set enrichment analysis
HBSS	Hank’s buffered salt solution
HGSOC	High-grade serous ovarian cancer
ICI	ICI182,780 (Fulvestrant)
IHC	Immunohistochemistry
IMEM	Improved Minimum Essential Medium
LMP	Low malignant potential
MsigDB	Molecular signatures database

OS	Overall survival
PBS	Phosphate-buffered saline
PDX	Patient-derived xenograft
PFS	Progression-free survival
PR	Progesterone receptor (also PGR)
qRT-PCR	Quantitative real-time polymerase chain reaction
RNA	Ribonucleic acid
RPCI	Roswell Park Cancer Institute
RPMI-1640	Roswell Park Memorial Institute medium 1640
RR	Relative risk
RT	Room temperature
Rx	Treatment
SD	Standard deviation
SDS	Sodium dodecyl sulfate
SEM	Standard error of the mean
SERM	Selective estrogen receptor modulator
SERD	Selective estrogen receptor degrader
TCGA	The Cancer Genome Atlas
TBS	Tris-buffered saline
UPMC	University of Pittsburgh Medical Center
ULA	Ultra low-attachment
Vhc	Vehicle

1.0 INTRODUCTION

1.1 OVARIAN CANCER

Ovarian cancer is the most common gynecologic malignancy and the fifth leading cause of cancer death in women[1]. An estimated 22,300 women in the United States will be diagnosed with ovarian cancer in 2016 and an estimated 14,300 (~40%) will succumb to the disease[1]. The poor survival rate is attributable to two main factors. Firstly, ovarian cancer lacks effective detection/screening methods and patients present with vague symptoms (e.g. gastrointestinal discomfort, appetite loss, weight gain, dull pelvic pain)[2,3]. As such, the disease is often diagnosed at an advanced, metastatic stage. The second factor is a paucity of effective treatment options. Development of successful treatment strategies for ovarian cancer has been impeded by the complex and heterogeneous biology of the disease: despite the uniform classification as "ovarian" cancer, the moniker represents a broad range of malignancies including epithelial ovarian cancer, germ cell stromal tumors (e.g. granulosa cell tumors and Sertoli-Leydig tumors), sex chord stromal tumors (e.g. yolk sac and choriocarcinomas), and small cell carcinomas[4]. Of these, epithelial ovarian cancers account for 95% of all cases and were the focus of this work.

1.1.1 Heterogeneity of epithelial ovarian cancer

Epithelial ovarian cancer is a diverse class of diseases in and of itself. It can be further divided into borderline tumors (also referred to as tumors of low malignant potential or LMPs) and invasive cancers. Invasive cancers are then further sub-classified into histologic subtypes including high-grade serous, which accounts for ~70% of cases; endometrioid (~10-15% of cases); clear cell (~10%); and mucinous (1.5%)[5,6]. Subtype is determined by pathologic review of a specimen collected at primary surgery. However, the subtypes are as distinct molecularly as they are histologically. While endometrioid and clear cell tumors share a propensity for ARID1A, CTNNB1, PIK3CA, and PTEN mutations[7], mucinous tumors most frequently harbor KRAS alterations[8]. Conversely, high-grade serous ovarian cancer (HGSOC) is characterized by ubiquitous p53 mutations, a propensity for DNA repair deficiencies, and rampant copy number aberrations but few recurrent somatic mutations[9,10]. Further, HGSOC contains multiple molecular subgroups, differentiated by gene expression profiles and patient outcomes[9,11],

These type-specific molecular alterations suggest ovarian cancer subtypes arise through unique mechanisms of transformation. Supporting this notion, the different subtypes are postulated to originate from different organs. Preclinical and clinical evidence suggests HGSOC primarily originates from intraepithelial lesions of the distal fallopian tube[12,13] whereas endometrioid and clear cell tumors are thought to arise from endometriosis lesions[14–18]. Mucinous tumors are believed to either be metastases to the ovary from primary gastrointestinal malignancies or arise from associated low malignant potential tumors[5]. Taken together, the varying tissues of origin and stark differences at the histologic and molecular level suggest that

"ovarian" cancer is not one disease but many; these distinct subgroups will likely require unique therapies to effectively treat patients.

1.1.2 Ovarian cancer treatment paradigms

All epithelial ovarian cancers, regardless of subtype, are currently given the same first-line treatment: aggressive cytoreductive ("debulking") surgery and platinum/taxane-based chemotherapy[19]. This treatment paradigm dates back to 1976 and the advent of cisplatin. Prior treatment for ovarian cancer relied on alkylating agents such as cyclophosphamide and melphalan[20]. However, a series of trials in the 70s and 80s demonstrated that most ovarian tumors had a remarkable sensitivity to platinum, even in the setting of resistance to alkylating agents[21–23]. The replacement of alkylating agents with taxanes as a partner for platinum further increased therapeutic response[24]. The current modality of carboplatin and paclitaxel co-treatment leads to ~80% patients achieving remission.

Based on the length of their initial remission, patients are classified into one of three groups: platinum sensitive (recurrence >6 months after therapy), platinum resistance (recurrence within 6 months of therapy), or platinum refractory (progression while on therapy)[25,26]. The favorable response to initial platinum prompts physicians to re-challenge tumors with platinum as second- and sometimes third-line therapy[25]. If tumors become platinum resistant, other cytotoxic regimens (e.g. doxorubicin, topotecan, gemcitabine) are given at the discretion of the oncologist. Despite the high platinum sensitivity in primary ovarian cancer, however, the majority of patients will develop chemotherapy resistance, relapse, and ultimately succumb to the disease[19]. Identifying targeted, personalized treatment strategies for ovarian cancer will be paramount for improving patient survival.

1.1.3 Targeted therapeutics in ovarian cancer

Numerous strategies for targeted therapy in ovarian cancer have been explored, in each case reporting only small response rates. A phase II trial of trastuzumab, a monoclonal antibody against Her2, reported partial or complete responses in 7.3% of patients and disease stabilization in 39%[27]. Similarly, a phase II study of gemcitabine plus pertuzumab, another Her2-targeted antibody, reported an overall response rate of 13.8% (compared to 4.6% for gemcitabine alone)[28]. Conversely, a trial evaluating lapatinib, a combined Her2/EGFR inhibitor, reported no objective responses but did observe disease stabilization in 8% of patients[29]. Other small molecule inhibitors including imatinib, and temsirolimus (mTOR) had similar results (summarized in Table 1). Hormonal agents such as mifepristone, a progesterone receptor (PR) and glucocorticoid receptor (GR) antagonist, have also been evaluated (discussed further in section 1.2). As a result of these low objective response rates, very few targeted agents have been evaluated in ovarian cancer in a phase III setting and only two targeted have been approved to date.

Table 1: Selected trials of targeted therapy in epithelial ovarian cancer

Drugs	Target(s)	Trials	Response (complete or partial)	Disease stabilization
Trastuzumab	Her2	Bookman et al. 2003[27]	7%	39%
Pertuzumab	Her2	Makhija et al. 2010, Gordon et al. 2006[28,30]	4.3 and 13.8%	NA or 6.8%
Lapatinib	Her2, EGFR	Garcia et al. 2012, Weroha et al. 2011	0 and 5%	8 and 16.6%
Erlotinib	EGFR, Her2	Vergote et al. 2014	0	0
Imatinib	Abl, PDGFR, c-kit	Coleman et al., 2006, Matei et al. 2008, Schilder et al., 2008[31–33]	0-21.7%	12.5-33%
Dasatinib	Src	Schilder et al. 2012[34]	0	20%
Temsirolimus	mTOR	Behbakht et al. 2011[35]	19%	24.1%
Sunitinib	PDGF	Campos et al. 2013[36]	8.3%	36%
Mifepristone	PR, GR	Rocereto et al. 2000, Rocerteo et al. 2010[37,38]	4.5 and 26%	NA or 12.5%

The first approved targeted agent for ovarian cancer was bevacizumab, an anti-VEGF antibody that inhibits angiogenesis[39]. Bevacizumab approval was based on several phase II and III trials that reported a significant improvement in progression-free survival (PFS) compared to controls[39]. However, this improvement amounted empirically to only an additional three months of PFS and in most trials involved combining Bevacizumab with conventional chemotherapy[39]. As such, Bevacizumab was approved for use in combination with a topoisomerase inhibitor. Bevacizumab in combination with chemotherapy comes with myriad side effects including hemorrhage, blurred vision, fatigue, and potentially fatal gastrointestinal perforations and at a hefty price: the drug costs $3,000-5000 / cycle[40,41].

The other approved targeted agent for ovarian cancer is olaparib, a poly-ADP ribose polymerase (PARP) inhibitor. Olaparib was approved for BRCA1/2 mutation carriers whose tumors have failed three previous rounds of chemotherapy[42]. Despite 3% of HGSOC tumors harboring somatic alterations in BRCA1 or BRCA2 and 18% harboring another form of homologous repair (HR) defect (e.g. RAD51 inactivation)[9], olaparib approval from the FDA only covers patients with germline BRCA1/2 mutations. However, a trial of olaparib in patients with any HR defect is now ongoing (NCT02392676).

The by and large failure of targeted agents in the ovarian cancer arena perhaps reflects poor patient rather than poor therapeutic selection. While several trials did select patients based on biomarker expression (e.g. imatinib trials[31,32], trastuzumab trial[27]), many of the clinical trials recruited patients regardless of target status (e.g. the lapatinib trials[29,43]). This “all-comers” approach could mute any subgroup-specific responses. While biomarker-based trials to date have still only reported low response rates, this should prompt further molecular and preclinical

studies to understand the biology of responsive tumors rather than abandonment of an entire therapeutic strategy.

1.1.4 Opportunities for personalized medicine in ovarian cancer

The unique genomic alterations in distinct histologic subtypes of ovarian cancer comprise many potential avenues for personalized therapy in ovarian cancer. Targeting BRCA1/2-deficient tumors with olaparib is one such strategy. Another example is MYC; MYC is amplified in >20% of HGSOC[9] and preclinical data suggests inhibiting bromodomain proteins (e.g. BRD4) is effective against MYC-driven cancers[44]. Further, preclinical studies have indicated ARID1A-deficient cancers can be successfully treated by targeting ARID1B[45]. While specific alterations are infrequent, looking at molecular subtypes by dysregulation of overall pathways (e.g. "PI3K-deficient tumors" as those harboring alterations in PIK3CA, PTEN, or AKT) may identify larger subpopulations with susceptibility to targeted treatments.

Also worth exploring are molecular subtypes that may be not be demarked by a genetic alteration but rather a distinct gene expression profile. For example, TCGA analysis of HGSOC identified a group of tumors with an immune-reactive gene signature[9]. One could postulate that this subgroup of HGSOC may be particularly sensitive to immunotherapy. Further, we recently identified a subset of HGSOC with poor outcome that may be driven by high expression of NR4A family members[46]. Similarly, estrogen receptor-alpha (ER) is expressed in ~70% of epithelial ovarian cancers, most frequently in HGSOC and ENOC subtypes[47–49]. Targeting ER has been incredibly successful for breast cancer therapy but its potential is under-utilized in ovarian cancer.

1.2 ESTROGEN IN OVARIAN CANCER PATHOBIOLOGY

ER is one of two estrogen receptor isoforms, α and β, which are encoded by separate genes on separate chromosomes (ESR1 on 6q and ESR2 on 14q, respectively)[50,51]. While ERβ expression is less prevalent in ovarian tumors[52–54], ER is expressed in ~80% HGSOC and ~75% of endometrioid ovarian cancer (Fig. 1)[49]. Reflecting the diversity of ovarian cancer subtypes described above, mucinous and clear cell tumors rarely express ER.

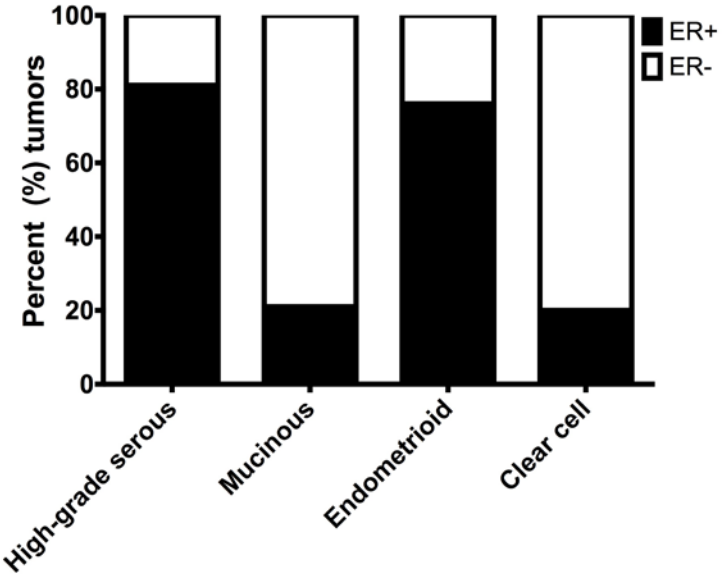

Figure 1: ER expression in ovarian cancer subtypes. Percentage of ER+ tumors was graphed based on data reported by Sieh and colleagues[49].

Hormone receptor expression in ovarian cancer carries biologic consequences. A recent study of over 2000 ovarian tumors revealed that while ER is not predictive of survival in HGSOC, co-expression of ER and PR portends better disease-specific survival (RR 0.71)[49]. In endometrioid ovarian cancer, ER alone was prognostic as was ER/PR co-expression (RR 0.41 and 0.38, respectively). This finding suggests a specific subset of HGSOC and endometrioid ovarian tumors may be hormonally driven. Importantly, the observation that ER alone is not

prognostic for survival in HGSOC suggests that while many serous tumors express ER, only a subset require it for progression. Nevertheless, even if only for a small subgroup of patients, hormone-dependence in both HGSOC and endometrioid tumors could be exploited therapeutically using existing FDA-approved drugs.

1.2.1 Targeting estrogen receptor in cancer

Inhibiting ER action ("endocrine therapy") has proven effective and safe in other malignancies. The notion began in the mid-1970s with the discovery of anti-estrogenic effects of tamoxifen. Tamoxifen, which originated as a failed contraceptive agent (ICI 46,474), was shown to competitively bind the estrogen receptor and, in doing so, inhibit proliferation of breast cancer cells[55,56]. Numerous clinical studies demonstrating the efficacy and favorable side effect profile of tamoxifen led to the establishment of endocrine therapy as the mainstay for breast cancer patients with ER+ tumors[57]. Three primary modalities of endocrine therapy now exist, each with a unique mechanism of action: selective ER modulators (SERMs, e.g. tamoxifen), selective ER degraders (SERDs, e.g. fulvestrant), and aromatase inhibitors (AIs, e.g. letrozole).

SERMs compete with estrogen for binding to ER[58]. The moniker "modulators" reflects the fact that the anti-estrogenic effects of SERMs depend on tissue context. In breast, SERMs antagonize ER activity whereas they have agonistic properties in the bone and endometrium[59,60]. Similar to SERMs, SERDs compete with estrogen for binding to ER[58]. However, SERDs are pure ER antagonists; further, they promote degradation of ER[61–63].

Rather than acting directly on ER, aromatase inhibitors work by reducing estrogen levels. Aromatase activity is responsible for conversion of androgens to estrogen in the adrenal glands and in peripheral tissues (e.g. adipose) and constitutes the primary source of post-menopausal

estrogen[64,65]. Further, aromatase expression has been detected in human cancers including breast and ovarian, suggesting AIs may work directly on the tumor in addition to decreasing systemic estrogen[66–68].

All three classes of endocrine therapy are currently used with success clinically. In addition to being extremely efficacious against hormonally driven malignancies, these therapies have very mild side-effect profiles[57,64]. Compared to the cytotoxic mainstays of ovarian cancer therapy, which come with side effects including nausea, vomiting, alopecia, and leukopenia[20,21], endocrine therapy produces hot flashes; dizziness; and bone, muscle, or joint pain. While still unpleasant, these side effects provide patients with a much better quality of life comparatively. Thus in addition to managing disease burden, endocrine therapy could provide ovarian cancer patients with a reprieve from the more debilitating side effects of standard-of-care chemotherapy.

1.2.2 Estrogen exposure and ovarian cancer risk

Pointing to an opportunity for endocrine therapy in ovarian cancer are numerous epidemiologic studies that link estrogen exposure to ovarian cancer pathogenesis. Prolonged estrogen exposure through nulliparity[69,70] and a greater number of menstrual years[71,72] has been reported to increase risk of ovarian cancer. Further, oral contraceptive (OC) use has been shown to confer a protective effect against epithelial ovarian cancer. Both prospective and case-control studies report ~30% decrease in lifetime ovarian cancer risk with ever-use of OCs[70,73,74]. Longer duration of use produces greater protection, with an approximate 20% decrease for every five years. Both estrogen and combined estrogen-progestin formulations have protective effects although it is debated whether estrogen-progestin formulations provide greater protection than estrogen alone. Presence of a single nucleotide polymorphism (SNP) in CYP19A1, the gene

encoding aromatase, has been associated with increased risk of ovarian cancer[75]. The SNPs in question, rs749292 and rs727479, promote increased aromatase activity (and thus increased estradiol levels)[75]. Additionally, recent data from patients with ductal carcinoma in situ (DCIS) suggests that patients receiving aromatase inhibitory therapy, which decreases estrogen levels, have a lower risk of ovarian cancer than those who received tamoxifen[76].

Perhaps suggesting the most causal link between estrogen and ovarian cancer is the association of post-menopausal hormone replacement therapy (HRT) use and risk. To this point, a centralized analysis of 52 epidemiologic studies (both prospective and retrospective) reported an increased risk of ovarian cancer for ever-users of HRT compared to never-users (RR 1.14 for all studies combined)[77]. Considering just prospective studies, thus eliminating potential contamination in control arms, risk was even higher (RR 1.20 for ever-users). Risk was greatest in current users or patients who had used HRT within the last five years (RR 1.37). Elevated risk was almost entirely attributable to increases in risk for high-grade serous (current or recent users in prospective studies, RR 1.53) and endometrioid tumors (RR 1.42). While risk decreased with time since last use, prior HRT use of $\geq$5 years produced a durable increase in risk.

This result was recapitulated by two other recent meta-analyses. These studies also found a link between duration of HRT use and ovarian cancer risk, with the greatest risk conferred by >10 years of use[78,79]. Notably, since the Women's Health Initiative (WHI) study, HRT use has decreased dramatically in the United States; with it, ovarian cancer incidence has decreased 2.4% per year[80]. Taken together, all of these epidemiologic studies clearly implicate estrogen in the etiology of epithelial ovarian cancer.

1.2.3 Clinical trials of endocrine therapy in ovarian cancer

In light of the associations between estrogen exposure and ovarian cancer risk and the frequency of ER+ tumors, several clinical trials have evaluated endocrine therapy in ovarian cancer (Table 2)[81–83] and three are ongoing (Table 3: Ongoing trials of endocrine therapy in ovarian cancer). Trials have encompassed the three main modalities of anti-estrogen therapy (SERMs, SERDs, and AIs). These trials have been small in cohort size, recruited patients who had been heavily pre-treated with chemotherapy, and did not routinely use ER status as inclusion criteria. Nevertheless, in each trial a subset of patients received clinical benefit (response or disease stabilization) from endocrine therapy.

Table 2: Summary of endocrine therapy trials in ovarian cancer

Drug	Trials (#)	Patients (n)	ER status	Prior chemo regimens	Response (CR or PR)	Stable Disease
Tamoxifen[81,84–94]	14	13 - 105	mixed or unknown	>1	6 -31%	6-83%
Aromatase Inhibitors[81,95–98]	7	22 - 54	+ or mixed	>2	4-17%	50-70%
Fulvestrant[99]	1	26	+	>2	4%	35%

These trials also indicate that endocrine therapy is effective even in the platinum-resistant setting. Timing of endocrine therapy (e.g. potential earlier introduction as a maintenance therapy) could improve response. Additionally, selection of the appropriate patient population will improve response rates. In breast cancer, expression of ER itself is sufficient to identify candidates for endocrine therapy. In ovarian cancer, however, even the endocrine therapy trials that did select for patients with ER+ tumors only saw clinical benefit in a subset of patients.

Further, "ER positivity" in ovarian cancer has not been well defined. The cut-offs for ER+ are frequently not reported (including in the aforementioned Lancet study) making it difficult to interpret associations (or lack thereof) with outcome[99,100]. When reported, cut-offs for ER+ ovarian tumors vary; for example, one recent study defined ER+ by H-score of >150, another used expression above or below the median H-score (90) in the study cohort[48,96]. In breast cancer, current treatment guidelines from the American Society of Clinical Oncology (ASCO) call a tumor ER+ if a histologic tumor specimen contains >1% ER+[101]. However, emerging data and recent discussions in the literature suggest that breast tumors with weak ER expression (1-9% ER+ cells) behave like ER- disease[102–104]. Understanding such thresholds will be critical to defining the predictive and prognostic role of ER in ovarian cancer.

Table 3: Ongoing trials of endocrine therapy in ovarian cancer

Trial	Drug(s)	Lead Investigator	Eligible tumors	Receptor status	Prior rx
PARAGON	Anastrazole	Richard Edmonson, MD	Epithelial ovarian cancer, endometrial cancer, primary peritoneal cancer, fallopian tube cancer, granulosa cell tumor, endometrial sarcoma, cervical sarcoma, sex cord stromal tumor	ER+/PR+,	Epithelial ovarian cancer with rising CA-125 after 1st line rx, platinum resistant/refractory disease
NCT01273168	Endoxifen	Alice Chen, MD	Hormone receptor-positive breast cancer or other solid tumors, desmoid tumors, gynecologic tumors (endometrial, ovarian, uterine, fallopian, peritoneal) tumors	Not required for gynecologic tumors	Progressed on 1+ prior standard-of-care rx
NCT02188550	Letrozole + everolimus	Kenneth Miller, MD	Relapse, refractory or persistent epithelial ovarian cancer,, fallopian tube cancer, primary peritoneal carcinoma, or endometrial cancer	Not required	Must have platinum-resistant/refractory disease or have progressed after 2nd-line platinum

1.2.4 Identifying endocrine-responsive ovarian cancer

Numerous studies have investigated the link between ER expression and endocrine response in ovarian cancer with mixed results. Two reports identified a significant association between quantified ER staining (e.g. AQUA scores) and response to letrozole or fulvestrant[105,106]. However, several other studies found no association[86,107,108]. This may be partially attributable to the inconsistent definitions of ER positivity discussed above (section 1.2.3) or differences in quantitation methods (AQUA score vs. H-score vs. Allred). Refining the role of ER in predicting endocrine response will be critical to selecting appropriate patient populations for endocrine therapy. Equally important will be the implementation of additional biomarkers to complement ER expression.

Three previous efforts have been made to identify biomarkers of endocrine response. The first study evaluated 14 estrogen-regulated genes as potential biomarkers of response in ovarian cancer patients who received letrozole[106]. They found ER targets such as TFF1, PLAU, and VIM associated with CA-125 response to letrozole. In a different study of the same cohort, they observed that IGBFP3, IGFBP4, and IGFBP5 associated with response. A separate report found VIM significantly associated with response to fulvestrant[105]. However, all of these studies looked at short, very focused lists of genes (<10 in a given study). Larger studies evaluating more comprehensive panels of putative biomarkers will be critical to identifying true biomarkers. Ideally these would be conducted in a prospective trial setting with pre- and post-treatment tissue collection, minimal treatment prior to endocrine therapy, and sufficient 'n' to account for a small group of responsive patients.

1.3 ESTROGEN REPEPTOR SIGNALING IN OVARIAN CANCER

1.3.1 Overview of estrogen receptor signaling

Classic ER signaling is stimulated by binding of the ligand, estradiol (E2), to the receptor (Fig. 2). Ligand binding produces a conformational change in the protein that facilitates receptor dimerization. Dimerized ER then binds DNA either directly at estrogen response elements (EREs) or indirectly through interaction with other transcription factors (e.g. AP1, SP1)[109]. Target genes activated after E2 stimulation vary based on the relative amounts of ER and ERβ, which have shared as well as distinct gene targets[110]. Targets of both receptor isoforms are divided between induced and repressed genes, dependent on the co-regulators recruited[111].

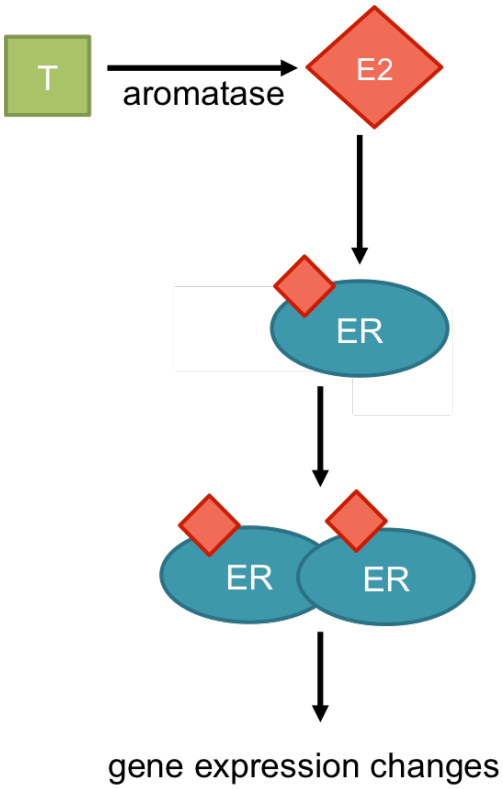

Figure 2: Canonical ER signaling. Estrogen (E2) is produced by aromatase through conversion from testosterone. E2 binds ER, promoting receptor dimerization. ER dimers then bind DNA to mediate transcription.

Co-regulators play a critical role in genomic ER signaling. Proteins such as SRC-1, SRC-2, and SRC-3 are recruited to ER after DNA binding, facilitating interactions between ER and general transcriptional machinery to form a larger complex[112]. Further, co-regulators can function as direct chromatin modifiers (e.g. histone acetyl-transferases) or recruit secondary co-regulators essential for regulation of gene transcription[112–114]. Co-regulators are largely shared between the two estrogen receptors (e.g. p160 family proteins, NCOR, SMRT) but some co-regulators display preferential binding for a given receptor (e.g. RIP140 for ERβ)[115]. Moreover,

the balance of co-regulators contributes to the tissue-specific effects of SERMs (e.g. tamoxifen), thus carrying significant consequences for endocrine response[116–118].

ER can also be stimulated independent of ligand via direct phosphorylation by kinases such as Src, MAPK, and Akt. Kinases act on S118, S167, and S305, inducing a conformational change that allows receptor dimerization and subsequent DNA binding[119]. Also suggested has been a non-genomic signaling cascade in which ER does not directly mediate transcription but rather activates other signaling molecules in the cytoplasm such as MAPK, PI3K, eNOS, SRC, and small G-proteins[120–122].

1.3.2 Interplay between ER and PR in ovarian cancer

Of particular note in ovarian cancer may be the interplay between ER and PR. PR is a canonically estrogen-induced gene and in breast cancer serves as a surrogate for active ER signaling[123,124]. Further, PR has recently been demonstrated to modulate ER signaling as a direct cofactor. Stimulation of PR by progestins promotes PR binding to ER and redirecting it to different sites in the genome[125].

PR is expressed in 31% of HGSOC and 67% ENOC, predominantly in an ER+ background[49]. Further, PR expression is prognostic for improved survival in HGSOC and ENOC[126]. This suggests that a subset of ER+ ovarian cancer maintains active ER signaling and that these tumors have distinct disease biology. Further, recent reports suggest that targeting PR with synthetic progestins induces senescence in ovarian cancer cells[127,128]. Clinical trials of PR agonists have produced mixed results (response rates of 0-47%)[129–131]. However, this may again be due to patient selection given the small percentage of ovarian tumors that express PR.

1.3.3 Preclinical studies of ER signaling in ovarian cancer

Preclinical studies have begun to investigate the role of ER and ERβ in ovarian cancer. Estrogen has been shown to promote proliferation *in vitro* and modulate expression of known ER target genes such as GREB1 in ovarian cancer cell lines and that E2-induced proliferation can be blocked by addition of tamoxifen or fulvestrant (ICI 182,780, herein referred to as ICI)[106,132,133]. Further, E2 has been reported to promote ovarian cancer cell migration, in part through ER-dependent up-regulation of survivin, and to protect cells from anoikis[134]. Over-expression of ERβ in ovarian cancer cell lines decreased proliferation and negatively regulated ER signaling[53,135]. Similar to results in the clinic, not all ER+ cell lines require estrogen for growth[133,136,137]. However, one must interpret cell line results with caution, given reports of misidentification of ovarian cancer cell lines (e.g. the widely used BG-1 cell line was identified to be MCF-7 breast cancer cells)[138]. Additionally, given the heterogeneity of ovarian cancer, preclinical results must be interpreted with regard to context of histologic subtype and underlying genetic alterations[139,140].

Experiments in animal models have also suggested a role for estrogen in ovarian tumorigenesis. E2 increased tumor growth in PEO1 and PEO4 cell line xenografts[132,141]. Treatment with the aromatase inhibitor letrozole improved survival and decreased tumor angiogenesis compared to control-treated animals with OVCAR-3 xenografts[142]. In a transgenic mouse model driven by SV40-Tag transformation of the ovarian surface epithelium, estrogen supplementation did not increase tumor burden but did accelerate the rate of tumor growth[143,144]. Oral contraceptives suppressed spontaneous ovarian tumor development in a hen model[145]. A transplantable ascites model in Wistar Rats also demonstrated endocrine responsiveness[146].

Similar to cell line studies, not all animal models have demonstrated endocrine response. In a popular mouse model of endometrioid ovarian cancer, driven by a *Kras*^{G12D}*;Pten*$^{-/-}$ transgene, treatment with estradiol or the SERM bazedoxifine had no effect on tumor growth[134]. Importantly, endocrine response has yet to be evaluated in patient-derived ovarian cancer models.

While these studies have scratched the surface of endocrine response in ovarian cancer, studies of ER downstream signaling are limited. Early studies focused on expression of known ER targets from studies in other cancer types (e.g. FOS, TFF1, cyclins, and IGFBPs)[136,147,148]. Only two large-scale gene expression studies have been conducted to date. The first was performed in PEO1 cells using a 1.2K gene array after 24 hours of E2 treatment and identified genes including CYR61, CTSD, and IGFBP3[149]. The second utilized a whole-genome (Affymetrix U133 Plus 2.0) array to compare expression of PEO4 xenografts treated +/- an E2 pellet for 11 weeks[132]. This analysis identified several known targets of ER including GREB1 and PGR. The limitation to both these studies is the duration of treatment. Due to the long exposure of E2, gene expression changes may reflect secondary responses just direct ER targets. While secondary responses may be important in E2-driven phenotypes (e.g. proliferation) in ovarian cancer, knowledge of direct ER targets will be critical to fully understanding mechanism of ER action in ovarian cancer.

Also important to understanding ER signaling in ovarian cancer will be identifying ER co-regulators. Studies to date have largely relied on the assumption that ER activates the same target genes and recruits the same co-regulators. Shared ER target genes between ovarian cancer and other malignancies would suggest similar co-regulator profiles. However, large-scale,

unbiased screens such as ChIP-Seq or mass spectrometry will be necessary to determine if ovarian cancer cells utilize unique ER cofactors.

1.3.4 Novel models of ovarian cancer

The modest improvements in clinical outcomes and limitations of existing cell line models have prompted a push for ovarian cancer models that more faithfully recapitulate human malignancy. These efforts have focused on the development of genetically engineered mouse models (GEMMs), culture of primary ovarian cancer cells, and establishment of patient-derived xenografts (PDXs).

Various ovarian cancer GEMMs have been established over the last almost two decades. Many models of HGSOC relied on a traditional view of ovarian tumorigenesis (i.e. restricted to the ovary)[150,151]. Recently a model recapitulating the evolution of HGSOC from the fallopian tube was developed. Malignant transformation of the fallopian tube secretory epithelium by a triple $Brca^{-/-};Tp53^{R270H/-};Pten^{-/-}$ transgene produces serous tubal intraepithelial carcinoma (STIC) lesions in the fallopian tube which progress into invasive tumors with HGSOC histopathologic features and peritoneal metastases[152]. Models of endometrioid ovarian cancer have also been effectively generated, the most common being a $KRas^{G12D};Pten^{-/-}$ transgenic[153,154]. Most recently, a model of clear cell carcinoma[7];,however, the model relies on transformation of ovarian surface epithelial cells and thus may not accurately reflect clear cell tumorigenesis. The downside of all GEMMs, of course, is that they are models of murine disease and rely on a predefined set of drivers. Thus, they fail to capture the genetic diversity of clinical ovarian cancer. This facet of disease biology is where patient-derived models come into play.

Several groups have established banks of ovarian cancer patient-derived xenografts (PDXs). PDXs, which rely on engrafting a piece of patient tumor into an immunocompromised host mouse, are currently regarded as the most faithful models of human disease[155,156]. Ovarian cancer PDXs, when engrafted orthotopically, mimic the intraperitoneal spread and, in some cases, significant ascites burden seen clinically[157,158]. Further, PDXs often demonstrate the same response to therapy observed in patient donors. In light of this, there are now ongoing clinical trials using PDX-guided treatment, including in ovarian cancer (e.g. NCT02312245). Success of such a trial could be a huge boon for ovarian cancer, especially with regard to developing personalized treatment strategies.

A newer system which could also have significant utility is the *ex vivo* tumor culture or "explant" model. Explant models entail culturing fragments of tumor on a gelatin sponge in a culture dish for up to a week[159]. This method gained popularity in the prostate cancer field, where it has been used to evaluate novel therapeutics against primary tumor tissue[159–162]. Unlike patient-derived cell lines or xenograft models, which can require months to establish[157,158,163], explants allow assessment of drug efficacy and pharmacodynamic response within 3-7 days. Explants have only been employed once to date in ovarian cancer[128]. However, the rapid nature and scalability (one small piece of tumor provides sufficient tissue for many replicates or treatment groups) of this assay system make it a promising complement to other model systems. Further, this model could also permit the assessment of intratumor heterogeneity, which may factor into response to targeted therapeutics.

1.4 IMPLICATIONS FOR PERSONALIZED THERAPY FOR OVARIAN CANCER

The heterogeneous nature of ovarian cancer suggests that personalized therapeutic strategies will be critical to improving patient outcomes. Advances in preclinical models of ovarian cancer, particularly patient-derived models, have laid the path for ovarian cancer research to make large strides forward in this arena Preclinical and clinical studies suggest that endocrine therapy could be an effective strategy in ovarian cancer if the correct patient population can be identified.

We hypothesized that ER drives ovarian cancer development and progression for a subset of tumors and that biomarkers of active ER signaling will identify patients most likely to respond to endocrine therapy. Based on epidemiologic and histopathologic analyses, hormone-responsive tumors are most likely to fall into the high-grade serous (HGSOC) and endometrioid (ENOC) ovarian cancer subtypes. In the following chapters, I describe studies to understand ER signaling and identify biomarkers of endocrine response across different subtypes of ovarian cancer. I initially study advanced HGSOC, the most common disease subtype, using preclinical models and primary patient tissue. Next I evaluate ER signaling during the progression from endometriosis, a hormonally-driven reproductive disease, to endometriosis associated ovarian cancers (EAOC). Finally, I assess the potential role of ER in early-stage ovarian tumors of low malignant potential. Our findings on ER function in epithelial ovarian cancer lay the groundwork for future studies of endocrine therapy in ovarian cancer and may have significant clinical ramifications for patients.

2.0 BIOMARKERS OF ER FUNCTION REFLECT ENDOCRINE RESPONSE IN HIGH-GRADE SEROUS OVARIAN CANCER

2.1 INTRODUCTION

High-grade serous ovarian cancer (HGSOC), the most common subtype of EOC, is an aggressive and often lethal disease with limited options for therapy. HGSOC patients typically respond to surgery and platinum-based chemotherapy as first-line treatment but the majority of patients will relapse and ultimately succumb to the disease. Identifying targeted, individualized treatment strategies for ovarian cancer will be essential for improving patient survival.

One promising but often-overlooked therapeutic strategy for HGSOC is targeting estrogen receptor-alpha (ER). ER is highly expressed in ~80% of HGSOC and estrogen exposure (e.g. through oral contraceptive use or post-menopausal hormone replacement therapy) affects risk of ovarian cancer[49,77,81,164]. In light of these observations, several clinical trials have evaluated endocrine therapy in ovarian cancer patients. Trials have been small, recruited heavily pre-treated patients, and did not routinely select patients based on ER status[81]. Nevertheless, in each trial, a subset of patients benefited from tamoxifen (~20% of patients[86]), aromatase inhibitors (~17%[96]), or fulvestrant (~40%[99]). However, even in trials that selected for patients with ER+ tumors, not all patients achieved clinical benefit. Thus, while endocrine therapy could

be successfully used in HGSOC, additional biomarkers are needed to select the appropriate patient population.

We sought to identify ovarian tumors likely to be ER-dependent and responsive to endocrine therapy. To achieve this, we characterized endocrine response with regards to growth, survival, and gene expression in HGSOC cell line and patient-derived xenograft (PDX) explant models. Based on our preclinical data, we built a gene signature of endocrine response and profiled tissue samples from ovarian cancer patients who received endocrine therapy. Gene expression biomarkers may identify patients who will benefit from therapy.

2.2 MATERIALS AND METHODS

2.2.1 Cell culture

PEO1 and PEO4 cell lines were provided by Dr. Thomas Krivak, who obtained them from HPA Cultures UK, and were cultured in DMEM (Invitrogen) + 10% FBS (Gibco). The OVCA432 cell line, also provided by Dr. Krivak, was maintained in RPMI-1640 (Invitrogen) + 10% FBS. OVSAHO and OVKATE cells were purchased from the Japanese Cell Repository Bank (JCRB) and maintained in DMEM + 10% FBS. CAOV-3 cells were purchased from the American Type Culture Collection and maintained in RPMI-1640 + 10% FBS. MCF-7 cells were cultured in DMEM + 10% FBS. Cells were cultured for <6 months. Mycoplasma testing was performed annually using the MycoAlert kit (Lonza). Cell line authentication was performed by short tandem repeat (STR) profiling.

Estradiol (E2) and 4-hydroxytamoxifen (4OHT) were purchased from Sigma (cat. #E8875 and #H6278, respectively). Fulvestrant (ICI182,780; ICI) was purchased from Tocris Biosciences (cat. #1047). E2, 4OHT, and ICI were solubilized in ethanol prior to use *in vitro.*

2.2.2 Hormone deprivation

Cells were hormone-deprived in charcoal stripped serum (CSS) as previously described[165]. Briefly, cells were washed 2X with serum-free, phenol red-free IMEM (Invitrogen #) and then put in IMEM + CSS (10% for PEO4, PEO1, OVCA432; 5% for MCF-7, OVSAHO, and OVKATE). Washes were repeated 3-5X per day for 3 days.

2.2.3 *In vitro* proliferation and viability assays

For standard proliferation assays, hormone-deprived cells were seeded in 96-well plates (Fisher #353072). After cells adhered (16-24 hrs), drug was added directly to the wells. Cell growth was analyzed after six days using the FluoReporter dsDNA quantitation kit (Molecular Probes) according to the manufacturer's instructions. Fluorescence was measured using a VictorX4 plate reader (Perkin-Elmer).

For assays in ultra-low attachment (ULA), cells were treated at the time of seeding and relative cell number was measured using the CellTiter-Glo assay (Promega G7573). Apoptosis was measured using the Caspase-Glo 3/7 Assay (Promega G8091). Luminescence was measured on a Promega GloMax plate reader. For both standard and ULA proliferation/viability assays, data are presented as the mean of three to six biological replicates +/- SD. ULA plates were

purchased from Corning (cat #3474). Data shown are representative of at least two independent experiments.

2.2.4 Cell line gene expression analyses

For microarray analyses, hormone-deprived PEO4 and PEO1 were plated in biological quadruplicates and treated with vehicle, 1 nM E2, 1 μM 4OHT +/- 1 μM E2, or 1 μM ICI +/- E2 for 3 hours. Cells were then rinsed with PBS and RNA was isolated using the GE Illustra RNAspin mini kit (cat #25-0500-70) according to the manufacturer's instructions. RNA quality was measured on a bioanalyzer to confirm an RNA integrity number (RIN) of >8. Gene expression was measured on Affymetrix U133A 2.0 arrays. The CEL files were read and expression data RMA normalized the using affy() package in R. T-tests performed for 5 comparisons using function limma in R, (E2 vs Vhc, ICI+E2 vs E2, 4OHT+E2 vs E2, 4OHT vs Vhc, and ICI vs Vhc). For each comparison, p-values and fold-changes were obtained for all genes. Significance was determined using a cut-off of $p<0.001$. Statistical analysis was performed by Soumya Luthra. Heat maps were generated using the Multiple Experiment Viewer (MeV: http://www.tm4.org/mev.html).

For NanoString analyses, cells were treated with vehicle, 1 nM E2, or 1 nM E2 + 1 μM ICI for 8 hours in biological triplicates. RNA was isolated as described above. NanoString nCounter assays were run following the manufacturer's protocol. Data were corrected to internal positive control probes and then to the geometric mean of five housekeeping genes.

2.2.5 Xenograft studies

All animal studies were approved by the University of Pittsburgh Institutional Animal Care and Use Committee. For PEO4 xenograft studies, C.B.17/IcrHsd-*Prkdc*^{scid}*Lyst*$^{bg\text{-}J}$ (SCID/Beige, Harlan) mice underwent ovariectomy followed by sub-cutaneous pellet implantation (placebo or 0.03 mg E2, Innovative Research of America). Two weeks after surgery, 10^6 PEO4 cells in 1:1 RPMI + matrigel were injected intraperitoneally (IP). Mice were monitored for 11 weeks after injection and then sacrificed for tissue harvest. Tissue was either fixed overnight in 10% neutral-buffered formalin (NBF) or flash frozen in liquid nitrogen. Frozen tissue was pulverized using a mortar and pestle and then processed for RNA isolation using the Qiagen RNEasy Kit.

Patient-derived xenografts (PDXs) were provided by Dr. Paul Haluska[157]. Fresh xenograft tissue was shipped overnight at 4 deg C and, upon arrival, was immediately processed for engraftment into SCID/Bg mice (Harlan). Tissue was processed by mechanical mincing in McCoy's 5A media + 1% anti/anti using surgical scissors. Minced tumor (0.1-0.2 cc of tissue in ~0.5 cc McCoy's) was injected IP using an 18-gauge needle. To passage PDX tumors, mice were sacrificed and necropsies performed in a sterile laminar flow hood. Tumor tissue was harvested from the mouse and processed for re-injection as described above.

2.2.6 Immunoblots

Cells were lysed in RIPA (50 mM Tris-HCl, 150 mM NaCl, 1 mM EDTA, 0.5% Nonidet P-40, 0.5% sodium deoxycholate, 0.1% SDS) with Halt Protease and Phosphatase Inhibitor (Pierce). Total protein was quantified using the BCA assay according to the manufacturer's instructions. (Thermo).

Twenty (20) micrograms of protein per lane was run on 10% SDS-polyacrlyamide gels and transferred to PVDF membranes. ER levels were evaluated using anti-ER antibody (6F11, Leica) and tubulin using (Sigma T6557-.2ML). Secondary antibodies were obtained from LiCor. The blot shown was performed by Dr. Michelle Boisen and is representative of three independent experiments.

2.2.7 *Ex vivo* cultures for rapid assessment of endocrine response

PDXs were cultured *ex vivo* using an established protocol for primary tumors[160–162]. Briefly, fresh PDX tissue was dissected in HBSS into ~1 mm^3 pieces. Tumor pieces were then transferred to 12-well dish. Each well contained a VetSPON gelatin sponge (Henry Schein, cat. #31550) partially submerged in 500 µL of explant media (IMEM + 5% FBS + 10 µg/mL insulin + 10 µg/mL hydrocortisone) + vehicle, 1 µM ICI, or 1 µM 4OHT. Three pieces of tissue were placed on each sponge. After three days of culture, 30 mg/mL BrdU (Invitrogen #00-0103) was added to media 4-6 hours before tissue collection. Tissue collected for immunohistochemical analysis was fixed for ~24 in 10% NBF. Tissue collected for gene expression analysis was lysed in Buffer RLT (Qiagen) + 1% beta-mercaptoethanol, vortexed and passed through an 18-gauge needle several times. RNA was isolated using the RNEasy Mini Kit (Qiagen) according to the manufacturer's protocol. cDNA conversion and qRT-PCR was performed using Bio-Rad iScript and Universal SYBR RT Supermix as according to the manufacturer's instructions. Primer sequences are listed in Appendix A. All primers were used at a 200 nM concentration in the final reaction mix. qPCRs were run in a 12-µL reaction volume in 96- or 384-well format using Bio-Rad CFX Real-Time Detection Systems. Immunohistochemical analysis is described below.

For PH045, PH053, and PH070, two sponges per treatment group (six explant pieces total) were used for each assay type (i.e. two sponges were set-up for RNA collection and two for fixation / eventual IHC). Two independent experiments were conducted for these three models, each experiment using a tumor from an individual mouse. PH242 was not available for a repeat experiment in sufficient time for the preparation of this thesis. Only one sponge (three explant pieces) was used for each treatment group for this model although several time points (day 1-3) were assessed.

2.2.8 Immunohistochemistry

PDX and explant IHC analysis was performed in the lab. Tissue sections were deparaffinized in a series of xylene washes and rehydrated in ethanol, PBS, and dH2O. Heat-induced antigen retrieval was performed in citrate buffer (pH 6.0) for 30 min using a boiling water bath. Endogenous peroxidases were blocked with H_2O_2 (Dako Peroxidase Block). Sections were then blocked in 5% BSA in PBS + 0.5% Tween-20 for 1 hour at RT. Sections were incubated in primary antibody overnight at 4 deg C. DAKO anti-mouse (K4001) secondary reagent was applied for 30 min at RT. Staining was visualized with 3,3'-diaminobenzidinetrahydrochloride (DAB) and slides were counterstained with hematoxylin. Antibodies are detailed in the table below.

BrdU staining was quantified by determining % Brdu+ cells (# BrdU+ cells / total cells * 100%) for a given field of view. For each treatment group, 10 fields of view were counted, spanning multiple explant pieces..

Table 4: Antibodies and dilutions for explant/PDX IHC

Antibody	Clone	Host	Vendor	Cat #.	Dilution
ER	6F11	Mouse	Leica	NCL-L-ER-6F11	1:50
BrdU	Bu20a	Mouse	Cell Signaling	5292S	1:200
Ki67	M1B	Mouse	Dako	M724001	1:300

Immunohistochemistry of clinical samples was performed by the research histology core at the University of Pittsburgh Medical Center. Antigen retrieval was performed in citrate buffer (pH 6) at 120 deg C. ER was stained using pre-dilute ER SP-1 clone antibody (Biocare Medical). Staining was detected using Envision Dual Link+ HRP Polymer and DAB (Dako). Hematoxylin was used for counterstaining.

2.2.9 Development of the E2sig and EndoRx panel

To design a comprehensive assay for estrogen response, we overlapped our microarray results with publically available preclinical studies of E2 response in breast, bone, ovarian, and endometrial cancer (Appendix B). Studies were downloaded from the Gene Expression Omnibus (GEO) and E2-regulated genes were analyzed by t-test (E2 vs. vehicle) with a cut-off of $p<0.001$. We also overlapped our data with genes which were differentially expressed between ER-positive and ER-negative tumors in The Cancer Genome Atlas (TCGA) breast and ovarian cohorts and with genes specific to "hormonally responsive" endometrial cancer (as defined by TCGA)[9,166,167]. The union of genes from each study type (*in vitro*, *in vivo*, and TCGA) was taken to determine E2-regulated genes for a given cancer type (e.g. ovary) except for breast cancer. Given the large number of genes identified by the numerous breast cancer studies, we used the intersection of these data sets. E2-regulated genes in each cancer type were then compared; this approach identified 207 genes that were estrogen-regulated in at least 3/4

cancer types (Fig. 9B). Ad hoc additions were then made including components of the ER signaling axis and genes which correlated with response in clinical trials of endocrine therapy in ovarian cancer[105,168]. This 236-gene set (the "E2sig") was validated *in silico* using the METABRIC and Van't Veer data sets and *in vitro* by NanoString assays in PEO4 and MCF-7 cells to confirm estrogen-regulation (Appendix B). Lastly, we added genes from the literature based on associations with endocrine resistance, tumor-stromal interactions, or immune response. The final 350-gene list was named the "EndoRx panel" and is provided in Appendix B.

2.2.10 Analysis of clinical specimens

Clinical samples were procured from the University of Pittsburgh Medical Center (UPMC), Fox Chase Cancer Center (FCCC), Roswell Park Cancer Institute (RPCI), and the University of Michigan (Mich). All clinical samples used contained >50% tumor and >50% viable cells as determined by a board-certified pathologist (E.E.). For RNA isolation and subsequent NanoString analysis, paraffin sections were scraped off of slides into microcentrifuge tubes. For each sample, four 5-um sections were used. Samples were deparaffinized using Deparaffinization Solution (Qiagen) and processed using the Qiagen AllPrep FFPE RNA / DNA isolation kit. RNA concentrations were measured using the Qubit (Invitrogen) broad range protocol. Gene expression of the EndoRx panel was measured on the NanoString nCounter according to the manufacturer's protocol. Data were analyzed using nSolver and R. We evaluated potential confounding batch effects between patients at different sites. Specifically, we compared time on endocrine therapy, overall survival, and gene expression (both overall patterns and total number of counts). These analyses are provided in Appendix B.

To identify genes associated with endocrine response, patients were stratified into groups based on duration of endocrine therapy: "responders" (≥120 days on endocrine therapy) and "non-responders" (<120 days). The 120-day cutoff was chosen based on discussions with practicing gynecologic oncologists (Drs. Robert Edwards and Michelle Boisen). Details of the statistical analysis are provided below under "Statistical methods." Analysis of tissue and clinical data was approved by local Institutional Review Boards.

2.2.11 Statistical methods

For preclinical studies, significance was determined using a p-value of 0.05 unless otherwise specified. Unpaired, two-tailed t-tests were used for experiments with two groups. For experiments with three or more groups, ANOVA was used followed by Tukey's post-hoc test.

For clinical samples, significance of differentially expressed genes was determined by likelihood ratio testing followed by Benjamini-Hochberg correction for multiple comparisons. Log-rank test was used to determine significance between Kaplan-Meier curves (alpha=0.05).

2.3 RESULTS

2.3.1 Endocrine response in HGSOC cell lines

To determine if estrogen mediated growth in ovarian cancer cells, we evaluated response to E2, ICI, and 4OHT in four HGSOC cell lines. ER was highly expressed in PEO1, PEO4, and OVCA432 cells at levels comparable to the hormone-responsive breast cancer cell line MCF-7.

Expression was more modest in OVSAHO cells (Fig. 3A). ERß was not expressed in any of the cell lines (not shown). E2 stimulated proliferation of PEO4 and PEO1 cells in a dose-dependent manner. This was abrogated by treatment with ICI and 4OHT (Fig. 3B), consistent with previous reports that E2 can promote ovarian cancer cell growth[132,169,170]. In contrast, E2 had no effect on proliferation of OVCA432 and OVSAHO cells.

We next hypothesized that expression of ER target genes (ERTGs) could distinguish ER-dependent versus -independent HGSOC cells. However, previous studies to identify ERTGs in HGSOC are limited[132,148] To create a more comprehensive picture of ER signaling and to capture primary ERTGs, we performed whole-genome microarrays in PEO4 and PEO1 cells after 3-hour treatment with E2, ICI +/- E2, or 4OHT +/- E2. E2 induced significant ($p<0.001$) gene expression changes in both cell lines (222 genes in PEO1, 293 in PEO4; Fig. 3C, Tables 12 and 13). Of these, 94 genes were E2-regulated in both PEO1 and PEO4 cell lines, including GREB1, CA12, DEPTOR, GFRA2, OFLM3, and SLC22A5. E2-regulation of these genes was validated by qRT-PCR in independent experiments (Appendix C).

E2-stimulated changes in gene expression were largely inhibited by ICI and 4OHT. Notably, ICI appeared to be more effective in blocking gene expression than 4OHT failed to block E2-mediated expression of 101 genes whereas ICI only failed to block 19 in PEO4 cells (Fig. 3C). This is likely attributable to agonistic effects of 4OHT as 4OHT modulated expression of several genes independent of E2 (Fig. 3C). These included genes such as BCL2A1, ARID5B, CXCL2, and TXNIP. However, 4OHT-regulation could not be consistently reproduced in independent qRT-PCR experiments (not shown).

Overlapping our array results with studies of E2-regulated genes in MCF-7 breast cancer cells (GEMS data[171]) revealed conservation of many known ER target genes (ERTGs) including

GREB1, MYC, and CCNG2 (Fig. 3D). IGFBP3, a well-characterized ERTG in HGSOC, was E2-repressed in both PEO1 and PEO4 cells but the p-value (0.014) did not reach our cut-off for

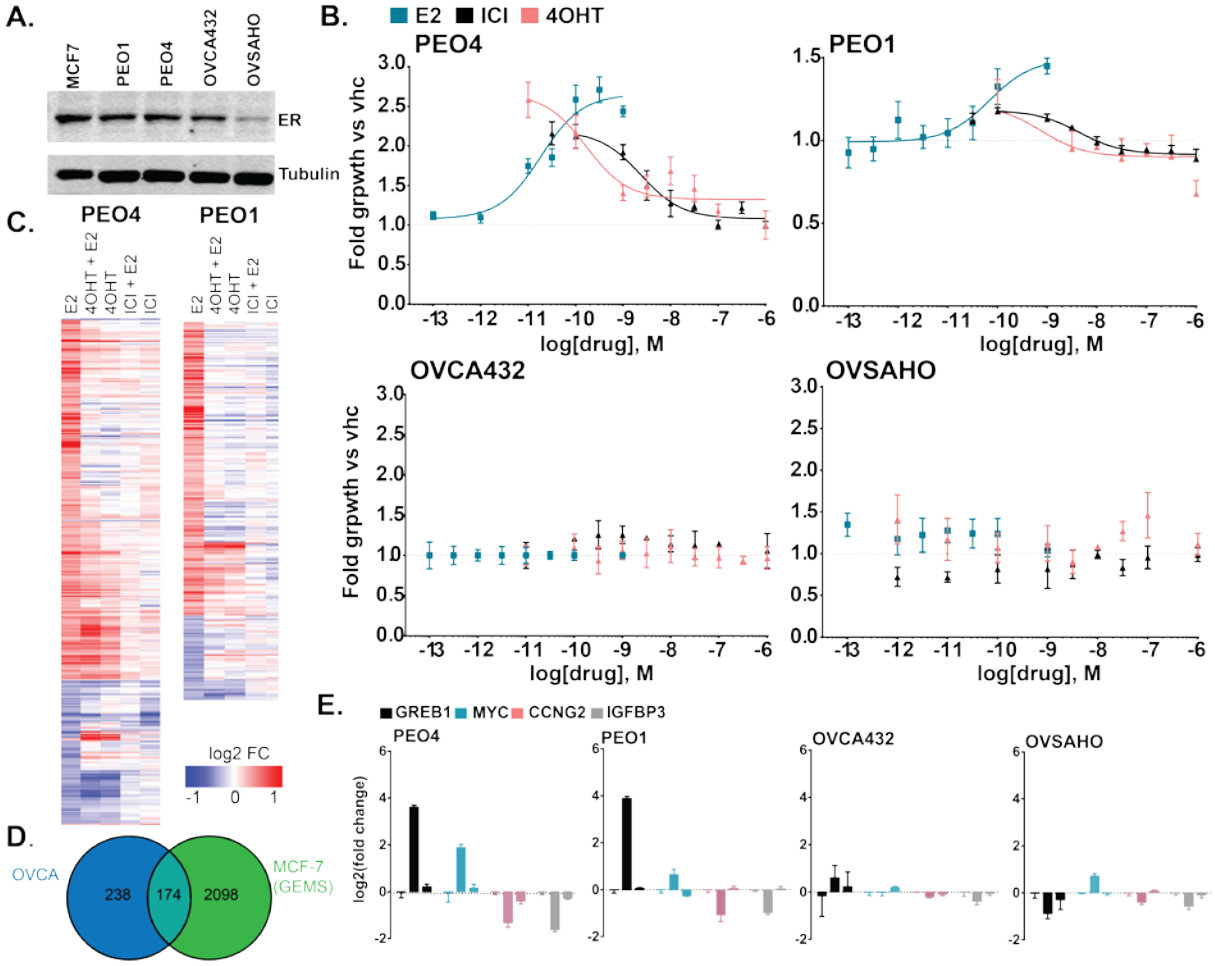

Figure 3: Endocrine response in HGSOC cell lines. A. Expression of ER in HGSOC cell lines. B. Effect of E2, ICI, and 4OHT on growth of HGSOC cells. Hormone-deprived cells were treated with increasing doses of E2, ICI, or 4OHT. ICI and 4OHT were added in the presence of 100 pM E2. Data are shown as fold change (FC) vs. vehicle. Points represent the mean of six biological replicates; error bars show standard deviation. Graphs are representative of ≥2C. Heat maps depicting gene expression changes (log2FC vs. vehicle) after treatment with E2 +/- 4OHT,or ICI in PEO4 and PEO1 cells. Genes shown are significantly regulated by E2 compared to vehicle ($p<0.001$). Microarray analysis was conducted by Soumya Luthra, MS. D. Overlap of E2-regulated genes in PEO1 and PEO4 cells versus MCF7 breast cancer cells (GEMS early data). E. Mean FC (treatment vs. vehicle, three biological replicates) of ERTGs in HGSOC cells. Gene expression was measured by NanoString after 8-hour treatment with Vhc, E2, or E2 + ICI. Error bars show standard deviation of three biological replicates.

significance in this experiment. This is likely attributable to the brief endocrine treatment, which enriches for immediate ERTGs. We were able to confirm its regulation and that of several other ERTGs (GREB1, MYC, CCNG2) by qRT-PCR (Fig. 3E). Expression of these genes was not significantly E2-regulated in OVCA432 and OVSAHO cells, consistent with the lack of proliferative response (Fig. 3E).

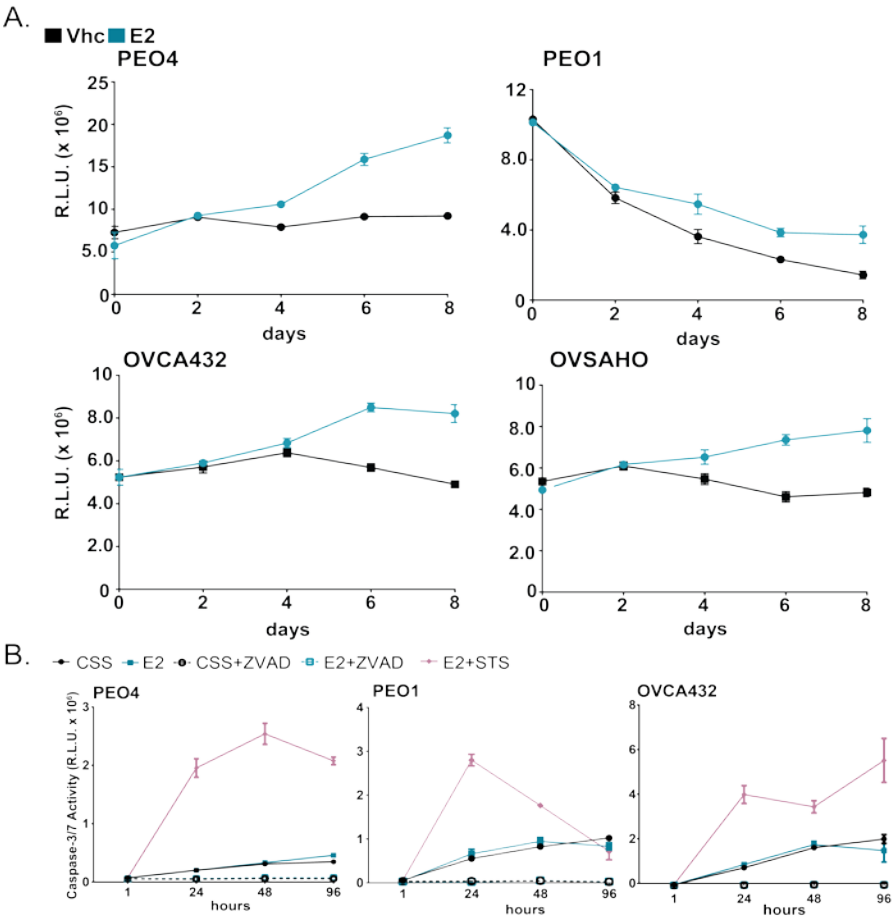

Figure 4: Endocrine response in an *in vitro* model of ascites. A. Hormone-deprived cells were plated in ULA +/- 1 nM E2. Total ATP was measured by CellTiter-Glo assay. Data are presented as blank-corrected luminescence (mean of six replicates + standard deviation). B. Hormone-deprived cells were treated with control, E2, ZVAD, or STS. Apoptosis was measured using CaspseGlo-3/7 assay.

We then evaluated how E2 affected models of more advanced disease. To mimic ascites, a common clinical manifestation in late-stage HGSOC, we seeded cells in ultra-low

attachment (ULA) plates. E2 increased viability of PEO1 and PEO4 cells in ULA, similar to standard conditions. Surprisingly, OVSAHO and OVCA432 cells, which were E2-independent under standard conditions, became E2-responsive in ULA (Fig. 4A). We asked if E2 was inhibiting anoikis (apoptosis from loss of cell matrix adhesions) in HGSOC cells. However, we saw no effect of E2 on caspase-3/7 activity in ULA (Fig. 4B).

In parallel, we assessed estrogen-dependence for PEO4 cells *in vivo* in mice +/- E2 pellet supplementation. E2 treatment increased tumor burden compared to placebo controls (Fig. 5). E2 also induced expression of canonical ERTGs (e.g. GREB1, MYC), consistent with *in vitro* studies (Fig. 5). Xenografts in both conditions expressed high levels of ER (Fig. 5). Taken together, these results suggest endocrine response is context-dependent and can promote features of advanced HGSOC.

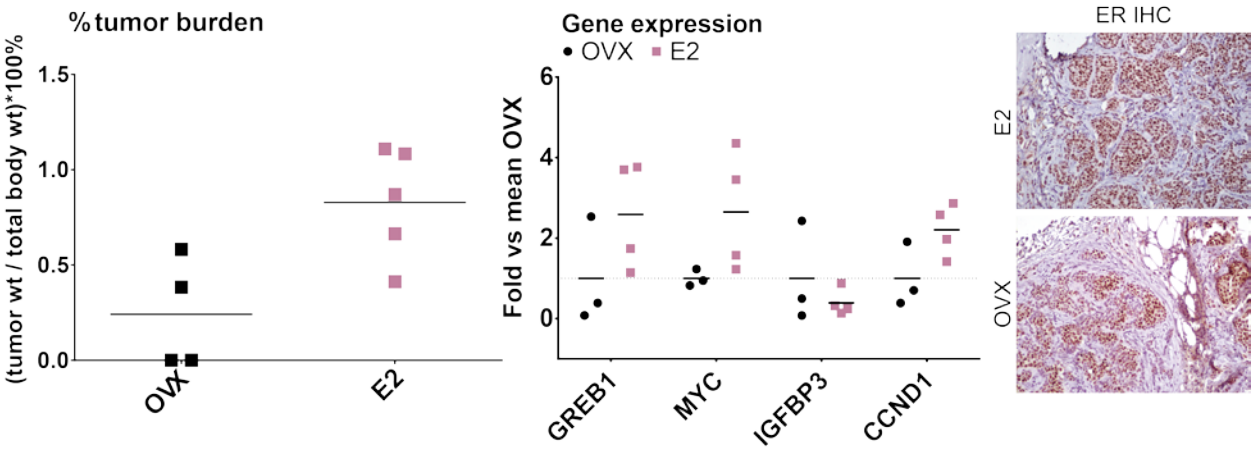

Figure 5: Endocrine response in cell line xenografts. PEO4 cells were injected IP into mice after ovariectomy (OVX) plus placebo or E2 pellet supplementation. Left: Tumor burden was measured after 11 weeks and calculated as (tumor weight / total body weight)*100%. Center: E2 modulates expression of ERTGs in PEO4 xenografts (qRT-PCR). Right: ER IHC in PEO4 xenografts.

2.3.2 Endocrine response in HGSOC patient-derived xenografts

To examine endocrine response in models more closely mimicking the complex biology of HGSOC, we utilized a panel of patient-derived xenograft (PDX) tumors (Tabel 6). Two of the models (PH045 and PH070) were exposed to neoadjuvant chemotherapy. One patient, the donor of PH070, had received previous endocrine therapy for breast cancer. The overall clinical features recapitulate and typical advanced grade and stage (Table 5) of clinical HGSOC. They also recapitulate the varying ER expression (Fig. 6). However, HGSOC PDXs often take months to form detectable tumors[157,158], limiting the feasibility of large-scale endocrine response studies *in vivo*. To circumvent this, we cultured PDX tumor fragments *ex vivo* as explants[172,173] to rapidly assess endocrine response (Fig. 7A).

Table 5: Clinical features of patient tumors used for PDX models

Model	Age at dx	Stage	Grade	Subtype	Chemo	Prior endo rx
PH045	66	3C	3	serous	Neoadj taxol/carbo, doxil, taxotere/carbo	no
PH053	70	3C	3	serous (PP)	taxol/carbo	no
PH242	70	4	4	serous	taxol/carbo, carbo, doxil, topotecan	no
PH070	62	3C	3	serous	Neoadj taxol/carbo	AI+Tam for BRCA

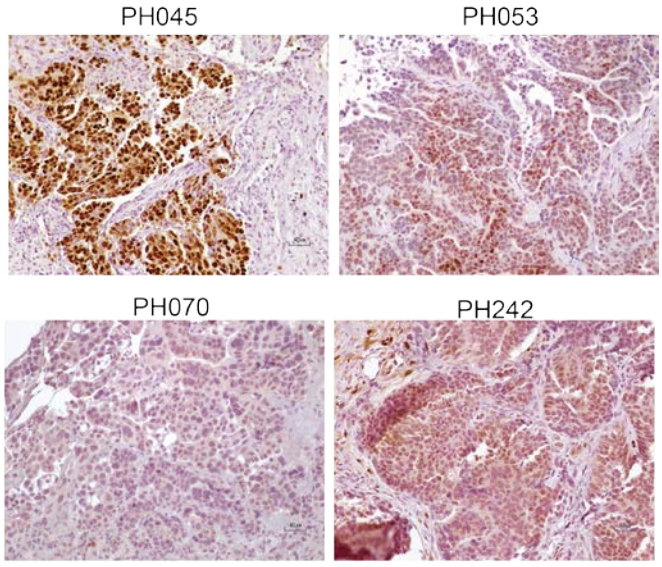

Figure 6: ER IHC in HGSOC PDXs. Tumors were collected when mice became moribund. (8-16 weeks after engraftment).

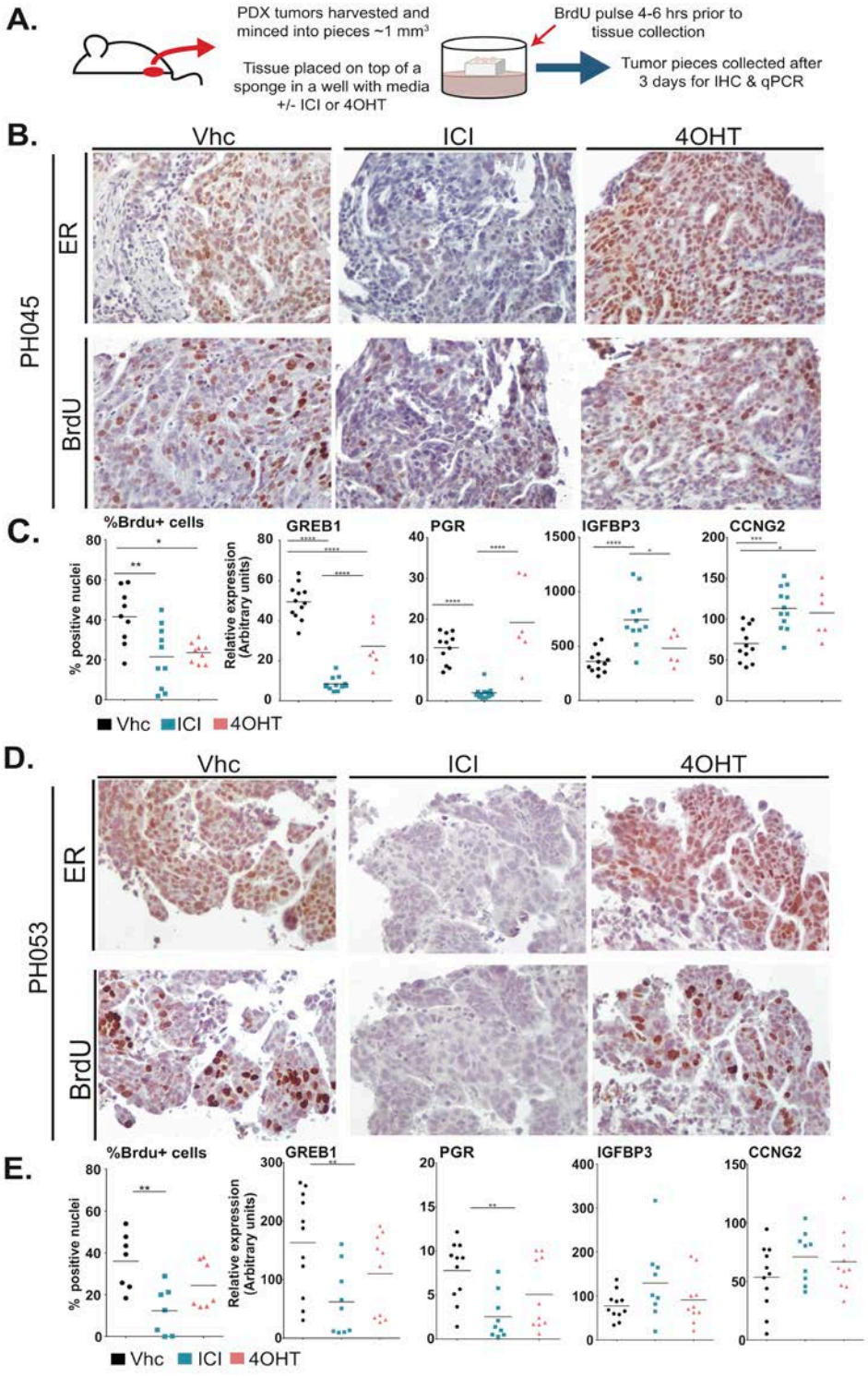

Figure 7: Endocrine response in PH045 and PH053 explants. A. Workflow for explant studies. B & C. ICI and 4OHT treatment decreases proliferation (B) and alters ER target gene expression (C) of PH045 explants. D & E. Effects of ICI and 4OHT treatment on PH053 explant proliferation and gene expression. For graphs in C & E, each dot represents an individual explant piece. Bars show mean expression. Asterisks indicate significance: ****, $p<0.0001$; ***, $p<0.001$; **, $p<0.01$; *, $p<0.05$. Significance determined by ANOVA.

ICI treatment decreased ER levels and reduced BrdU incorporation of PH045 explants (Fig. 7B). The median change in BrdU incorporation after ICI treatment was -50% (range 8% to -95%). Decreased proliferation was complemented by repression of ERTGs including GREB1 and PGR (Fig. 7C). Similarly, expression of ER-repressed genes CCNG2 and IGFBP3 was increased by ICI treatment. 4OHT modestly reduced BrdU incorporation. While the median change vs. vehicle was similar between ICI and 4OHT (-50% vs. -40%), ICI produced a greater maximal decrease (95% vs. 58%) and more robust change ($p=0.005$ vs. $p=0.014$). 4OHT also had less-pronounced effects on gene expression, suggesting ERTGs could be a useful metric of drug efficacy.

ICI and 4OHT also decreased proliferation and gene expression of PH053 (Fig. 7D & 7E). Intriguingly, ICI again produced a more significant decrease in proliferation than 4OHT ($p=0.0049$ vs. n.s.). ICI did not block proliferation or gene expression of PH242 and PH070, consistent with these tumors being ER-poor and ER-negative, respectively, in explant culture (Fig. 8). This suggests explant models mimic the variable response to endocrine therapy seen clinically.

We also tried to mimic AI therapy by growing explants in hormone-deprived conditions (IMEM + 10% CSS). However, this produced no significant changes in gene expression relative to vehicle / hormone-replete control. Further, addition of E2 did not produce significant effects on gene expression (not shown). Similarly, there were no significant changes in BrdU incorporation between hormone-replete (IMEM + FBS), CSS, or CSS + E2 conditions (not shown). Given that addition of ICI to CSS altered gene expression relative to CSS alone, these may be attributable to residual hormones in the explant cultures rather than a resistance to estrogen deprivation.

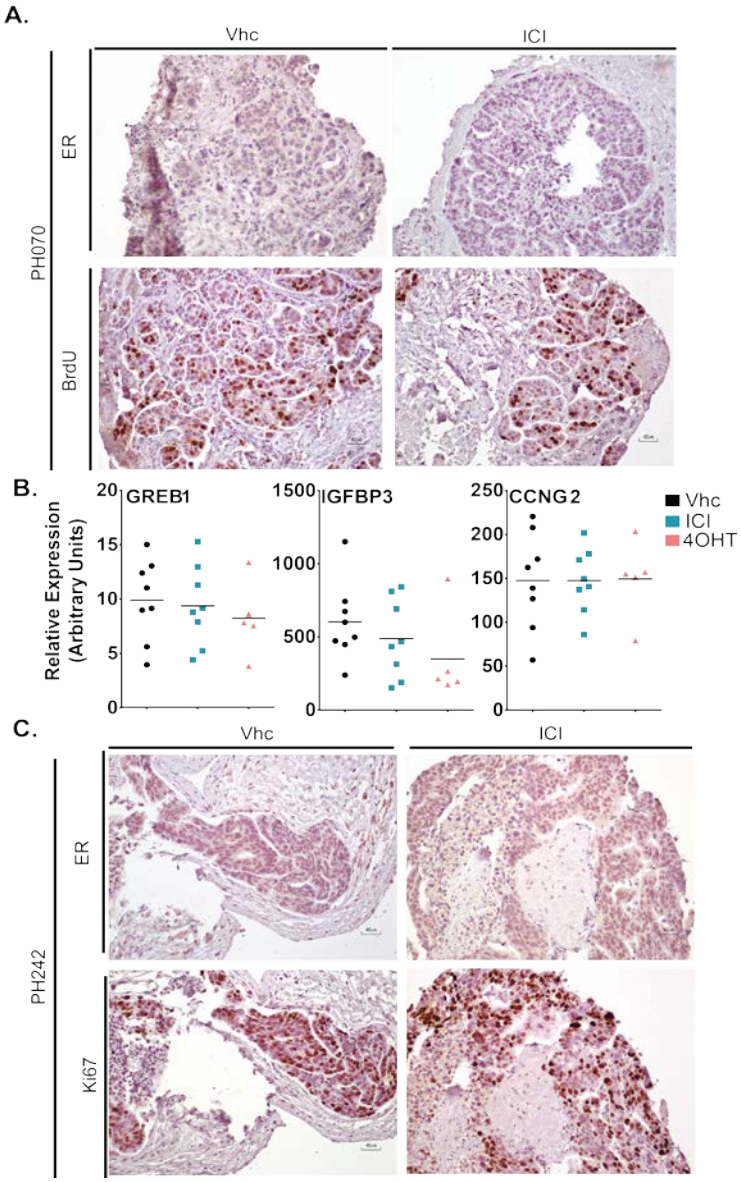

Figure 8: Endocrine response in PH070 and PH242 explants. PH070 and PH242 PDX tumors were grown as explants. IHC and gene expression analyses were performed after three days of explant culture.

2.3.3 Identifying genes associated with clinical endocrine response

Because modulation of ERTGs corresponded with proliferative response in HGSOC models (Figs. 3 & 7), we hypothesized that their expression could predict clinical response to endocrine therapy. To test this, we procured specimens from four medical centers from 70 ovarian cancer patients who received endocrine therapy (tamoxifen and/or an AI) (Table 6). The median age at diagnosis was 63 and the majority (85%) of patients presented at late stages (III or IV). Median age at diagnosis was 63 and the majority (85%) of patients presented at late stages (III/IV). Patients from RPCI were significantly older ($p=0.0009$) than patients from the other three sites. There was no significant difference in overall survival between patients at different centers (Appendix D). There was also no significant difference in stage, grade, or pre-endocrine therapy CA-125 levels, suggesting endocrine therapy was used at a similar point in the disease course at each site..

Fig. 9A depicts a sample patient timeline. Upon initiation of endocrine therapy, patients are typically maintained on treatment until disease progression. We had pre- and post-treatment CA-125 measurements for 45 / 70 patients; for 41 patients, CA-125 was higher when endocrine therapy was stopped (not shown). Thus, we used duration of endocrine therapy as a surrogate for therapeutic response. There was no association between clinical characteristics (age, stage, and grade) and time on endocrine therapy.

Table 6: Clinical features of OVCA patients who received endocrine therapy[*]

	RPCI (N=20)	UPMC (N=17)	FCCC (N=9)	Mich (N=26)
Age at dx	72.7 ± 7.3	60.1 ± 9.8	56.8 ± 7.5	59.5 ± 15.0
Primary/Recur	17/3	17/0	6/3	30/0
Grade				
Low	0	2	1	3
High	20	15	8	23
Stage				
Early (1-2)	0	1	3	2
Late (3-4)	20	12	6	28
Pre-endo CA-125 (# censored)	419 ±639 (1)	283 ±503 (6)	463 ±785 (5)	105 ±143 (0)
Days on endo rx	405 ± 647	383 ± 356	168 ± 115	192 ± 275
Min	22	38	31	30
Max	2850	908	396	1470
Survival after endo rx (days)	687 ± 866	959 ± 641	665 ± 639	628 ± 742
Overall survival (days)	1961 ± 1361	2497 ±1470	2129±1104	1554 ± 1212

To identify ERTGs and ER regulators critical to endocrine response, we designed the EndoRx panel gene signature (see methods, Fig. 9B) and measured expression in tumor specimens. Patients were dichotomized based on duration of endocrine therapy: those who received therapy for $\geq$4 months were considered "responders" while those treated for <4 months were "non-responders." Of the various gene sets incorporated into the EndoRx panel, ERTGs had some of the strongest associations with endocrine response. IGFBP3 was significantly lower (q=0.015) in patients who responded to endocrine therapy (Fig. 9C). PGR, MYC, and PDGFRL trended towards differential expression (Table 7), with MYC and PGR being elevated and PDGFRL being decreased in responders relative to non-responders.

[*] Descriptive statistics were determined by Tianzhou Ma. For external sites (RPCI, FCCC, Mich), clinical data were provided by the collaborating physician.

Interestingly, ESR1 also trended towards higher expression in responders ($q<0.25$, $p=0.003$). Previous attempts to link ER expression with endocrine response in ovarian cancer have produced mixed results so we further measured ER by IHC and H-scoring (Fig. 9D). H-scores ranged from 0 to 270 (median=60, Fig. 9E). Surprisingly, ESR1 expression and H-score had only a modest correlation (corr=0.41). However, patients with an H-score above the median were more likely to benefit from endocrine therapy ($p=0.002$, Fig. 9F). H-score had greater predictive power for endocrine response than ESR1 (not shown).

Finally, we asked how IGFBP3 compared to ER as an indicator of endocrine response. To do this, we regressed time on endocrine therapy against IGFBP3 and found it was a better discriminator than H-score ($p=0.0002$ vs $p=0.003$, Figure 9G). We then designated patients as ER^{high} or ER^{low} (H-score above or below 60, respectively) and $IGFBP3^{high}$ or $IGFBP3^{low}$ (above or below third-quartile IGFBP3 expression). Patients with $ER^{high}/IGFBP3^{low}$ tumors had the best response to endocrine therapy (Fig. 9H). While only four patients had $ER^{high}/IGFBP3^{high}$ tumors, two of them had a dramatically shorter time (<30 days) on endocrine therapy. Strikingly, patients with $ER^{low}/IGFBP3^{high}$ tumors had significantly worse outcomes than their $ER^{low}/IGFBP3^{low}$ counterparts (Figure 9H, $p=0.023$). Patients with $ER^{low}/IGFBP3^{low}$ tumors had outcomes comparable to patients with $ER^{high}/IGFBP3^{low}$ tumors, suggesting some ER^{low} tumors retain active ER signaling. Together, these observations suggest that direct assessment of ER function better denotes endocrine response than ER levels alone.

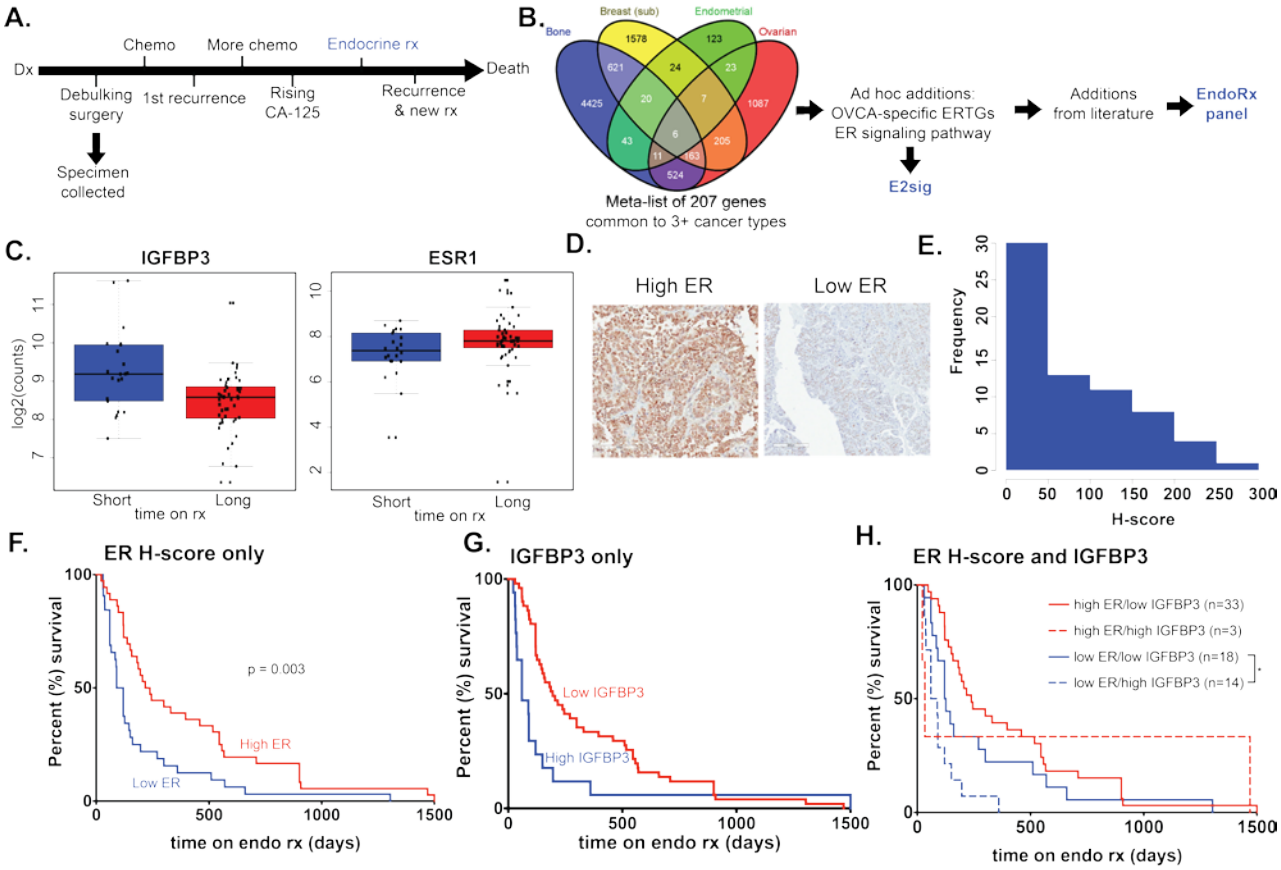

Figure 9: Identifying ERTGs associated with clinical response to endocrine therapy. A. Timeline of a typical ovarian cancer patient. After diagnosis (dx), treatment starts with debulking surgery and chemotherapy. Endocrine therapy is typically given after multiple rounds of chemotherapy if patients have a "biochemical" recurrence, determined by rising serum CA-125 levels. Endocrine therapy is continued until the patients progress by CA-125 or visual evidence of disease. B. Workflow for the design of the EndoRx panel. Meta-analysis was done in collaboration with Soumya Luthra and Uma Chandran, PhD. C. IGFBP3 expression is higher in patients who don't respond to endocrine therapy compared to those who do. The converse is true for ESR1. Analysis was done by Charles Ma. D. Representative IHC stains of ER in our patient cohort. E. Distribution of H-scores. F. Patients with a higher H-score have better response to endocrine therapy. G. Kaplan-Meier analysis of association between IGFBP3 expression and time on endocrine therapy. H. Low IGFBP3 expression identifies subgroups of high- and low-ER tumors that are more endocrine responsive.

Table 7: ERTGs associated with endocrine response in patients.

Gene	logFC	p-value	q-value
IGFBP3	-0.8283	9.01E-05	0.0158
ESR1	0.9252	0.00256	0.227
PGR	1.1479	0.00726	0.228
MYC	0.5562	0.00770	0.228
PDGFRL	-0.5322	0.0135	0.257

2.4 DISCUSSION

Clinical trials of endocrine therapy suggest that a specific subset of ovarian cancer patients benefits (response or disease stabilization) from endocrine therapy. However, unlike for breast cancer, selecting patients based on ER status (positive vs. negative) is not sufficient to predict response in HGSOC. Implementing biomarkers that complement ER expression will be critical to identifying appropriate patient populations for endocrine therapy.

Three studies have previously tried to identify biomarkers of endocrine response[105,106,168]. These studies all utilized a small panel of IHC markers. We pursued a comprehensive profile of potential biomarkers by designing the EndoRx panel. Our analysis indicated lower IGFBP3 was significantly associated with prolonged endocrine response (Fig. 9). This corroborates a previous report that IGFBP3 immunoscore correlates with response to letrozole[106]. IGFBP3 expression was more strongly associated with endocrine response than H-score (Fig. 9). Further, IGFBP3 expression was able to identify a subgroup of low-ER patients who still benefited from endocrine therapy. Given that IGFBP3 is ER-regulated in HGSOC (Figs 3 & 7, ref. 23), our results suggest that a direct output of ER function is a better indication of endocrine responsiveness than ER expression alone.

With the exception of IGFBP3 and TFF1, the latter trending towards an association ($q<0.3$, $p=0.023$), our analysis did not find strong associations between endocrine response and previously reported biomarkers[105,106,168]. This could be attributable to differences in methodology (gene expression vs. IHC) or cohort size (ours is the largest to date). Though VIM expression was previously shown to be associated with fulvestrant response[105], difference in

therapy may account for the discrepancy; independent classes of endocrine therapy may require different predictive markers.

Our EndoRx panel was designed based on studies in models that recapitulate the varying endocrine response seen in clinical HGSOC. PEO1 and PEO4 cells were endocrine responsive in standard culture conditions whereas OVCA432 and OVSAHO were not. However, OVCA432 and OVSAHO cells became ER-dependent in ULA, suggesting ER has unique roles in different stages of ovarian cancer biology. This observation also emphasizes the necessity of translational models such as PDXs or tumor explants to fully understand the role of ER in HGSOC.

We provide the first evidence of endocrine response in patient-derived HGSOC models. ICI produced a greater effect on explant gene expression and proliferation than 4OHT, suggesting that modality of endocrine therapy will be an important consideration in HGSOC therapy. Selective ER modulators (SERMs, e.g. 4OHT) exhibit partial agonism in certain tissues and cancer types[165] whereas selective ER degraders (SERDs, e.g. ICI) are pure antagonists. Potential tamoxifen agonism in HGSOC has not been explored but tamoxifen was reported to promote fallopian tube and ovarian lesions in canines[174]. Further comparisons of ICI and 4OHT with other SERMs and SERDs will be necessary to understand any differential class effects in HGSOC.

Our explant studies also suggested heterogeneous endocrine response across regions of HGSOC tumors: response to both 4OHT and ICI varied in terms of both proliferation and gene expression between explant pieces. It is possible that interactions between different regions would allow a response of the tumor in bulk. However, strategies for combination therapy should also be considered. Two such possibilities are MAPK and Src, which have been shown to

crosstalk with ER and drive endocrine resistance in ovarian cancer[141]. Co-targeting PGR is also promising given its interaction with ER[125] and recent reports demonstrating PGR agonists induce senescence in ovarian cancer cells[125].

Our analysis is somewhat limited by its retrospective nature. Modality of endocrine therapy and number of previous therapies vary across patients. Prospective studies with post-treatment specimen collection, standardized timing of endocrine therapy, and sufficient power to compare different endocrine agents will be necessary to solidify the utility of any biomarkers. Such future studies could involve a "window trial" of neoadjuvant endocrine therapy, in which endocrine therapy is given for a brief period prior to primary debulking surgery and standard-of-care chemotherapy. In a window trial setting, pre-treatment specimens could be collected to evaluate ER status and expression of putative predictive markers (e.g. IGFBP3); post-treatment specimens could be collected at the time of surgical debulking and assessed for pharmacodynamic markers (e.g. loss of ER expression for fulvestrant-treated patients, changes in ERTG expression compared to untreated tumor) and proliferative markers.

In summary, ER modulates growth, survival, and gene expression in a subset of HGSOC and endocrine-responsiveness is context dependent. Moreover, targeting ER can be effective in patients. Targeting ER with ICI and 4OHT modulates expression of MYC, PGR, and IGFBP3 in preclinical models of HGSOC. Moreover, expression of these genes reflects clinical endocrine response. Our findings may enable the selection of HGSOC patients who would benefit from endocrine therapy.

3.0 UNDERSTANDING ER SIGNALING IN OVARIAN CANCER

3.1 INTRODUCTION

We and others have described effects of ER on ovarian cancer growth and survival in preclinical models (Chapter 2). However, the mechanisms by which ER executes these effects have not been thoroughly elucidated. To this point, there are only two previous studies of ER-mediated transcription (discussed in Chapters 1 and 2) in addition to the study we performed in Chapter 2. There are no studies to date evaluating the role of these downstream targets in E2-regulated phenotypes in ovarian cancer. Further, the co-regulators of ER signaling (either classical or non-genomic) in ovarian cancer have not been well characterized.

Previous reports have suggested crosstalk between ER and kinase signaling pathways in ovarian cancer. Specifically, Src and MEK have been suggested to directly phosphorylate ER, driving ligand-independent activity and endocrine resistance[141,175]. In breast cancer, ligand-independent activation of ER by mTOR/PI3K signaling has been described as a mechanism of endocrine resistance[176,177] and targeting mTOR in combination with an AI is now an effective therapeutic strategy[178,179]. Endocrine response can also be affected by crosstalk with cytokine signaling (e.g. IL-6/STAT3 pathways)[180,181].

Herein, we sought to understand the mechanism of ER signaling, with a focus on the shift in endocrine responsiveness in OVCA432 and OHSAHO as described above. We

investigated the role of ER target genes in driving E2-mediated growth and survival. We also investigated potential crosstalk between ER and other signaling pathways including IL-6/STAT3. Understanding effectors of ER signaling in ovarian cancer will help better identify patients with endocrine-responsive tumors and identify possible nodes for combination therapy.

3.2 MATERIALS AND METHODS

3.2.1 Cell culture

PEO1, PEO4, OVSAHO, and OVCA432 cells were cultured and hormone-deprived as described in Chapter 2. Proliferation assays and survival assays were performed with FluoReporter and CellTiter-Glo kits as described in Chapter 2.

E2, 4OHT, and ICI were obtained from Sigma (E2, 4OHT) or Tocris Biosciences (ICI) and dissolved in ethanol. The following inhibitors were purchased from Tocris Biosciences and solubilized in sterile DMSO: U1026 (MEK), Saracatinib (Src), LY294002 (PI3K), Stattic (STAT3), and Staurosporine (pan-kinase). OSI-906 (IGF1R/Insulin Receptor inhibitor) was purchased from Selleckchem and SNS-314 (AURORAK inhibitor) from ApexBio. Both were solubilized in DMSO. Recombinant IL-6 was obtained from Life Technologies (#10395-HNAE-5) and was dissolved in sterile ddH2O prior to use *in vitro*.

3.2.2 Transient knockdown

Transient knockdown was performed using Dharmacon siRNA smart pools (cat # for DEPTOR and # for SLC22A4). Hormone-deprived cells were reverse transfected with 25 nM siRNA using Lipofectamine RNAiMAX (Life Technologies). RNA was measured by qRT-PCR 48 hours after transfection. Cell growth was measured six days after transfection.

3.2.3 Gene expression analyses in HGSOC cell lines

For qRT-PCR analyses, RNA was isolated using the GE Illustra RNAspin Mini Kit as described in Chapter 2. Bio-Rad iScript RT Supermix and Universal SYBR Supermix were used for cDNA conversion and PCR, respectively. Primer sequences are listed in Chapter 2 (Table 9). Cells seeded in 2-D were treated ~16 hours after plating to allow time to adhere. Cells seeded in ULA were treated immediately after plating.

For NanoString assays, hormone-deprived cells were treated with vehicle, E2, or E2 + ICI for 8 hours as described in Chapter 2. RNA was isolated as above. Expression of the E2sig was measured on the NanoString nCounter as described in Chapter 2.

3.2.4 Immunoblots

Cells were lysed in RIPA as described in Chapter 2. Cells in 2-D were rinsed with PBS in the culture vessel and then scraped in RIPA. Cells in ULA were collected by centrifugation and rinsed with PBS. The pellet was then lysed in RIPA. Protein content was quantified by BCA assay as described in Chapter 2. Twenty to thirty (20-30) µg protein per lane was run on 10%

SDS polyacrylamide gels and transferred to PVDF membranes. Blots were imaged using either the Olympus LiCor Phosphoimager or chemiluminescence or X-ray film. The antibodies used were: ER (Leica NCL-L-ER-6F11, used at 1:500), pER S118 (clone 16J4, CST #2511, used at 1:1000), pSTAT3-Y705 (CST, 1:1000), STAT3 (CST, 1:1000), and Tubulin (Sigma, used at 1:5000). Secondary antibodies used were either anti-rabbit IgG (CST #7074, used at 1:2000 or 1:5000) or anti-mouse IgG (Sigma #T6557, used at 1:2000). Immunoblots for ER in figs. 11 and 12 were performed by Dr. Michelle Boisen. The blot in figure 15 was performed by Elizabeth Nelson.

3.3 RESULTS

3.3.1 Evaluating DEPTOR as a potential mediator of endocrine response

Through the microarray studies in Chapter 2, we identified DEPTOR as an E2-induced gene in HGSOC. DEPTOR, which is also E2-regulated in breast and endometrial cancers, interacts with mTORC1 and 2 to modulate signaling[182,183]. Given this observation and known interactions between ER and mTOR in other cancer types[176,177], we postulated that DEPTOR may contribute to E2-stimulated proliferation in ovarian cancer.

To investigate this, we transfected PEO4 cells with DEPTOR-targeted siRNA and measured growth and gene expression after E2 treatment. After 48 hours, transient knockdown completely abrogated E2-stimulated DEPTOR expression (Fig 10). However, knockdown had no effect on E2-induced expression of GREB1, nor did it impact E2-stimulated proliferation in 2-D (Fig 10).

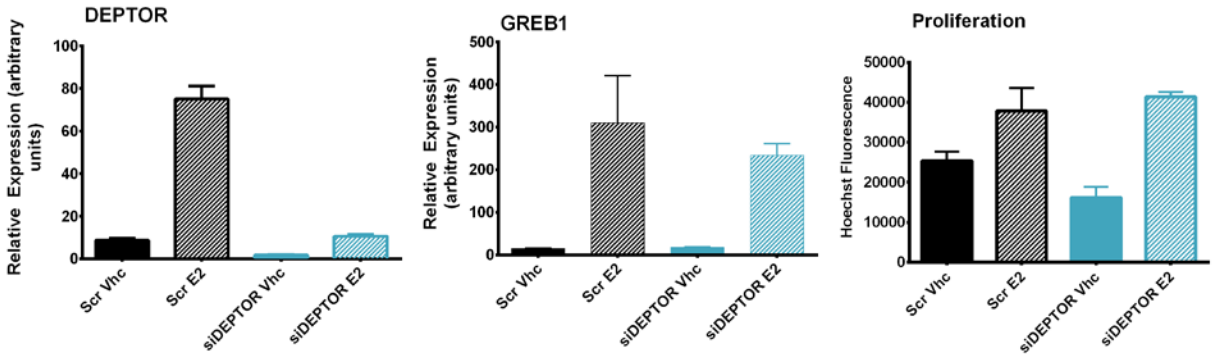

Figure 10: Effects of DEPTOR KD. A. DEPTOR-targeted siRNA blocks E2-induced expression. Gene expression was measured by qRT-PCR 48 hours after reverse transfection and 24 hours after E2 treatment. B. DEPTOR knockdown has no effect on E2-induced GREB1 expression. Gene expression was measured as in A. C. DEPTOR knockdown does not affect 2-D growth. Proliferation was measured six days after transfection by FluoReporter.

3.3.2 Using changes in ER signaling between 2-D and ULA to identify ERTGs critical to growth

Rather than continue to work through targets identified solely from the microarray, we sought to prioritize targets more likely to contribute to E2-driven growth. Given the shift we observed in endocrine response between 2-D and ULA (Chapter 2), we postulated that evaluating ER signaling in ULA would help us identify genes and co-factors critical to endocrine response. In light of this, we first compared ER expression between the two conditions. After 24 hours in culture, ER expression was higher for PEO1, PEO4, OVCA432, and OVSAHO cells in ULA than in standard culture conditions (Fig. 11). Similarly, ESR1 mRNA levels increased in ULA (Fig. 11), suggesting that higher ER levels in ULA are attributable to elevated transcription.

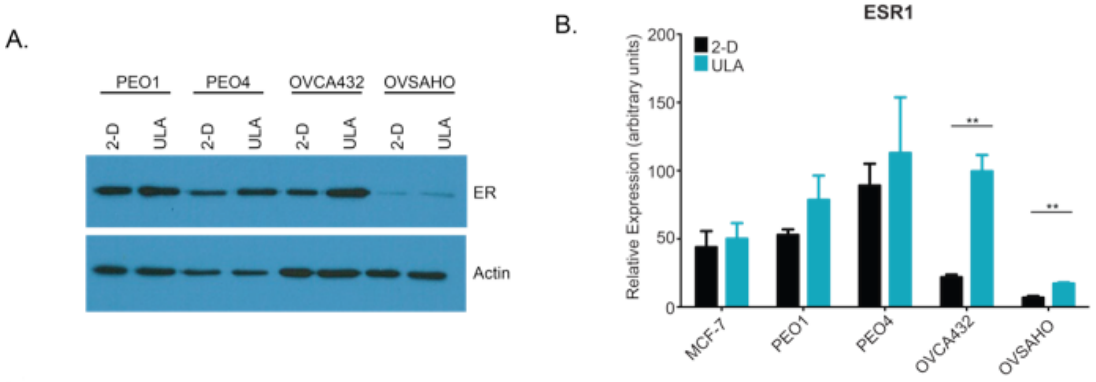

Figure 11: ER expression in 2-D and ULA. A. ER protein levels measured after 24 hours in 2-D or ULA (M Boisen). Representative blot of three independent experiments. B. ER (ESR1) mRNA levels after 24 hours in 2-D or ULA. Graph shows the average of three independent experiments. Error bars shown standard error of the mean. qRT-PCR was performed by Ravi Patel.

To confirm this, we compared ER turnover between 2-D and ULA. Hormone-deprived cells were treated with vhc, E2, ICI, or 4OHT for 4 and 24 hours. In PEO1 cells, E2 treatment led to ER degradation (Fig. 12). ICI also degraded ER, consistent with its known mechanism of action. Similarly, 4OHT stabilized ER expression. In PEO4, OVCA432, and OVSAHO cells, E2 did not degrade ER but ICI and 4OHT degraded and stabilized ER, respectively (Appendix

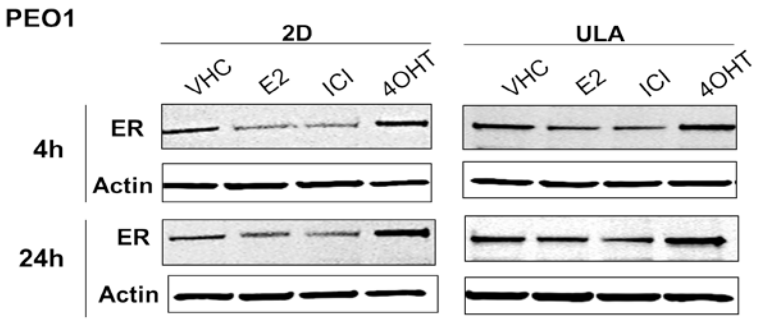

Figure 12: ER degradation in PEO1 cells in 2-D and ULA. Hormone-deprived PEO1 cells were plated in 2-D or ULA and treated with vhc, 1 nM E2, 1 µM ICI, or 1 µM 4OHT. ER levels were measured by immunoblot after 4 or 24 hrs. Blots performed by M. Boisen

E). Notably, ER turnover did not differ between 2-D and ULA, further indicating that the change in ER levels is caused by increased transcription.

We hypothesized that this increase in ER expression would lead to concomitant increases in canonical ER signaling. To evaluate this, we plated PEO1, PEO4, OVCA432, and OVSAHO cells in 2-D or ULA and treated with vehicle, E2, or E2+ICI. After 8 hours of treatment, we collected RNA and evaluated expression of the E2sig (n=236 genes, described in Chapter 2). As expected, E2 treatment induced robust changes in gene expression in PEO1 and PEO4 cells in both culture conditions (Fig. 13A). These were largely abrogated by addition of ICI. E2 produced much more modest effects on gene expression in OVCA432 and OVSAHO cells, consistent with their lack of endocrine response in 2-D. Surprisingly, the number of genes

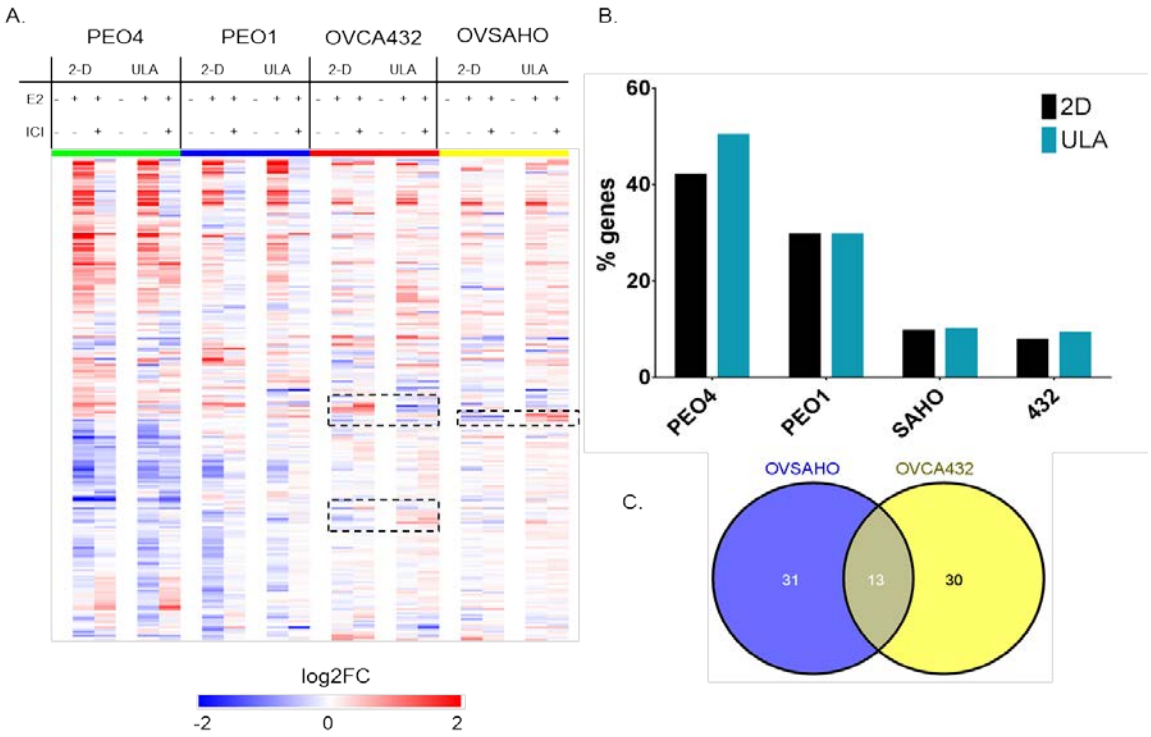

Figure 13: ER-mediated transcription in 2-D vs. ULA. A. Heat map of E2sig expression in HGSOC cells after 8-hour treatment with Vhc, E2, or E2 + ICI. Heat map is colored by log2FC vs. vehicle control (2-D is normalized to 2-D, ULA to ULA). B. Percentage of genes on the E2sig significantly E2-regulated in both conditions for each cell line. C. Overlap of genes differentially regulated between 2-D and ULA in OVSAHO and OVCA432 cells.

significantly regulated by E2 did not differ between 2-D and ULA for any cell line (Fig. 13B). There were, however, a small subset of genes that exhibited differential E2-regulation between 2-D and ULA (dashed lines on Fig. 13A, Fig. 13C) in OVCA432 and OVSAHO cells. Some of these genes were repressed in 2-D but induced in ULA. Others were E2-regulated in the same direction but had greater relative FC in ULA. This latter category included GREB1 and SLCC22A4, both of which were more strongly induced by E2 in ULA. We thus postulated that these two genes might contribute to E2-driven growth. We addressed this by transiently knocking down SLC22A4 in several cell lines. SLC22A4-targeted siRNA decreased expression of SLC22A4 but had no effect on growth or survival in ULA (Fig. 14). This suggests that increased induction of SLC22A4 may be a consequence of heightened endocrine responsiveness, rather than a mediator of it. However, other phenotypes (e.g. 2-D growth, anti-estrogen

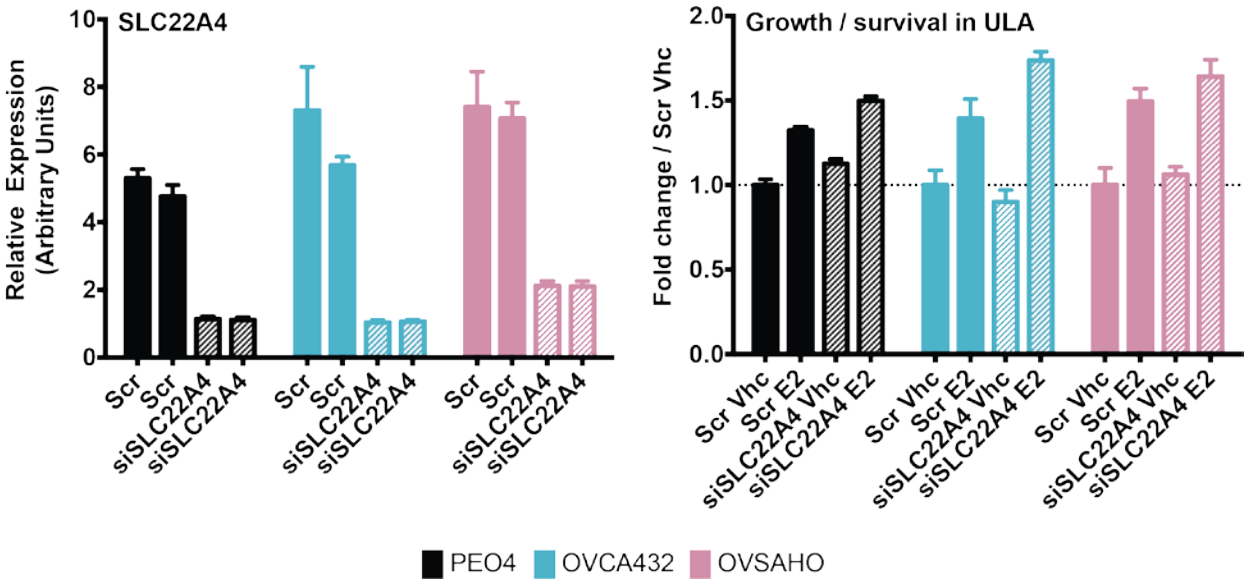

Figure 14: Effects of SLC22A4 knockdown on cell growth and survival in ULA. A. Hormone-deprived cells were transiently transfected with scrambled control or SLC22A4-targeted siRNA and treated with 1 nM E2. Expression was measured by qRT-PCR 48 hours after transfection. Biological duplicates are shown side by side. B. Growth in ULA was measured by CellTiter-Glo six days after transfection.

response) need to be evaluated before SLC22A4 can be ruled out as an effector of ER signaling.

3.3.3 Identifying pathways that crosstalk with ER

Overall cellular architecture changes with three-dimensional context (2-D vs. 3-D [matrigel] vs. suspension [ULA]). Thus, our observations regarding the activation of endocrine response in low attachment in OVCA432 and OVSAHO cells (Chapter 2) is suggestive of ER crosstalk with cell membrane or cytoskeletal cues. It is likely that ER signaling in ovarian cancer cells is mediated in part by interaction with kinase signaling cascades and that targeting these pathways may modulate ER function. To address this, we asked what pathways drive ER-independent growth in 2-D. We screened a small panel of compounds that inhibit MEK, PI3K, IGF1R, AURORAK, STAT3, and SRC, respectively against hormone-deprived cells. Each cell line had slightly different sensitivity to inhibitors (Fig. 15). However, the Src inhibitor Saracatinib

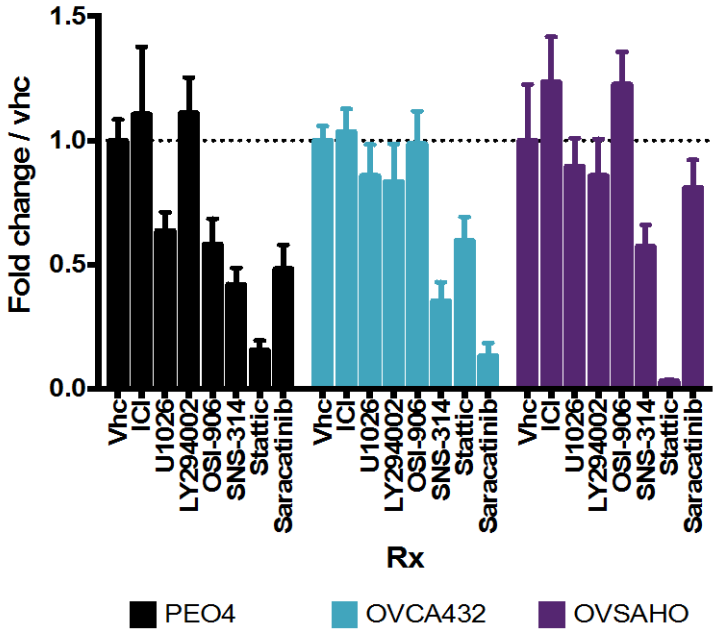

Figure 15: Small screen of targeted agents in HGSOC cells. Hormone-deprived cells were treated with 1 µM of the indicated inhibitor. Growth in 2-D was measured by FluoReporter after six days.

partially abrogated growth in all cell lines. Further, Stattic, an SH2 domain mimetic that inhibits STAT3 dimerization[184], significantly blocked proliferation in PEO4, OVSAHO, and OVCA432 cells. This is consistent with previous reports that STAT3 can drive proliferation in HGSOC[185,186].

3.3.4 Evaluating crosstalk between ER and IL-6/STAT signaling

Given that STAT3 inhibition prevented ER-independent cell growth in multiple cell lines, we then compared effects of Stattic in 2-D to those in ULA. There was no difference in potency or maximal efficacy of Stattic between conditions (Fig. 16). Further, response to Stattic was not affected by addition of E2 (Fig. 16). Despite this, we decided to further investigate potential crosstalk between STAT3 and ER signaling based on reports that IL-6-driven STAT3 activity can alter endocrine response[180,187,188]. Rather than asking if E2 treatment affected STAT3 inhibition, we asked whether STAT3 activation affected ER activity.

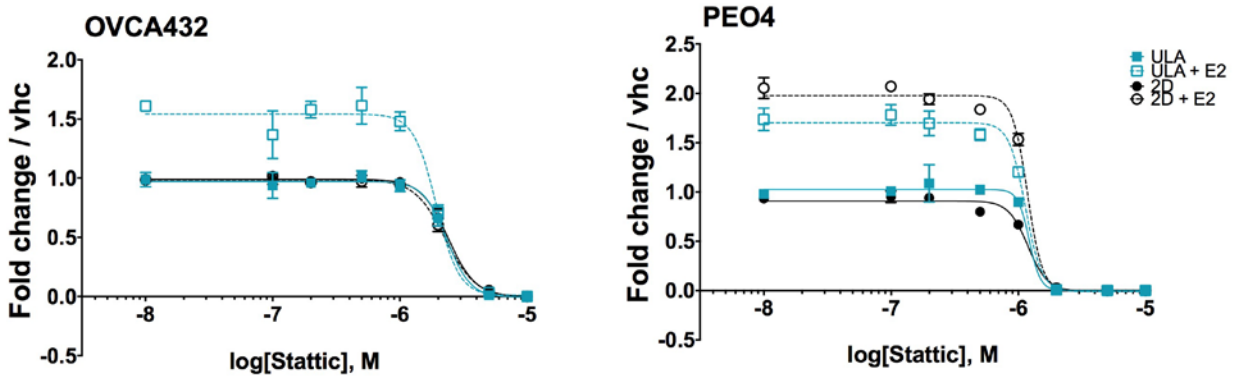

Figure 16: Effect of Stattic on proliferation of OVCA432 and PEO4 cells. Cells were hormone-deprived and treated with increasing doses of Stattic +/- 1 nM E2. Growth was measured after six days by CellTiter-Glo.

Our first approach was to test whether STAT3 activation affected ER-mediated transcription. Thus, PEO1 cells were hormone-deprived and subsequently treated with increasing doses of IL-6 or E2 for 24 hours. Treatment with 10 ng/mL IL-6 significantly enhanced E2-induced expression of GREB1 and DEPTOR in PEO1 cells (Fig 17A). In light of this, we expected that IL-6 stimulation would enhance E2-stimulated growth in HGSOC cells. However, IL-6 had no effect on E2-stimulated proliferation of PEO1 cells in 2-D (Fig. 17B). We also hypothesized that IL-6 mediated STAT3 induction led to increased activation of ER. To

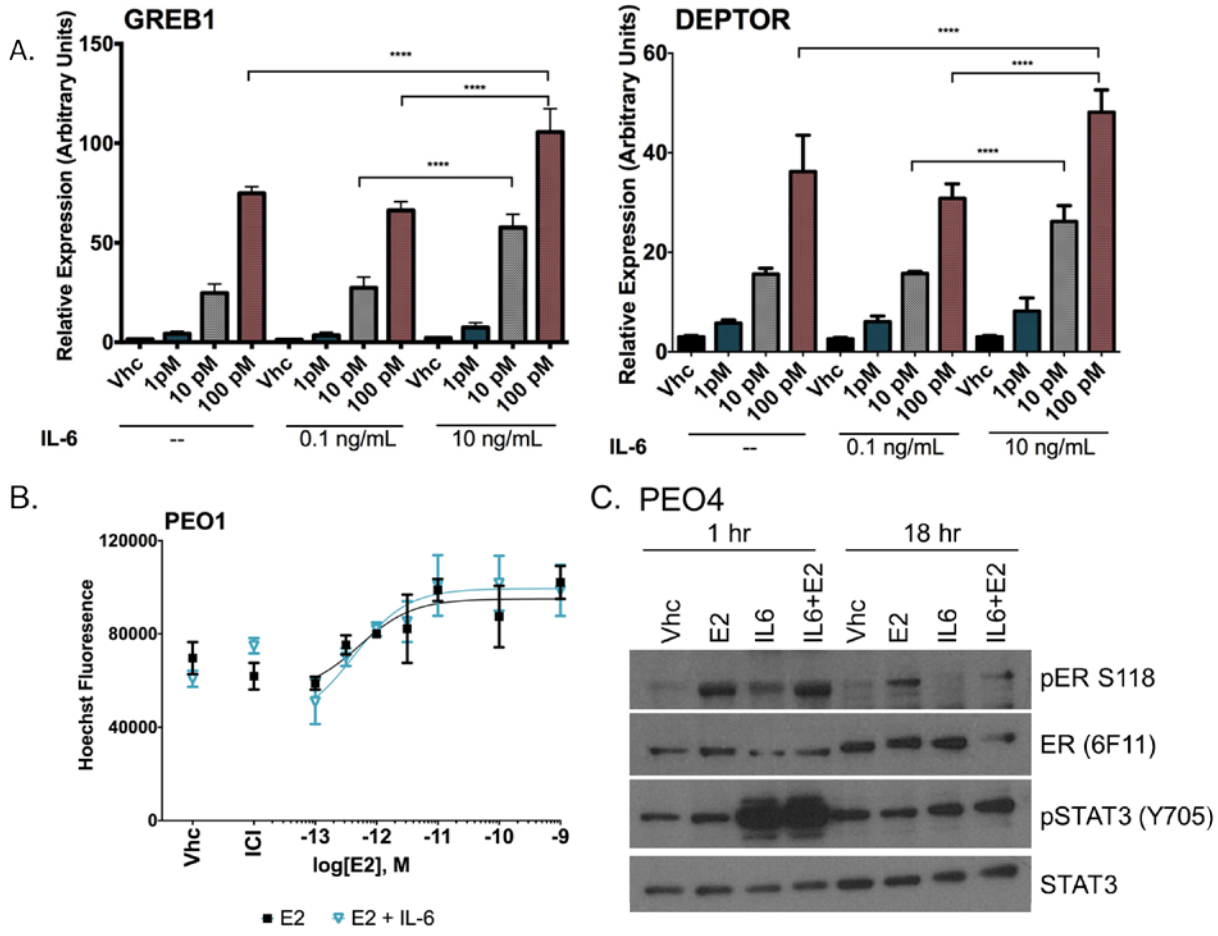

Figure 17: Potential crosstalk between IL-6/STAT3 and ER in HGSOC. A. Effects of IL-6 treatment on E2-mediated gene expression. Hormone-deprived PEO1 cells were treated with increasing doses of E2 or IL-6 as indicated. Gene expression was measured by qRT-PCR 24 hours after treatment. B. Effects of IL-6 on E2-stimulated growth. PEO1 cells were hormone-deprived and treated with increasing concentrations of E2 +/- 10 ng/mL IL-6. Growth was measured by FluoReporter after six days. C. Effects of IL-6 on ER phosphorylation. Cells were treated with 1 nM E2, 10 ng/mL IL-6, or the combination for 1 or 18 hours as indicated.

evaluate this, we measured phosphorylation of ER at S118. Cells were hormone-deprived and treated with vhc, E2, IL-6, or the combination for 1 or 18 hours. IL-6 treatment induced STAT3 phosphorylation and had no effect on ER phosphorylation (Fig. 17C). However, we have not yet evaluated the effect of IL-6 on other phosphorylation sites (e.g. S167) or on E2-mediated growth in ULA. It is possible that ER and IL-6/STAT3 crosstalk in these contexts.

3.4 DISCUSSION

The heterogeneous response to endocrine therapy in ovarian cancer imparts a need to understand mediators of ER signaling as both biomarkers of response and potential nodes for combination therapy. In Chapter 2, we described identification of ERTGs that reflected active ER signaling. Herein, we sought to understand how these target genes and other potential effectors (e.g. kinase signaling cascades) affected E2-driven growth and survival in HGSOC.

Endocrine response in HGSOC cells changes based on three-dimensional context, specifically in ultra-low attachment versus adherent conditions (Chapter 2). This corresponded with increased ER levels in ULA compared to 2-D. This was due to upregulation of ESR1 at the mRNA level. We postulated that increased ER expression would lead to increased ER transcriptional activity, which would help us identify drivers of E2-driven proliferation. Surprisingly, we observed very few changes in E2-regulated gene expression between 2-D and ULA, even in OVCA432 and OVSAHO cells. Among those were GREB1 and SLC22A4. GREB1 is required for ER-mediated proliferation in MCF-7 cells and has recently been identified as a co-factor for ER[188–190]. Thus, one could speculate that GREB1 has the same role in HGSOC. SLC22A4 is a solute carrier and has been implicated in chemotherapy

resistance[191,192]. While SLC22A4 knockdown had no effect on E2-stimulated growth in ULA, we did not evaluate how it affected response to ICI or 4OHT. Importantly, our phenotypic studies were limited to growth assays in ULA. Characterizing the effects of SLC22A4 knockdown on other phenotypes (e.g. 2-D growth, spheroid formation, *in vivo* growth, potency of E2 [EC50]) will be critical before ruling out a role for it in endocrine responsiveness. Additionally, we did not evaluate the role of GREB1. This should be an avenue for future study.

The context-dependent change in endocrine response also suggests that ER may interact with the cell membrane or with cytoplasmic signaling components. To assess this potential signaling, we performed a small screen of targeted agents in hormone-deprived cells. This screen suggested that inhibiting STAT3 completely abrogates E2-independent growth in HGSOC cells. Further, STAT3 inhibition blocked growth equally well in the presence of E2. The dependence on STAT3 was intriguing because STAT3 activation has been demonstrated into induce tamoxifen resistance in ovarian cancer cell lines[181]. IL-6 stimulation, which leads to phosphorylation of STAT3, enhanced ER-induced expression of GREB1 and DEPTOR. IL-6 treatment alone had no effect on expression of either gene, suggesting IL-6 treatment is somehow modulating ER signaling. However, IL-6 treatment had no effect on ER phosphorylation at S118. IL-6/STAT3 pathway activation could have stimulated ER phosphorylation at an alternative site (e.g. S167, S305) and this should be investigated further. Moreover, lack of changes in ER phosphorylation does not rule out the possibility that these two signaling pathways could be interacting at the DNA-binding level. To this point, STAT3 has been previously shown to modulate GREB1 expression in MCF-7 cells[188]. Additional studies such as ChIP re-ChIP assays would help determine if STAT3 is recruited to the same DNA binding sites as ER upon co-stimulation with E2 and IL-6. Further, RNA-seq analysis after

treatment with E2, IL-6, or the combination could identify additional genes that are synergistically regulated by E2 and IL-6. Notably, however, co-stimulation did not affect E2-driven proliferation in 2-D. Future studies should first evaluate effect of IL-6 on other E2-driven phenotypes such as growth in ULA before delving into mechanistic analyses.

Our inhibitor screen identified several other pathways that may interact with ER in HGSOC cells as well and thus could be possible targets for combination therapy. Notably, Saracatinib, which inhibits Src, was very effective at blocking growth of OVCA432 cells and partially inhibited growth of PEO4 and OVSAHO cells. Src has been reported to promote fulvestrant resistance in PEO1 cells via direct interaction with ER, which leads to its sequestration in the cytoplasm[141]. Future studies should expand upon potential interplay between Src and ER and the role of Src as a driver of endocrine resistance. Additionally, experiments such as reverse phase protein arrays (RPPA) will provide more insight into potential drivers of E2-independent growth in HGSOC and create a comprehensive picture of changes in ER signaling in different contexts. Similarly, ER localization should be evaluated after treatment with E2, ICI, or 4OHT in both 2-D and ULA.

Another important area of future investigation is estrogen metabolism. Several groups have reported expression of aromatase, which produces estradiol, in epithelial ovarian tumors[193–196]. Further, estrone sulfatase activity has been detected in advanced stage ovarian tumors and correlated with worse outcome[197]. Intratumor estrogen metabolism could have significant implications for endocrine therapy. One could speculate that tumors expressing steroidogenic enzymes may be more hormonally driven. Alternatively, ovarian tumors lacking steroidogenic enzymes or the enzymes necessary to convert estrone into the more potent ligand estradiol may be less endocrine responsive. Future studies should investigate expression and activity of

enzymes such as aromatase, estrone sulfotransferase, and steroid sulphatase in clinical specimens. Further, expression and activity of these enzymes should be compared across preclinical models to assess their potential contributions to endocrine responsiveness.

In summary, we determined that IL-6/STAT3 activation might interact with ER signaling; however, the phenotypic consequences of this crosstalk remain unclear. Larger-scale studies such as RNA-seq and RPPA will be necessary to fully understand this crosstalk and elucidate other effectors of endocrine response and resistance in HGSOC.

4.0 EVOLUTION OF ESTROGEN SIGNALING IN THE PROGRESSION FROM ENDOMETRIOSIS TO ENDOMETRIOSIS-ASSOCIATED OVARIAN CANCER

4.1 INTRODUCTION

Endometriosis is a common condition, affecting 6-10% of women of reproductive age and 35-50% of women with infertility[198,199]. It is defined as presence of endometrial glands at extra-uterine sites, frequently in the pelvis[199]. While endometriosis is regarded largely as a benign condition, endometriotic lesions can undergo transformation to specific subtypes of invasive ovarian cancer[16,200]. Illustrating this, a pooled analysis of case-control studies revealed odds ratios of 3.05, 2.11, and 2.04 for the development of clear cell (CCC), endometrioid (ENOC), and low-grade serous ovarian cancers for patients with a self-reported history of endometriosis compared to those without[201]. Further, approximately 60-80% of CCC and ENOCs present in the setting of atypical endometriosis. As such, these subtypes are often referred to as endometriosis-associated ovarian cancers (EAOC). However, the mechanisms underlying the progression from endometriosis to EAOC are poorly understood.

Identifying biomarkers and pathways associated with the transition from endometriosis to cancer is an active area of research. Recent reports have identified differences in microRNAs profiles between healthy patients, those with endometriosis, and those with EAOC[202]. Immunologic pathways, particularly the complement cascade, have also been implicated as a

factor in the transformation from endometriosis to EAOC[203]. One pathway that has been understudied to date, however, is estrogen signaling

Estrogen is a known driver of endometriosis, contributing to both proliferation of the ectopic uterine tissue and inflammatory response[199,204]. Hormonal therapy (e.g. estrogen-progestin contraceptives or GnRH agonists) is typically prescribed to regulate proliferation of endometriotic implants[199]. Estrogen has also been implicated in ovarian cancer progression (e.g. through hormone-replacement therapy use, discussed in Chapter 1.0), particularly for the endometrioid subtype. Taken together, these clinical observations suggest that estrogen may contribute to progression of endometriosis to EAOC.

Here we investigate estrogen signaling during the progression of endometriosis into EAOC using a cohort of tissue samples from healthy controls, patients with both benign and atypical endometriosis, patients with endometriosis diagnosed concurrently with ovarian cancer, and patients with EAOC. Using a comprehensive gene signature of estrogen response (the E2sig), we identified gene expression changes associated with each disease state. Understanding changes in estrogen signaling during disease progression will help determine if ER is a putative driver of transformation from endometriosis to EAOC.

4.2 MATERIALS AND METHODS

4.2.1 Clinical specimens

Clinical specimens were shared with us by Dr. Anda Vlad's lab. Tissue samples were obtained from patients at the University of Pittsburgh Medical Center undergoing pelvic surgery for

indications including fibroids, pelvic pain, endometriosis, pelvic mass, and confirmed or suspected ovarian malignancy. Tissue inclusion was contingent upon adequate samples of benign endometriosis, atypical endometriosis, endometriosis within the vicinity of an EAOC collected at the time of primary surgery (referred to herein as "concurrent endometriosis"), or endometriosis-associated cancers (clear cell or endometrioid ovarian cancer) as determined by a pathologist (E.E.). "Concurrent" cancers were defined as any epithelial ovarian cancer with endometriosis identified within the pathologic specimen following surgical resection. Dr. Vlad's lab also procured samples of normal endometrium from patients without a diagnosis of endometriosis or cancer to use as controls. All tissue samples underwent an independent pathology review by a staff pathologist prior to inclusion in this study. Corresponding patient demographic characteristics, clinical disease characteristics, and treatment factors were abstracted from patient charts. All work was approved by the Institutional Review Board (IRB) at the University of Pittsburgh.

4.2.2 RNA extraction and NanoString analysis

FFPE sections were processed using the RNEasy FFPE Kit (Qiagen) by Dr. Swati Suryawanshi according to the manufacturer's instructions. Expression of the E2sig (described in Chapter 2) was measured using a custom code set for the NanoString nCounter platform. RNA (100 ng) was prepared for NanoString analysis according to the manufacturer's protocol. Data were normalized to internal positive controls and to the geometric mean of five housekeeping genes. Additional details of the analysis are provided below under "statistical analysis."

4.2.3 Immunohistochemistry

Immunohistochemistry (IHC) for both ER (SP-1 clone) and FGF18 (Sigma, used at 1:500) was performed by the Department of Pathology at Magee-Womens Hospital of the University of Pittsburgh Medical Center. Stained slides were then reviewed and scored by a staff pathologist (E.E.). ER staining was quantified by H-scoring.

4.2.4 Statistical analysis

Gene expression for each sample was normalized to the mean expression of that gene in the normal endometrium. To identify genes differentially expressed across the four tissue types, we performed ANOVA with a significance cut-off of $q<0.05$. The 158 genes identified by ANOVA were used for the remaining statistical analysis.

For comparisons to preclinical profiles of hormone receptor signaling, we utilized publicly available data from the Gene Expression Omnibus (GEO). For ER signaling, we used the following studies: GSE50695, GSE3529, GSE22600, and GSE38234. For ERβ signaling we used GSE1153 and GSE42347; for PR, GSE46715. Hormonally regulated genes were classified as those significantly altered by treatment compared to vehicle control. The heat map show log2 fold change (hormone vs. vehicle). Statistical analysis was performed by Tianzhou (Charles) Ma.

4.2.5 Gene set enrichment analysis (GSEA)

GSEA was performed by Dr. Matthew Sikora. To evaluate signatures similar to the E2sig, all 236 genes were overlapped against gene sets in the C2 (curated gene set) collection of the molecular signatures database (MsigDB). To identify gene signatures activated in EAOC, up-regulated and down-regulated in EAOC relative to normal endometrium were compared to a cancer-specific subset of gene sets in MsigDB C2. Up-regulated genes comprised those in clusters 1 and 2 (Fig. 18); down-regulated genes were those in clusters 3 and 4.

4.3 RESULTS

4.3.1 Identification of differentially expressed genes between normal, endometriosis, and cancer tissues

We evaluated 83 samples from patients with benign endometriosis (n=19), which includes both ovarian (n=11) and non-ovarian endometriosis (n=8); atypical endometriosis (n=11); concurrent endometriosis (n=9); and EAOCs (n=21). Also included were 23 samples of normal endometrium with an equal distribution between the proliferative and secretory phases. The sociodemographic and disease characteristics of this patient cohort are summarized in Table 8. Not surprisingly, the patients with concurrent endometriosis and EAOC were older than those with benign and atypical endometriosis (median age of 70 and 57.5 versus 39 and 47 years old, respectively). The majority of patients with EAOC presented at an early stage (15 patients, 71%) and had tumors of endometrioid and clear cell histologies (14, 66% and 5, 24% respectively).

The majority of patients with endometriosis were premenopausal while the majority of patients with EAOC were postmenopausal at the time of surgery.

To profile estrogen signaling in patient samples, we analyzed expression of the E2sig. The E2sig is a 236-gene panel genes identified by a meta-analysis of estrogen-regulated genes across breast, ovarian, endometrial, and bone cancer (described in Chapter 2.2.9).

Table 8: Overview of patients with endometriosis or EAOC[†]

	Benign endo. (n=19)	**Atyp. endo. (n=11)**	**Con. endo. (n=9)**	**EAOC (n=21)**
Median age (range)	39 (25-74)	47 (34-50)	70 (49-75)	57.5 (47-77)
Body mass index	27.6	30.6	27.4	29.6
Menopausal status				
Premenopausal	10	7	2	2
Postmenopausal	1	1	3	11
Unknown	8	3	3	8
Cancer stage	N/A	N/A	(concurrent)	
Early (I-II)				15 (71%)
Late (III-IV)				6 (29%)
Tumor histology	N/A	N/A	(concurrent)	
Clear Cell				5 (24%)
Endometrioid				14 (66%)
Serous				1 (5%)
Adenocarcinoma NOS				1 (5%)

Given the discrepancy in age between endometriosis and cancer patients, we first evaluated if expression of the E2sig changed based on menopausal status. To do this, we compared expression of the entire gene set across samples from normal endometrium. Pre-menopausal and post-menopausal patients did not cluster separately (Appendix F). Further, a t-

[†] Clinical data were compiled by Dr. Michelle Boisen and Dr. Swati Suryawanshi

test comparison identified no genes significantly different between these two groups. Thus, any changes observed in expression are likely due to differences in tissue biology rather than hormonal status of the patient.

We next evaluated how estrogen signaling changes during the progression from benign endometriosis to EAOC. ANOVA identified 158 genes with significantly different ($q<0.05$) expression between different disease states and these genes separated into four distinct clusters (Fig. 18A). Expression of genes in cluster 1 (C1, n=37) is higher endometriosis specimens compared to normal endometrium and highest in EAOC (e.g. FGF18, ESR2). Cluster 2 (C2, n=60) represents genes that are highly expressed in the EAOC specimens compared to all endometriosis specimens and includes MUC1, PAX8, TP53, and NRIP1. Cluster 3 (C3, n=20)

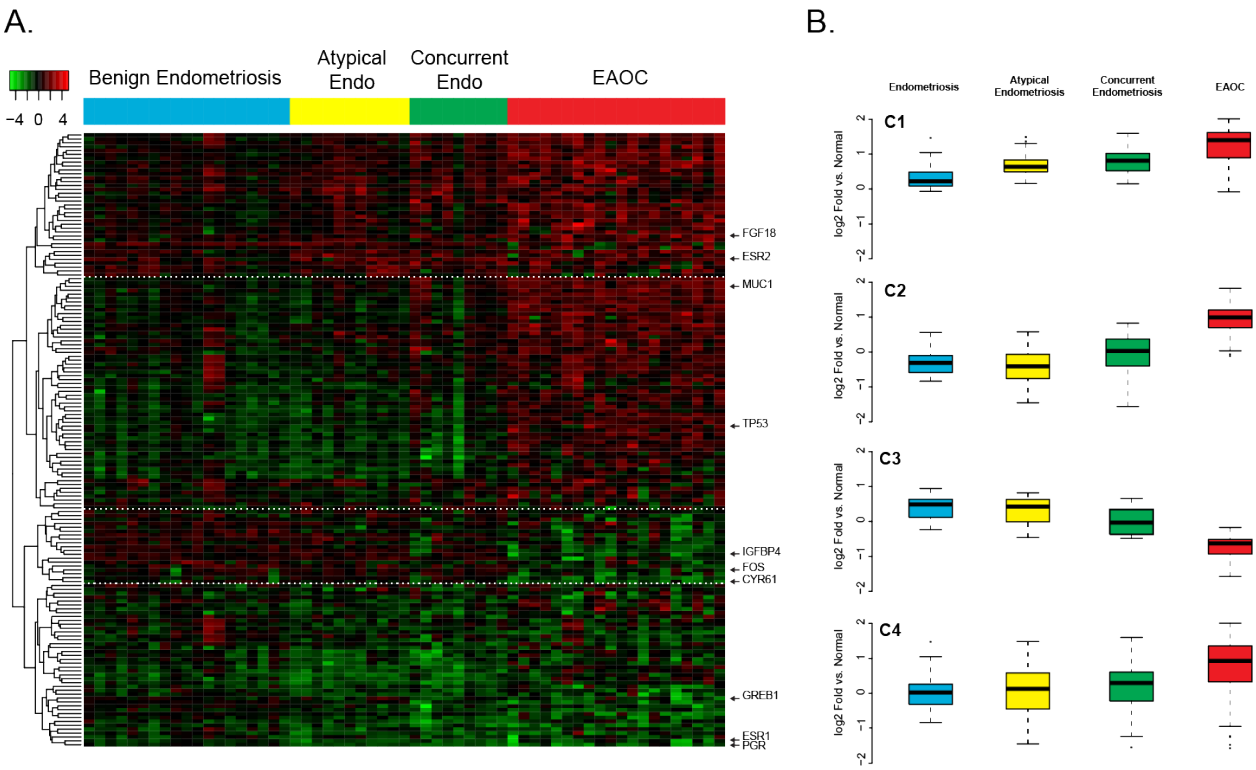

Figure 18: Differentially expressed genes between endometriosis and EAOC. A. ANOVA identified 158 genes of the E2sig with significantly ($q<0.05$) different expression between normal endometrium, endometriosis, and endometriosis-associated cancers. Unsupervised clustering reveals four distinct gene clusters. B. Average expression of gene clusters across tissue types. Differential expression analysis was performed by Tianzhou Ma.

comprises genes that are more highly expressed in endometriosis tissue than in the EAOC and includes IGFBP4 and FOS. The final cluster (C4, n=41) consists of genes that are expressed at lower levels in both endometriosis and EAOC than in normal endometrium and includes GREB1, ESR1, and PGR. The full list of genes in each cluster is provided in Appendix F.

4.3.2 Changes in hormone receptor expression and canonical ER signaling in EAOC

The ANOVA results identified significant changes in expression of the hormone receptors ER (ESR1), ERβ (ESR2), and progesterone receptor (PGR). Expression of ESR2 increases incrementally from normal endometriosis to EAOC (Fig. 19). Conversely, PGR expression decreases from normal endometriosis to EAOC. ESR1 expression is decreased in benign and atypical endometriosis but increases again in EAOC.

We further investigated ER expression by immunohistochemistry. This also suggested a decrease from benign endometriosis to EAOC (Fig. 20); median H-score decreased in intensity from normal endometrium to benign endometriosis to EAOC and had a modest but significant correlation (corr=0.43, p=0.016) with ESR1 levels.

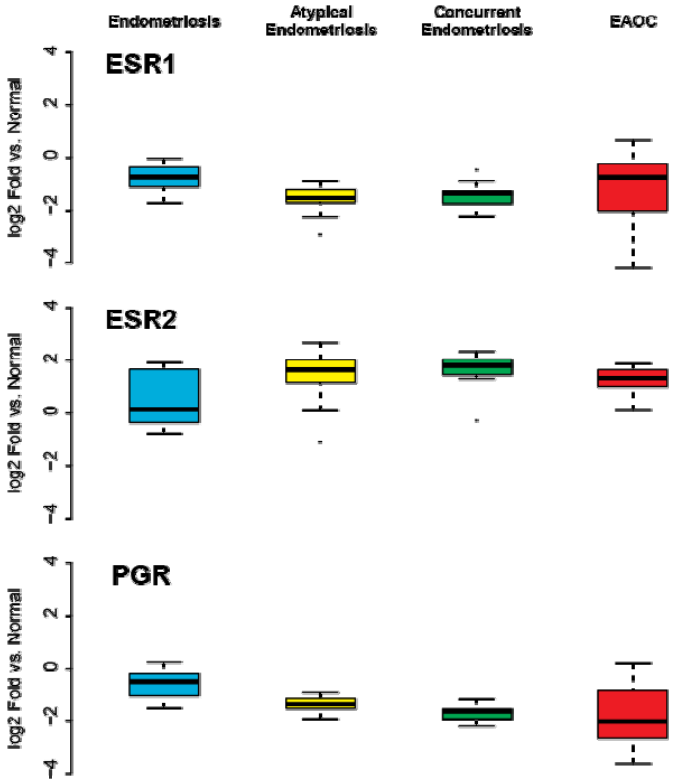

Figure 19: Hormone receptor expression in endometriosis and EAOC. Expression of ESR1, ESR2, and PGR as measured by NanoString.

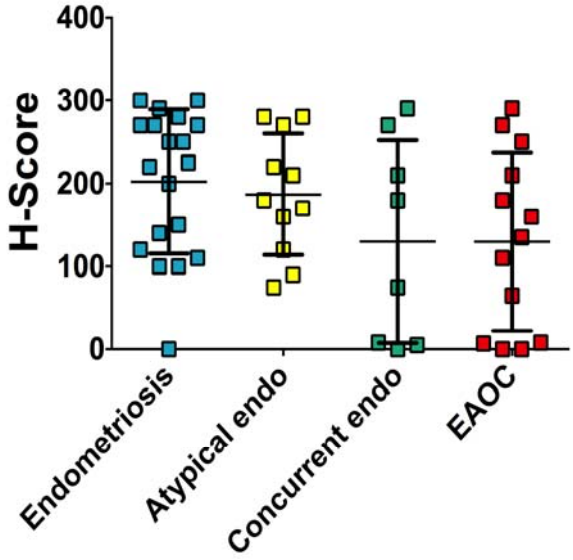

Figure 20: ER H-scores in endometriosis and EAOC. ER expression in clinical samples was evaluated by IHC and H-scoring. H-scoring was performed by Dr. Esther Elishaev.

We next asked if gene expression patterns in EAOC represented active ER signaling. To do this, we compared expression of the 158 differentially expressed (DE) genes to four gene expression studies of estrogen treatment in breast cancer cell lines, ovarian cancer cell lines, and endometrial cancer cell lines[132,165,205,206]. We also included one study of gene expression in MCF7 breast cancer cells performed in our lab (Appendix B). This comparison revealed that some components of canonical ER signaling are maintained in EAOC (Fig. 21), including high expression of NRIP1. However, much of canonical gene regulation is deactivated, as indicated by the decrease of GREB1 and PGR. The same analysis was performed comparing our cohort to profiles of ERβ and PGR signaling; no similarities were found between our data and these signatures (data not shown)[110,111,207].

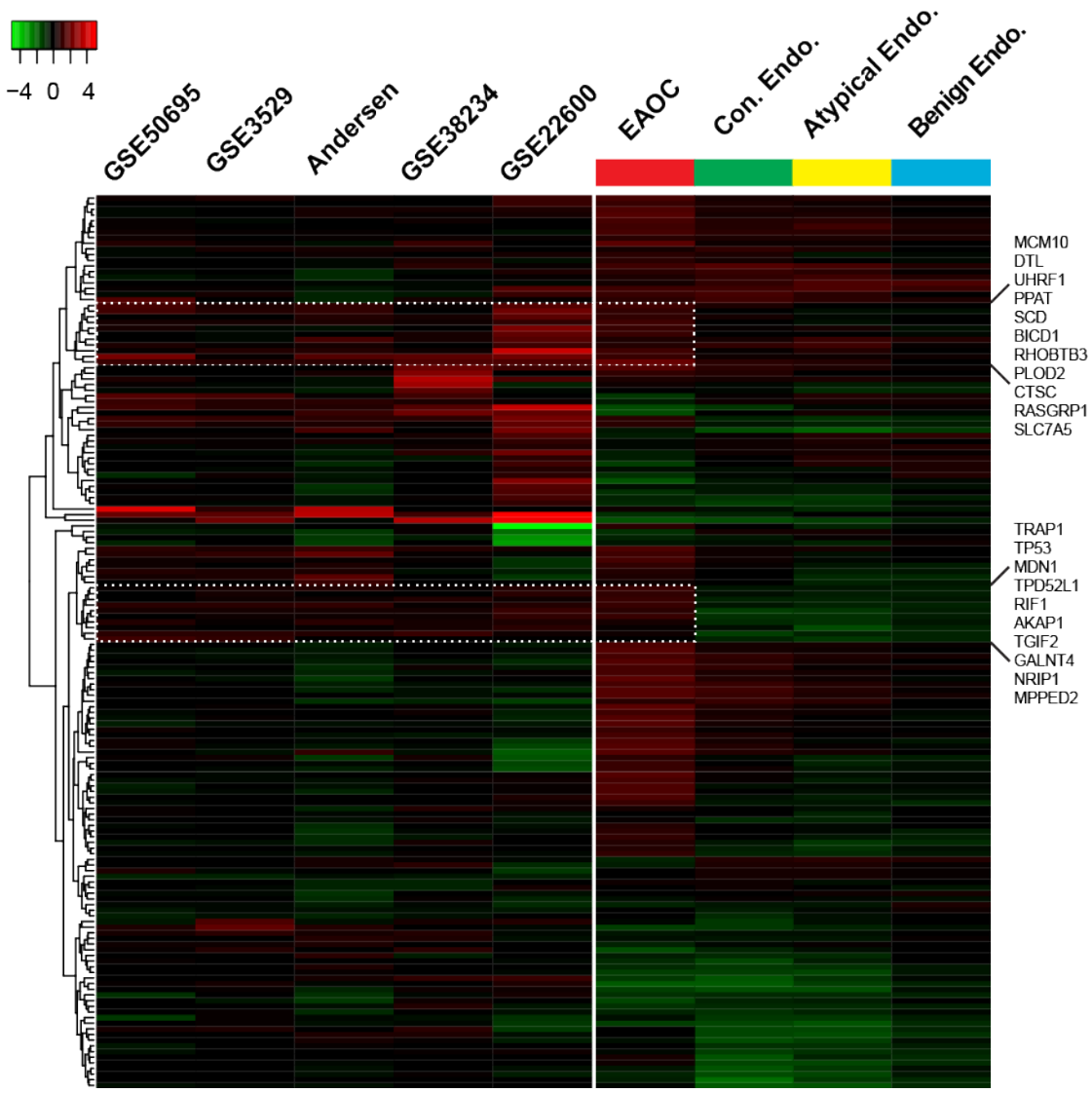

Figure 21: Expression profiles of endometriosis and EAOC tissues compared to ER signaling in preclinical cancer models. Gene expression of our cohort was compared to expression data from five studies following estrogen treatment in breast cancer (GSE50695, GSE3529, Andersen), ovarian cancer (GSE22600), and endometrial cancer (GSE28234) cell lines. Cell line studies are colored by FC of E2 treatment vs. vehicle control, patient samples FC vs. normal. Analysis was performed by Tianzhou Ma.

Since the preclinical studies in GEO specifically represent activated ER in cancer, we performed Gene Set Enrichment analysis (GSEA) against the Molecular Signatures Database (MSigDB) to evaluate ER signaling in a more unbiased manner (Fig.21). GSEA identified

extensive overlap with ER signaling signatures, consistent with the signature design. Despite this initial enrichment, however, GSEA did not identify any activated ER-related signatures among genes over-expressed in EAOC compared to normal endometrium. Conversely, among under-expressed genes in EAOC vs. normal endometrium, GSEA identified signatures related to endocrine resistance and loss of ER function where these genes were similarly under-expressed. These observations suggest that, consistent with decreased ER expression, EAOC inactivate canonical ER signaling, and may actively transition to an ER-independent phenotype.

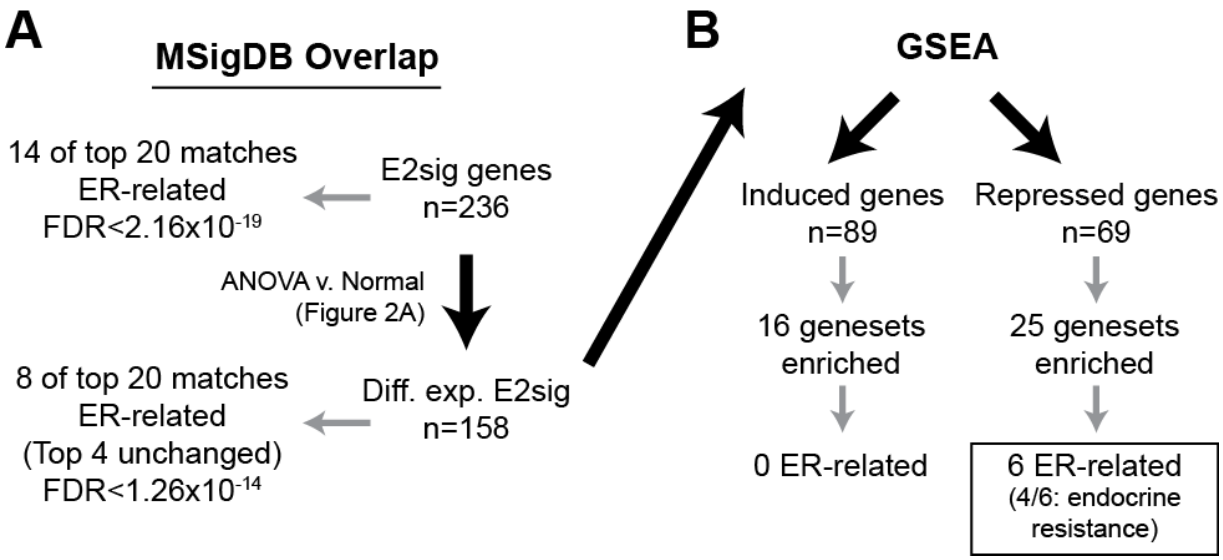

Figure 22: Consort diagram for GSEA. A. Genes from the E2-signature were overlapped against gene sets in the C2 collection (irrespective of expression changes). B. GSEA was performed using a focused subset of the C2 collection (see Methods); multiple comparisons corrections were omitted due to the small size of the gene list. GSEA was performed by Dr. M. Sikora.

4.3.3 High expression of FGF18 in EAOC

Given this shift in ER signaling, genes most highly expressed in EAOC (C1 and C2) likely represent de-repressed ER targets. To this point, among genes in cluster C2 is IGFBP3, which is

a known ER-repressed target in ovarian cancer[168]. De-repression of these genes may impact tumorigenesis; for example, FGF18 (cluster 1) overexpression has recently been identified as a poor prognostic marker in HGS ovarian cancer[208]. FGF18 also modulates migration and invasion of ovarian cancer cells[208]. In our cohort, FGF18 mRNA expression increased with increasing malignancy of the disease state (Fig, 23). In light of these observations, we further investigated expression of FGF18 in EAOCs by immunohistochemistry. FGF18 was highly expressed in a subset of EAOCs (Fig. 23). Given its demonstrated role in HGSOC and elevated expression in EAOC, de-repression of FGF18 may promote EAOC progression.

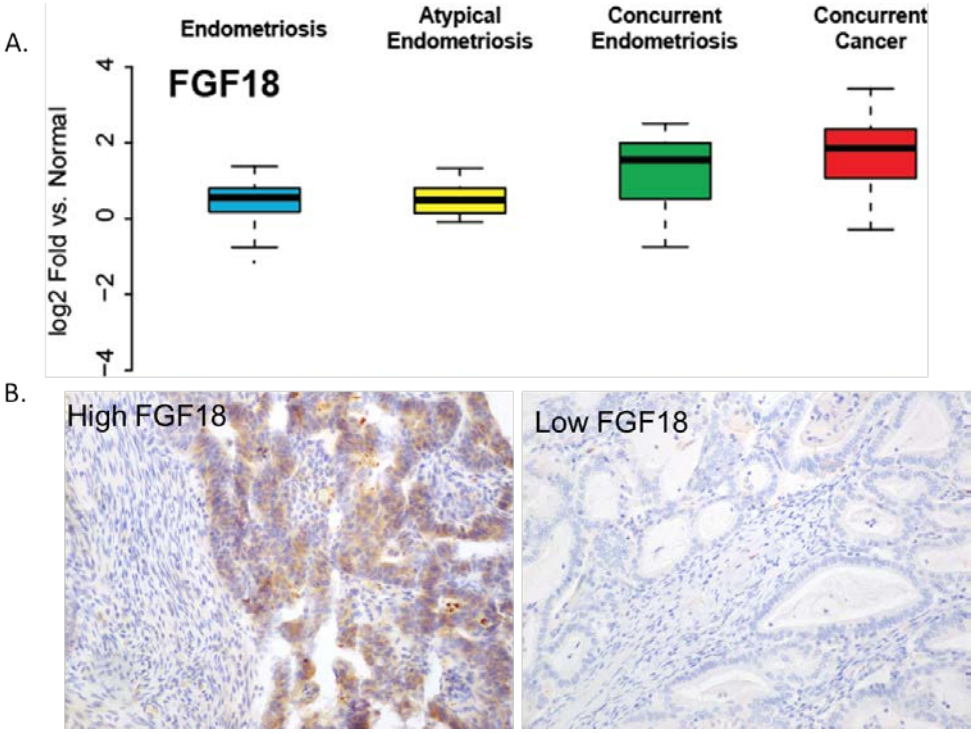

Figure 23: FGF18 expression in endometriosis and EAOC. A. FGF18 expression across different tissue types. B. Representative staining of FGF18 in EAOC samples.

4.4 DISCUSSION

Endometriosis and ovarian cancer are both estrogen-responsive disease entities. Given this shared pathway, we investigated how ER signaling evolves during progression from endometriosis to EAOC by profiling a comprehensive signature of estrogen-regulated genes in patient tissue. Surprisingly, our results indicate that canonical ER signaling is largely inactivated during the progression from endometriosis to EAOC; rather, gene expression in EAOC mirrors profiles of estrogen resistance.

The overall loss of canonical ER signaling in the transition from endometriosis to EAOC has not previously been reported. However, this notion is supported by several studies of the complex interplay between hormone receptors in endometriosis. ER and PR levels have been shown to be significantly lower in endometriosis compared to normal endometrium while ERβ was elevated[209]. Further, ERβ was reported to regulate ER in endometriosis-derived stromal cells[210,211]. Knockdown of ERβ in endometriotic stromal cells resulted in increased ER mRNA and protein levels while ERβ overexpression in endometrial stromal cells led to decreased ER. This is particularly intriguing in light of our observation that ESR2 mRNA levels are elevated in EAOC compared to normal endometrium. ERβ is generally thought to be anti-proliferative and to antagonize pro-proliferative effects of ER[212–215]. However, this may be dependent on tissue context. To this point, a study in endometriosis-derived stromal cells reported treatment with E2 significantly increased the proportion of cells in S-phase, which was blocked by siRNA knockdown of ERβ[211]. This suggests that estrogen regulates proliferation in endometriosis through activation of ERβ rather than ER. Further supporting this notion is a recent report of increased ERβ activity in a mouse model of endometriosis. This elevated ERβ activity led to

decreased apoptosis and increased proliferation in ectopic endometriotic lesions[209]. One could postulate that a shift from ER to ERβ signaling could factor into transformation from endometriosis to EAOC. This would be consistent with our finding that canonical ER signaling is largely deactivated in EAOC.

Inactivation of canonical ER signaling is reflected by the decrease in genes such as GREB1, IGFBP4, and PGR. Loss of PR could carry significant consequences for proliferation of these tissues as progesterone signaling abrogates estrogen-induced proliferation of normal endometrium. In addition, progestins have been suggested to have an anti-inflammatory role in the endometrium. In light of this and a recent finding that inflammation factors into progression from endometriosis to EAOC[203], there may be significant overlap between the hormonal regulation and inflammatory regulation of disease progression. Indeed, targeting ER with ligands that also decreased inflammation was shown to block progression of endometriosis in a preclinical model[204]. The interplay between estrogen signaling and inflammation in transformation of endometriosis to EAOC should be a focus of future study,

While components of canonical ER signaling were decreased in EAOC, there was a subset of ER-induced genes that remained highly expressed in EAOC (e.g. NRIP1). NRIP1, which encodes for RIP140, is a nuclear receptor co-regulator. RIP140 has been previously shown to interact with both ERβ and ER in ovarian cancer cell lines to promote proliferation[135]. This observation suggests that activation of these genes despite down-regulation of ER could promote transformation to EAOC.

Another possibility based on the shift in ER signaling is that de-repression of ER target genes promotes EAOC growth and the development of endocrine resistance. Supporting this notion is the increased expression of FGF18 in EAOC. FGF18 is estrogen-repressed in our

HGSOC models (Appendix F) and has previously been described as a driver of tumorigenesis and poor prognostic marker in HGSOC[208]. Our results further support a role for FGF18 as a driver of ovarian tumorigenesis.

Potential interplay between the ERs and FGF18 in the development of EAOCs has not been described in the literature. However, broader FGFR signaling has been implicated in endocrine resistance in breast cancer[165,216–219]. Future investigations should focus on understanding crosstalk between FGF18 and the ERs and on the potential of FGF18 as both a biomarker and therapeutic target.

A limitation of our analyses is that the small cohort of EAOCs did not provide enough power to compare clear cell carcinomas to endometrioid tumors. Previous reports have indicated that only 6% of clear cell tumors express ER and PR, whereas the majority (63%) of endometrioid tumors express both receptors[49,220]. Further endometrioid tumors are reported to have higher expression of ERβ than clear cell tumors[221]. One could postulate that these two histologic subtypes may diverge in their hormone response. However, larger cohorts will be necessary to compare differences in ER signaling between the two groups.

In summary, expression profiles of primary tissue samples suggest ER expression and classical signaling decreases during the progression of endometriosis to EAOC. Several ER-induced genes remain highly expressed in EAOC (e.g. NRIP1) and may contribute to estrogen-dependent EAOC progression. Similarly, de-repression of ER target genes such as FGF18 may facilitate the transformation of endometriosis into EAOC.

5.0 HORMONE RECEPTOR EXPRESSION AND SIGNALING IN OVARIAN TUMORS OF LOW MALIGNANT POTENTIAL

5.1 INTRODUCTION

Ovarian tumors of low malignant potential (LMP), or borderline tumors, are a unique entity defined by atypical epithelial proliferation without stromal invasion[6]. They comprise approximately 15% of all epithelial ovarian tumors and, similar to invasive ovarian cancer, are sub-classified by histology[222]. LMP ovarian tumors carry a favorable with approximately 70% being diagnosed at stage I and a 5-year overall survival of greater than 90%[223]. However, almost 20% of these patients will be diagnosed under the age of 40 and thus fertility conservation becomes a critical consideration during surgical counseling[222].

The primary treatment for LMP tumors is surgical resection. The recurrence risk is 6-36% depending on stage at time of original diagnosis, extent of surgical resection and certain high-risk pathologic features[224–227]. Recurrent tumors are treated again by surgical resection because these tumors are largely unresponsive to cytotoxic chemotherapy[228]. In the same vein, adjuvant chemotherapy does not improve progression-free or overall survival for those diagnosed with more advanced disease[229].

Currently, the ability of LMP tumors to undergo malignant transformation is undetermined. LMP tumors do not constitute a distinct precursor or preinvasive lesion; however,

when patients recur, they can present with secondary LMPs or with invasive tumors. Given that cytotoxic chemotherapy has little effect on late stage and non-resectable recurrent disease, new strategies for adjuvant therapy are needed to prevent recurrence.

Epidemiologic data suggest a role for steroid hormones in the etiology of LMP tumors, as has been previously noted for invasive ovarian cancer (described in Chapter 1). Increasing parity and lactation have been reported to correlate with a reduced risk of LMP tumors[230]; conversely, unopposed estrogen use and obesity correlated with an increased risk of tumor development. Further corroborating this is a recent study demonstrating that >60% of serous LMP tumors demonstrate ER expression and >80% express PR[48]. Studies of endocrine response in ovarian cancer have primarily been conducted with models of invasive ovarian cancer; however, there may still be a role for steroid hormones in the development of ovarian LMP tumors, particularly given the expression of ER and PR. If LMPs have active hormone signaling, they may be treatable with adjuvant endocrine therapy. The objective of the work herein was to investigate the role of hormone receptors in ovarian LMP tumors.

5.2 MATERIALS AND METHODS

5.2.1 Clinical specimens

FFPE tissue samples were procured from patients with ovarian tumors of low malignant potential treated at the University of Pittsburgh Medical Center from 1990-2010. All specimens were obtained from the Health Sciences Tissue Bank at Magee-Womens Hospital of UPMC. Samples were reviewed by a board-certified pathologist to ensure accurate diagnosis and tissue quality for

subsequent molecular analysis. Clinicopathologic data was abstracted from medical charts by Dr. Sarah Taylor. All studies were approved by the University of Pittsburgh Institutional Review Board (IRB).

5.2.2 Immunohistochemistry

Immunohistochemistry was performed by the Department of Pathology at the Magee-Womens Hospital of UPMC. Tissue sections were stained with Ventana CONFRIM anti-ER (SP1), CONFIRM anti-PR (1E2), and ERβ (AbD Serotec) antibodies. ER and PR immunohistochemistry (IHC) was performed using the Ventana BenchMark ULTRA IHC staining module as described by the provider (Ventana Medical Systems, Inc., Tucson, AZ). ERβ-1 was stained using protocol described by Stabile et al.[231]. Briefly, tissue sections were deparaffinized and placed in dH_2O. Diva antigen retrieval was performed (Biocare Medical). Slides were cooled and rinsed in dH_2O, endogenous peroxidase quenched with 3% H_2O_2 and slides placed in working TBS. Slides were incubated with CAS Block (Invitrogen) then with working primary antibody. Slides were washed in TBS buffer, incubated with Mach4 Universal Probe (Biocare Medical). Slides were washed with TBS buffer, incubated with Dako Substrate Chromagen, rinsed in ddH2O and counterstained and dehydrated. Normal ovarian tissue, normal cervical tissue, and invasive breast carcinoma tissue were used as positive controls for ERβ. H-scoring for ER was performed by Dr. Rohit Barghava. Tumors were considered positive or negative for a given hormone receptor based on the following scores: <50, negative; 51-100, weak positive; 101-200, intermediate positive; >200, strong positive.

5.2.3 RNA isolation and NanoString assays

RNA was isolated by Dr. Sarah Taylor from FFPE cores using Qiagen RNeasy Mini Kit. Gene expression of the E2sig was performed using the NanoString nCounter platform as described in Chapter 2.

5.2.4 Statistical Analysis

NanoString data were corrected for an internal positive control and then normalized to the geometric mean of five housekeeping genes using nSolver. Unsupervised hierarchical clustering of NanoString data was performed using the Multiple Experiment Viewer (MeV*)* to identify genes differentially regulated between serous and mucinous LMPs. To determine which of these differences were statistically significant, we used a non-parametric t-test followed by a Bonferroni adjustment for multiple comparisons with a cut-off of $p<0.01$.

5.3 RESULTS

5.3.1 Hormone receptor expression in LMP tumors

Thirty-eight patients were included in this study. Median age at diagnosis was 37.5 (range 18-69). Twenty-six (68.4%) underwent surgical staging at the time of primary surgery. Notably, over half (52.6%) of these patients underwent fertility sparing surgery at the time of initial surgical resection. All patients had stage I disease. The histological subtypes were divided

between 20 serous and 18 mucinous tumors. Average length of follow-up was 48 months (range 1-124). At time of last follow-up, all patients except one were alive. That one patient passed away from recurrent, progressive cervical cancer. Four patients (10.5%) had recurrences during clinical follow-up.

We first evaluated expression of ER, ERβ, and PR by immunohistochemistry and H-scoring (Fig. 24). The median H-score for ER was 135 (range 0-295), ERβ was 20 (0-120), and PR was 85 (range 0-265). When separated by histologic subtype median H-score for the serous subtype was 257.5 for ER (range 90-295), 30 for ERβ (0-120), and 175 for PR (range 15-265). The median H-score for the mucinous subtype was 0 for ER (range 0-150), 0 for ERβ (0-40), and 0 for PR (range 0-170). Based on these scores, all of the serous tumors were ER and PR positive and six of 20 (30%) were ERβ positive. Only one of the 18 mucinous tumors (5.6%) was positive for both ER and PR; all of the mucinous samples were negative for ERβ.

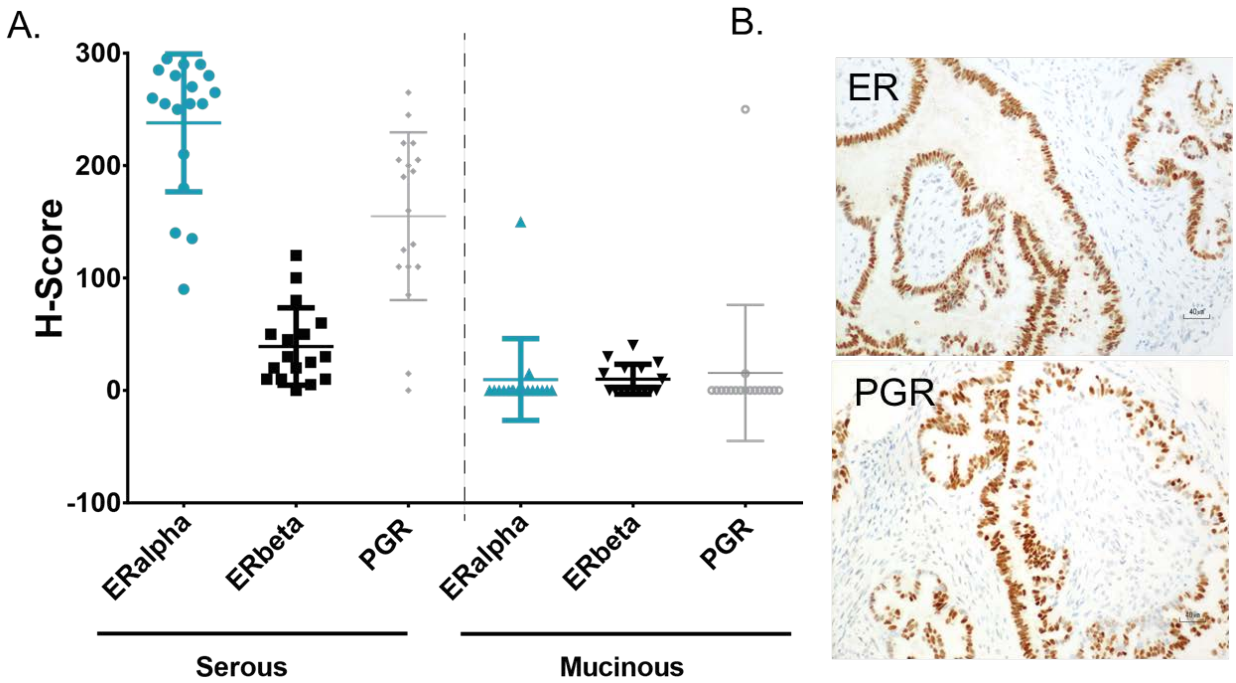

Figure 24: Hormone receptor expression in ovarian LMP tumors. A. H-scores of hormone receptors in serous and mucinous LMPs (determined by Dr. R Bharghava). B. Representative staining of ER and PGR in serous LMPs.

5.3.2 Analysis of ER signaling in LMPs

Based on the differential staining patterns noted between the serous and mucinous subtypes, we sought to better understand hormone receptor expression patterns at the RNA level as well as downstream signaling. To accomplish this, we analyzed mRNA expression of ER, ERβ, PR, and he E2sig (Chapter 2). From the NanoString analysis, ERα and ERβ mRNA expression was found to be mutually exclusive. ERβ mRNA levels were elevated in the mucinous LMP tumors and ERα mRNA expression higher in the serous samples (Fig. 25). We further compared protein expression to mRNA expression. Overall ER protein expression, represented by H-scores, correlated strongly with ER mRNA expression (r^2=0.5606, Fig. 26). PR protein expression correlated with PR mRNA expression (r^2=0.42), even when examined by histologic subtype, serous (r^2=0.74) and mucinous (r^2=0.59) (data not shown). However, ERβ expression did not correlate with mRNA expression of ESR2 (r^2=0.038, not shown).

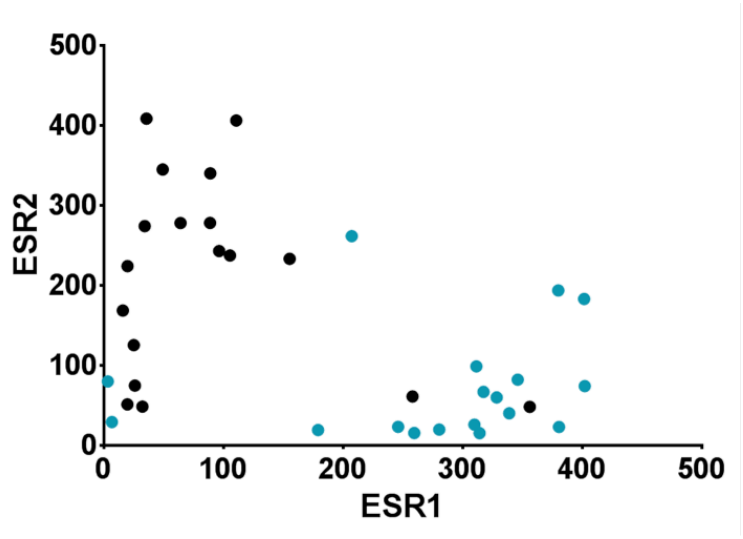

Figure 25: ESR1 and ESR2 are mutually exclusive in LMPs. NanoString data of ESR1 and ESR2 expression in LMP tumors. Blue dots represent serous tumors and black dots represent mucinous.

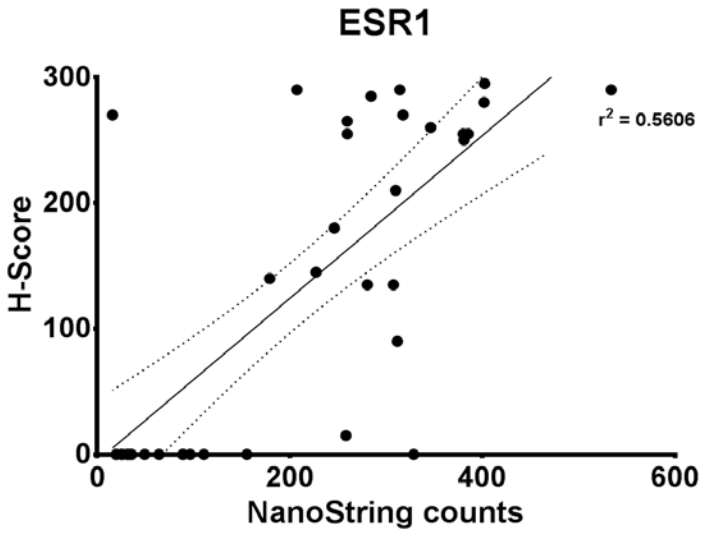

Figure 26: Correlation of ER mRNA and H-score. ER H-score was plotted against the normalized NanoString counts for ESR1 and fit to a linear regression. Solid line shows the best-fit regression and dashed lines show the 95% confidence interval.

Hierarchical clustering of all of the genes in the E2sig revealed a clear separation of serous from mucinous subtypes (Fig. 27). Notably, expression of canonical ER-induced genes (e.g. GREB1, DEPDC6) was higher in the serous subtypes while expression of the co-regulators, (NCOAs and NCORs) was higher in the mucinous subtypes. Upon further investigation, 44 genes showed a statistically significant difference ($p<0.01$) between the serous and mucinous subtypes. Genes higher in the mucinous tumors included PRLR, PRKCD, and TMPRSS2. Genes higher in serous tumors included ESR1, FGF18, and ARL4C.

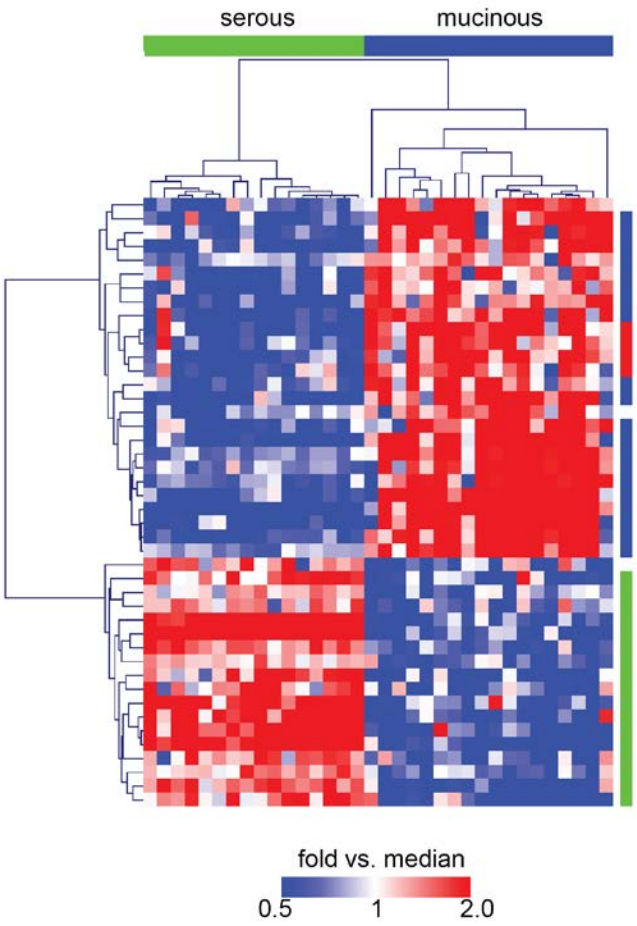

Figure 27: Differentially expressed genes between serous and mucinous LMPs. T-tests followed by Bonferroni correction identified genes in the E2sig with significantly different expression between serous and mucinous LMPs.

5.4 DISCUSSION

Ovarian tumors of low malignant potential are a unique entity that lack an invasive component but have the capacity to recur and possibly become invasive. Given that 70% of these tumors were diagnosed as stage I disease, it is not surprising that all of the samples in this study fell into this category. However, even with this early stage of diagnosis, four patients (10.5%) were noted to have recurrence of disease during their follow-up. Frequently, these tumors are amenable to surgical resection at the time of recurrence. However, LMP tumors exhibit a poor response to chemotherapy, limiting options to treat recurrent disease, which may not be amenable to resection, or advanced stage LMP tumors with high risk of recurrence. Thus, new strategies for adjuvant treatment are critically needed.

Previous case reports have shown that LMP tumors can be successfully treated with endocrine therapy. Additionally, a phase II study of letrozole reported a response rate of 30% in 13 patients with advanced or recurrent low-grade serous carcinoma and low malignant potential tumors[232] and this response correlated with ER/PR status of the tumors. These data suggest that endocrine therapy can be effectively used in the LMP tumor setting. However, a critical step in implementing such a regimen will be prospectively defining the appropriate patient population. Previous reports on hormone receptor expression in LMP tumors suggest that serous and endometrioid subtypes express ER and PR and in turn might benefit from hormonal therapy. In our study, we investigated expression of ER, ERβ, and PR at both the mRNA and protein level. Further, we evaluated ER function by measuring expression of the E2sig.

We found high levels of ER and PR expression in serous LMPs and high expression of downstream ER targets (e.g. GREB1), suggesting that these tumors may have active hormone

signaling. Interestingly, mucinous tumors had significantly higher levels of ERβ mRNA but this did not correlate with high levels of ERβ protein expression when examined by IHC. This finding is intriguing and should be validated by staining with an additional ERβ antibody. If reproducible, this discrepancy could be attributable to post-transcriptional and translational modification and should be an area of future investigation[233,234]. In light of the contrasting, hormone receptor expression, it was surprising that mucinous tumors expressed higher levels of NCOAs and NCORs than serous LMPs. However, we did not assess expression of other nuclear receptors (e.g. androgen receptor, glucocorticoid receptor) which may still be involved in mucinous tumor biology.

Given that mucinous tumors largely did not express ER or PR, the striking differences in gene expression (shown by discrete clustering of serous and mucinous tumors) suggest that this separation is likely more attributable to underlying lineage differences between the two histologies rather than differences in estrogen signaling. Additional large-scale analyses (e.g. genome-wide RNA-seq, RPPA) are warranted to better understand the differences between these two subtypes and identify avenues for targeted therapy in mucinous LMPs.

6.0 DISCUSSION

Ovarian cancer is a rare but often-fatal disease comprised of multiple unique subtypes. To date, ovarian cancer treatment paradigms have been driven by a 'one-size-fits-all' strategy that regards the different histologic types as one unified disease. However, the lack of improvements in patient outcomes over the last four decades[235] and the low response rates to targeted therapies suggest a critical need to implement more personalized strategies.

An often-overlooked strategy for ovarian cancer treatment is targeting ER through endocrine therapy. Endocrine therapy is well-tolerated in patients, has been a tremendous success in breast cancer, and can also be effective in ovarian cancer, indicated by preclinical studies and clinical trials (discussed in Chapters 1 and 2). However, identification of the appropriate ovarian cancer patient population is paramount to its clinical success. Unlike in breast cancer, ER status alone has not proven sufficient to predict endocrine response in ovarian cancer; thus, additional biomarkers are needed.

Our findings suggest that outputs of ER function (e.g. ERTG expression) can be harnessed to identify hormonally responsive ovarian tumors. Implementation of such biomarkers in the clinic could identify patients who are likely to respond to endocrine therapy and ultimately have profound results for ovarian cancer patients. If prospective trials based on our risk score or other biomarkers were successful, this could produce a paradigm shift in ovarian cancer treatment.

Biomarker-driven trials will be challenging, however, given the rarity of the disease (9.4 cases in per 100,000 women for the disease in total[236]), particularly for non-HGSOC tumors. To organize trials of sufficient size and power will require coordination across multiple centers, likely through efforts of cooperative groups such as the Gynecologic Oncology Group.

An important consideration for investigations of endocrine therapy in ovarian cancer will be comparisons of different drug classes. Reports that tamoxifen exposure is associated with lesions in the fallopian tube and ovary[174,237], greater efficacy of ICI versus 4OHT in explant studies (Chapter 2), and the observation that AIs confer less risk for ovarian cancer in ductal carcinoma in situ patients than tamoxifen[76], particular attention should be given to efficacy of SERMs versus other endocrine agents.

An additional consideration for the implementation of endocrine therapy is that intratumor heterogeneity will require endocrine therapy to be combined with another agent to completely abrogate tumor growth. Further, even if endocrine therapy is successful as a single agent, one could envision the emergence of endocrine resistance as is seen in breast cancer[238,239]. Future studies should investigate the mechanism(s) of ER signaling, specifically with regard to crosstalk with other pathways (e.g. STAT3). Effectors and co-factors for ER will identify putative targets for combination treatment with endocrine therapy. Importantly, these studies should be performed and interpreted in subtype-specific contexts.

Such studies will require a more thorough characterization of endocrine response in EAOC and LMP tumors. To date, such studies have been limited by a paucity of representative preclinical models for these disease subtypes. This could be partially alleviated by use of explant models. We derived the explant models for our studies from PDX tumors (Chapter 2) but these could also be derived from primary patient tissue.

Explants provide a unique opportunity to study ER signaling in epithelial ovarian cancer. In addition to serving as a platform to evaluate for drug efficacy, explant models could be used to characterize ER signaling in a more clinically relevant setting. Advances in technology (e.g. RNA-seq, ChIP-Seq, and SILAC) now allow profiling of the transcriptome, cistrome, and proteome from small tissue inputs. This renders these analyses amenable to smaller culture systems such as explants, enabling the rapid evaluation of signaling in primary tissue.

In summary, endocrine therapy is a promising treatment strategy for epithelial ovarian cancer. The studies herein describe identification of a risk score for ER activity in HGSOC, changes in ER signaling during development of ENOC and CCC, and expression of ER and downstream canonical targets in LMP tumors. These studies lay the groundwork for future preclinical investigations of ER signaling in ovarian cancer, which will be enhanced by more sophisticated technologies and disease models. Further, prospective clinical trials taking into consideration markers of ER function may observe better response rates than those which did not use any biomarkers as inclusion criteria. Ultimately, such work may facilitate the use of endocrine therapy as a “personalized medicine” approach to ovarian cancer treatment.

APPENDIX A

PRIMER SEQUENCES

Primer sequences for studies in Chapter 2 and 3 are provided in the table below.

Table 9: Primer sequences

Gene	Forward (5'->3')	Reverse (5'->3')
RPLP0	TAAACCCTGCGTGGCAATC	TTGTCTGCTCCCACAATGAAA
GREB1	GGTTCTTGCCAGATGACAATGG	CTTGGGTTGAGTGGTCAGTTTC
ESR1	GAGTATGATCCTACCAGACCCTTC	CCTGATCATGGAGGGTCAAATC
IGFBP3	CACAGATACCCAGAACTTCTCC	CAGGTGATTCAGTGTGTCTTCC
CCNG2	GTTTGGATCGTTTCAAGGCG	CCTCTCCACAACTCATATCTTCAC
PGR	TCGCCTTAGAAAGTGCTGTC	GCTTGGCTTTCATTTGGAACG
MYC	GCTGCTTAGACGCTGGATTT	GAGTCGTAGTCGAGGTCATAGT
DEPTOR	TTGTGGTGCGAGGAAGTAAG	CCGTTGACAGAGACGACAAA
SLC22A4	ATTCTGTGGAGGAGCTAAA	CCATAGCAGCAAAGACATAA

APPENDIX B

ENDORX PANEL NANOSTRING CODE SET

This appendix provides additional details on the EndoRx panel, which encompasses the E2sig. Genes in the E2sig were identified by a meta-analysis of E2-regulated genes in breast, ovarian, endometrial, and bone cancer (described in section 2.2.9). The lists of studies are provided below. Data from GEO were downloaded, processed, and analyzed by Soumya Luthra and Dr. Uma Chandran.

Table 10: Studies used in the E2sig.

Tissue	GEO DataSet	GEO accession OR 1st author	Platform	Samples used
Bone	GDS884	GSE1153	Affy U95A	U2OS-Era vhc 1+2, U2OS-ERa E2 4h 1+2, U2OS-ERa E2 8h 1+2, U2OS ERa E2 24h 1+2
Bone	GDS1094	GSE2292	Affy Human HG Focus Target	ERa Cont A-F, ERab Cont A-F, ERa E2 A-D, ERab E2 A-E
Bone	GSE21769	GSE21769	Illumina humanWG-6	U2OS_ERa_doxy_rep1-3, U2OS_doxyE2_rep1-3
Bone	NA	Krum	Affy U133 Plus 2.0	http://research4.dfci.harvard.edu/brownlab//datasets/index.php?dir=Krum%20U2OS%20Data/
Bone	NA	Hartmaier	Affy Human Gene 1.0 ST	all
Breast	GSE1045	GSE1045	Affy U133A	WT control A+B, MDA-MB-231 expressing WT ER 1 hr A+B, MDA-MB-231 expressing WT ER 2hr A+B
Breast	GDS3285	GSE11324	Affy U133 Plus 2.0	all

Breast	GDS3217	GSE11352	Affy U133 Plus 2.0	12hr untreated control rep1-3, 12hr E2-treated rep1-3, 24hr untreated rep1-3, 24hr E2-treated rep1-3
Breast	GDS3283	GSE11506	Affy U133 Plus 2.0	all
Breast	GDS1873	GSE2225	Affy U133A	control rep 1-3, estrogen treated rep1-3
Breast	GSE26834	GSE26834	Affy U133A 2.0	SFM control (3hr) rep1-2, E2-treated (3hr) rep1-3, SFM control (24hr) rep 1-3, E2-treated (24hr) rep1-3
Breast	GDS1549	GSE3529	Affy U133A	all
Breast	GDS2770	GSE4006	Affy U133A	Ad+veh rep1+2, Ad+E2 rep1+2
Breast	GDS2367	GSE4025	Affy U133A	Ad+veh rep1+2, Ad+E2 rep1-3
Breast	GDS3105	GSE6800	Affy U133 Plus 2.0	24h_DMSO_1+2, 24h_Estradiol_1+2
Breast	GDS881	GSE848	Affy HG U95A	control A+B, E2 8h A+B
Breast	GDS3315	GSE8597	Affy U133 Plus 2.0	MCF7_EtOH_24_rep-14, MCF7_E2_24h_rep1-4
Breast	GSE3834	GSE3834	Affy U133A and U133A Plus 2.0	All
Breast	NA	NA	Affy U133A 2.0	TCGA
Endometrial	GSE38234	GSE38234	Illumina HiSeq 2000	T47D_DMSO_R1+2, T47D_E2_R1+2, ECC1_DMSO_R1+2, ECC1_E2_R1+2
Endometrial	GDS3604	GSE3013	Affy U95A v 2	EECs from stage I control, Eecs from stage I estrogen, EEC from stage II control, EEC from stage II estrogen -- no replicates
Endometrial	NA	NA	Affy U133A 2.0	TCGA
Endometrial	GSE3762	GSE3762	MRC Human Known Gene Oligo	24h E2 & control -- control data available through ArrayXpress: http://www.ebi.ac.uk/arrayexpress/experiments/E-GEOD-3762
Ovary	GSE22600	GSE22600	Affy U133A 2.0	All
Ovary	NA	Andersen	Affy U133A 2.0	3h E2 and 3H Vhc
Ovary	NA	NA	Affy U133A 2.0	TCGA

The design of the EndoRx panel is described Chapter 2. Table 11 lists all of the genes in the panel and their associated groupings. Selection of the genes in the E2sig is described above. The “endocrine rx” genes were chosen by literature searches for genes associated with endocrine response and resistance. “Immune” genes were chosen based on known roles in immune response. The last set of genes in the code set, “tumor/stroma interactions (McLean GOIs)”,

were added at the request of our collaborator Dr. Karen McLean based on her research interest in the microenvironment and its effect on endocrine therapy response.

Table 11: Genes in the EndoRx NanoString code set

No.	Gene	Annotation
1	ABAT	E2sig
2	ADM	E2sig
3	AKAP1	E2sig
4	ALDH3A2	E2sig
5	ARHGAP26	E2sig
6	ARID1A	E2sig
7	ARID5B	E2sig
8	ARL4C	E2sig
9	ARNTL	E2sig
10	ASB13	E2sig
11	ASCL1	E2sig
12	ATP2A3	E2sig
13	BCAR3	E2sig
14	BCL2L11	E2sig
15	BICD1	E2sig
16	BMP7	E2sig
17	C19orf6	E2sig
18	C1orf116	E2sig
19	C20orf160	E2sig
20	C5orf13	E2sig
21	C6orf89	E2sig
22	CA12	E2sig
23	CA8	E2sig
24	CALD1	E2sig
25	CAMK2D	E2sig
26	CAMSAP1	E2sig
27	CBY1	E2sig
28	CCNG2	E2sig
29	CDC25A	E2sig
30	CDCA7	E2sig
31	CDK6	E2sig
32	CEP68	E2sig
33	CGNL1	E2sig
34	CHN2	E2sig
35	CISH	E2sig
36	CITED2	E2sig
37	CLASP2	E2sig
38	COCH	E2sig

39	CPD	E2sig
40	CTSC	E2sig
41	CUEDC1	E2sig
42	CYB561	E2sig
43	CYP26B1	E2sig
44	CYR61	E2sig
45	DAAM1	E2sig
46	DEPDC6	E2sig
47	DHRS3	E2sig
48	DKK1	E2sig
49	DNAJB4	E2sig
50	DTL	E2sig
51	DUSP1	E2sig
52	EGFR	E2sig
53	EHF	E2sig
54	ENPP5	E2sig
55	EPHA4	E2sig
56	ESR1	E2sig
57	ESR2	E2sig
58	EZR	E2sig
59	FAM174B	E2sig
60	FAM46C	E2sig
61	FBXO32	E2sig
62	FGF18	E2sig
63	FJX1	E2sig
64	FLVCR2	E2sig
65	FOS	E2sig
66	FOXA1	E2sig
67	FZD6	E2sig
68	GALNT10	E2sig
69	GALNT4	E2sig
70	GAS6	E2sig
71	GATA3	E2sig
72	GCLM	E2sig
73	GFRA2	E2sig
74	GINS2	E2sig
75	GNAS	E2sig
76	GREB1	E2sig
77	GSN	E2sig
78	HELLS	E2sig
79	HIP1	E2sig
80	HNF1B	E2sig
81	HOXD3	E2sig
82	ID2	E2sig
83	IFNAR2	E2sig

84	IGFBP3	E2sig
85	IGFBP4	E2sig
86	IGFBP5	E2sig
87	IL12A	E2sig
88	IL24	E2sig
89	INPP4A	E2sig
90	INPP4B	E2sig
91	ITGB4	E2sig
92	ITPK1	E2sig
93	KIAA1217	E2sig
94	KIAA1467	E2sig
95	KLF5	E2sig
96	KRT4	E2sig
97	LEF1	E2sig
98	LIFR	E2sig
99	LIMK2	E2sig
100	LONRF2	E2sig
101	LRP8	E2sig
102	MARCKS	E2sig
103	MBOAT1	E2sig
104	MCM10	E2sig
105	MDN1	E2sig
106	MLPH	E2sig
107	MPP7	E2sig
108	MPPED2	E2sig
109	MPZL2	E2sig
110	MTUS1	E2sig
111	MUC1	E2sig
112	MXD4	E2sig
113	MYB	E2sig
114	MYBL1	E2sig
115	MYC	E2sig
116	MYLIP	E2sig
117	NCF2	E2sig
118	NCOA1	E2sig
119	NCOA2	E2sig
120	NCOA3	E2sig
121	NCOR1	E2sig
122	NCOR2	E2sig
123	NETO2	E2sig
124	NFIA	E2sig
125	NFIB	E2sig
126	NRIP1	E2sig
127	NXT1	E2sig
128	OLFM1	E2sig

129	OLFML3	E2sig
130	ONECUT2	E2sig
131	OSBPL11	E2sig
132	OSBPL3	E2sig
133	OTUB2	E2sig
134	PAX8	E2sig
135	PCDH7	E2sig
136	PDGFRL	E2sig
137	PDK3	E2sig
138	PDZK1	E2sig
139	PGR	E2sig
140	PHLDA1	E2sig
141	PKIB	E2sig
142	PKNOX2	E2sig
143	PKP2	E2sig
144	PLAU	E2sig
145	PLOD2	E2sig
146	PODXL	E2sig
147	POLR3E	E2sig
148	PPAT	E2sig
149	PPP1R3C	E2sig
150	PRKCD	E2sig
151	PRLR	E2sig
152	PSD3	E2sig
153	PTPRE	E2sig
154	PTPRH	E2sig
155	PVT1	E2sig
156	RAB17	E2sig
157	RAI14	E2sig
158	RARA	E2sig
159	RASGRP1	E2sig
160	RBBP8	E2sig
161	RCAN3	E2sig
162	RDX	E2sig
163	REPS2	E2sig
164	RHOBTB3	E2sig
165	RHOF	E2sig
166	RHOQ	E2sig
167	RIF1	E2sig
168	RND3	E2sig
169	RNF144A	E2sig
170	RNF19A	E2sig
171	RNF213	E2sig
172	RNF41	E2sig
173	SAMD4A	E2sig

174	SARDH	E2sig
175	SCD	E2sig
176	SEC14L2	E2sig
177	SEMA3B	E2sig
178	SHB	E2sig
179	SIX1	E2sig
180	SLC22A4	E2sig
181	SLC22A5	E2sig
182	SLC25A29	E2sig
183	SLC2A1	E2sig
184	SLC30A1	E2sig
185	SLC35A3	E2sig
186	SLC35F2	E2sig
187	SLC39A14	E2sig
188	SLC7A2	E2sig
189	SLC7A5	E2sig
190	SLC7A6	E2sig
191	SLC9A3R1	E2sig
192	SMTNL2	E2sig
193	SORBS2	E2sig
194	SOX11	E2sig
195	SPDEF	E2sig
196	STOX2	E2sig
197	SYBU	E2sig
198	SYNJ2	E2sig
199	SYT1	E2sig
200	SYT7	E2sig
201	TANK	E2sig
202	TAP2	E2sig
203	TAPBP	E2sig
204	TBC1D9	E2sig
205	TFF1	E2sig
206	TGFA	E2sig
207	TGIF2	E2sig
208	THBS1	E2sig
209	TIPARP	E2sig
210	TJP3	E2sig
211	TLE3	E2sig
212	TM4SF1	E2sig
213	TMPRSS2	E2sig
214	TP53	E2sig
215	TPBG	E2sig
216	TPD52L1	E2sig
217	TRAF5	E2sig
218	TRAP1	E2sig

219	TRPS1	E2sig
220	TSC22D1	E2sig
221	TSKU	E2sig
222	TSPAN5	E2sig
223	TUBB2A	E2sig
224	TXNIP	E2sig
225	UBE2H	E2sig
226	UHRF1	E2sig
227	USP25	E2sig
228	USP53	E2sig
229	VIM	E2sig
230	WT1	E2sig
231	YPEL2	E2sig
232	YRDC	E2sig
233	ZBTB38	E2sig
234	ZFP36L2	E2sig
235	ZMIZ1	E2sig
236	ZWILCH	E2sig
237	ABL	Endocrine rx
238	AGR2	Endocrine rx
239	AKT1	Endocrine rx
240	AKT3	Endocrine rx
241	AP-1	Endocrine rx
242	ARHGDIA	Endocrine rx
243	BCAR1	Endocrine rx
244	BCL2	Endocrine rx
245	BIK	Endocrine rx
246	ERBB2	Endocrine rx
247	ERBB3	Endocrine rx
248	ESRRG	Endocrine rx
249	FGF17	Endocrine rx
250	FGFR1	Endocrine rx
251	FGFR2	Endocrine rx
252	FGFR4	Endocrine rx
253	HOXB13	Endocrine rx
254	IGF1R	Endocrine rx
255	IL17BR	Endocrine rx
256	IL6	Endocrine rx
257	JNK (MAPK8)	Endocrine rx
258	JUN	Endocrine rx
259	KGF	Endocrine rx
260	KRAS	Endocrine rx
261	MAPK	Endocrine rx
262	MET	Endocrine rx
263	NFKB	Endocrine rx

264	NOTCH1	Endocrine rx
265	NOTCH4	Endocrine rx
266	PAX2	Endocrine rx
267	PDGFRA	Endocrine rx
268	PDGFRB	Endocrine rx
269	PELP1	Endocrine rx
270	PIK3CA	Endocrine rx
271	PTEN	Endocrine rx
272	SF3B3	Endocrine rx
273	SNCG	Endocrine rx
274	SRC	Endocrine rx
275	STAT1	Endocrine rx
276	STAT3	Endocrine rx
277	STC2	Endocrine rx
278	TGFBR2	Endocrine rx
279	USP9X	Endocrine rx
280	WNT4	Endocrine rx
281	ABCF1	HKG
282	OAZ1	HKG
283	RPLP0	HKG
284	SDHA	HKG
285	**ARG1**	Immune
286	BCL2L1	Immune
287	CCL2	Immune
288	CCL22	Immune
289	CCL5	Immune
290	CCR2	Immune
291	CCR4	Immune
292	CCR7	Immune
293	CD3	Immune
294	CD4	Immune
295	CD8	Immune
296	CTLA4	Immune
297	CXCL10	Immune
298	CXCL11	Immune
299	CXCL12	Immune
300	CXCL9	Immune
301	CXCR3	Immune
302	CXCR4	Immune
303	EOMES	Immune
304	FASL	Immune
305	FOXM1	Immune
306	FOXO1	Immune
307	FOXP3	Immune
308	GZMA	Immune

309	GZMB	Immune
310	IDO	Immune
311	IFNG	Immune
312	IL10	Immune
313	IL10RA	Immune
314	IL8	Immune
315	IRF1	Immune
316	LAG-3	Immune
317	NOS2	Immune
318	PD-1	Immune
319	PD-L1	Immune
320	Prf1	Immune
321	PTGS2	Immune
322	RORc	Immune
323	T-bet	Immune
324	Tcf1	Immune
325	TGFB1	Immune
326	TIM-3	Immune
327	TNF	Immune
328	BIRC5/survivin	Tumor / stroma interaction (McLean GOI)
329	BMP2	Tumor / stroma interaction (McLean GOI)
330	BMP4	Tumor / stroma interaction (McLean GOI)
331	BMP6	Tumor / stroma interaction (McLean GOI)
332	CCND1	Tumor / stroma interaction (McLean GOI)
333	CCNE2	Tumor / stroma interaction (McLean GOI)
334	CDH1	Tumor / stroma interaction (McLean GOI)
335	CEBPB	Tumor / stroma interaction (McLean GOI)
336	COL1A1	Tumor / stroma interaction (McLean GOI)
337	DDIT3	Tumor / stroma interaction (McLean GOI)
338	GADD45A	Tumor / stroma interaction (McLean GOI)
339	GP130	Tumor / stroma interaction (McLean GOI)
340	IHH	Tumor / stroma interaction (McLean GOI)
341	IL6R	Tumor / stroma interaction (McLean GOI)
342	LIF	Tumor / stroma interaction (McLean GOI)
343	MMP2	Tumor / stroma interaction (McLean GOI)
344	MMP7	Tumor / stroma interaction (McLean GOI)
345	MMP9	Tumor / stroma interaction (McLean GOI)
346	PAPP-A	Tumor / stroma interaction (McLean GOI)
347	SHH	Tumor / stroma interaction (McLean GOI)
348	SPARC	Tumor / stroma interaction (McLean GOI)
349	TWIST	Tumor / stroma interaction (McLean GOI)

The 207 genes identified by meta-analysis (Fig. 9) were validated *in silico* by supervised clustering of data from METABRIC and van't Veer et al (performed by Soumya Luthra)[240]. E2sig expression was sufficient to separate ER+ from ER- breast tumors (A). We also measured expression of the entire E2sig in PEO4 and MCF7 cells to confirm E2-regulation (B). Cells were hormone-deprived as described in Chapter 2 and treated with vehicle or 1 nM E2 (3 hours for PEO4, 24 hours for MCF7). Heat maps depict fold change vs. vehicle control.

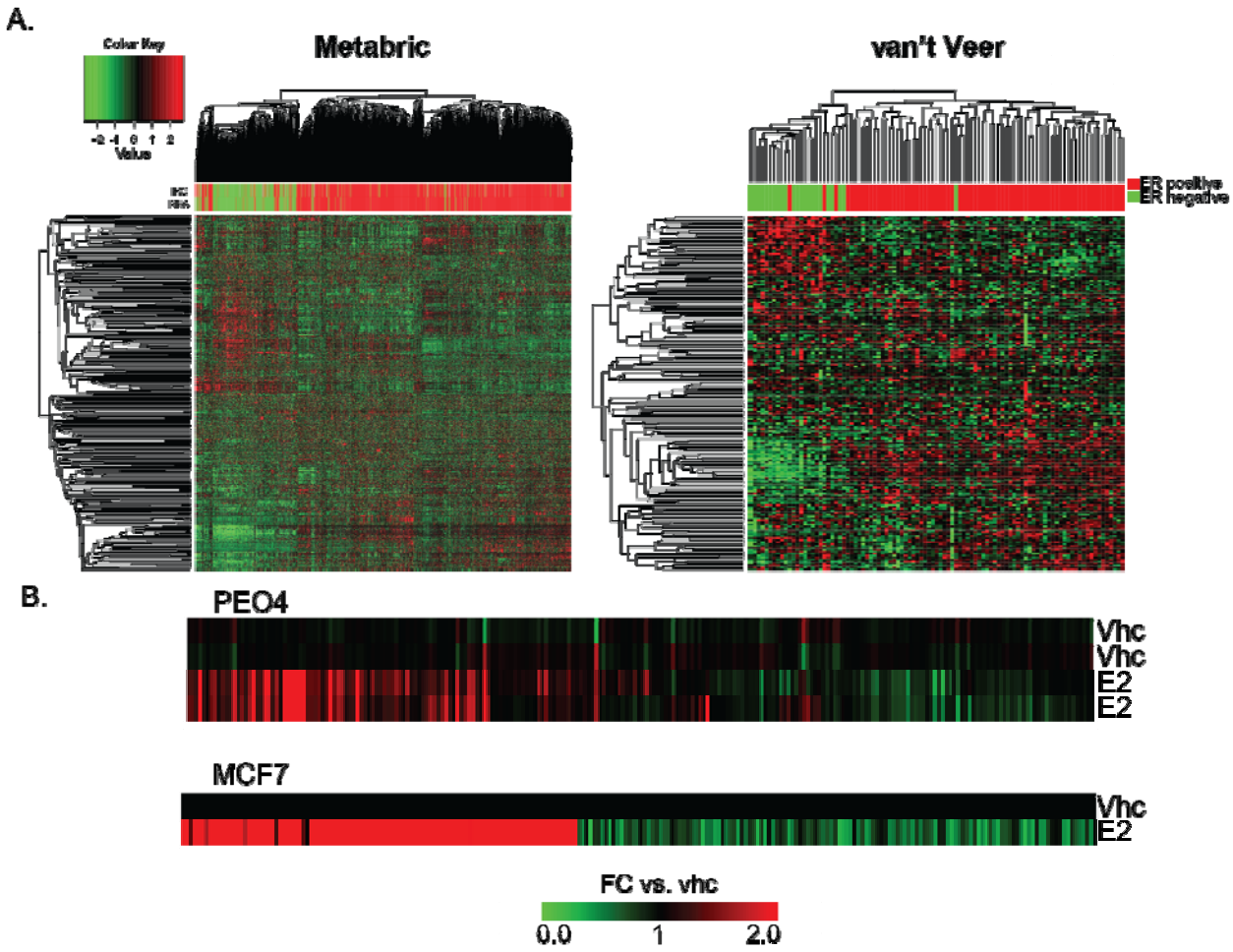

Figure 28: Validation of the E2sig. A. Expression of 207 genes separates ER+ from ER- breast tumors in two independent studies. Analysis performed by S. Luthra. B. Changes in expression of the E2sig after estrogen treatment in PEO4 and MCF-7 cells. Heat maps depict fold change vs. vhc control.

APPENDIX C

E2-REGULATED GENES IN PEO1 AND PEO4 CELLS IDENTIFIED BY MICROARRAY

This appendix contains lists of genes significantly E2-regulated in PEO1 and PEO4 cells identified by microarray studies (described in Chapter 2). Genes are listed in the order corresponding to the heat maps in Fig. 3, Chapter 2. The tables show log2FC vs. vehicle control.

Table 12: Ordered gene lists from PEO1 microarray heat maps in Fig. 3

Symbol	E2	4OHT+E2	4OHT	ICI+E2	ICI
ZNF37BP	0.368	-0.009	-0.055	0.083	0.075
AP3M2	0.216	-0.111	-0.152	-0.022	-0.030
OVOL2	0.305	-0.380	-0.458	-0.163	-0.193
GAL	0.273	-0.009	-0.057	0.069	0.041
OBTB1	0.436	-0.253	-0.369	0.005	-0.118
SLC29A3	0.414	-0.301	-0.386	-0.146	-0.204
SATB2	0.354	-0.240	-0.246	-0.121	-0.166
RHOBTB3	0.570	-0.011	-0.030	0.106	0.051
PLCL2	0.393	-0.129	-0.130	-0.029	-0.077
OLFML3	0.643	-0.296	-0.349	-0.102	-0.230
INHBB	0.457	-0.291	-0.345	-0.147	-0.218
SDPR	0.281	-0.284	-0.273	-0.152	-0.083
IRX5	0.394	-0.269	-0.270	-0.147	-0.108
SLC22A4	0.454	-0.148	-0.122	0.069	-0.067
INPP4B	0.279	-0.028	-0.001	0.079	0.042
PTHLH	0.281	0.030	0.020	0.113	0.084
MECOM	0.494	-0.118	-0.145	0.078	-0.022

HERC1	0.279	-0.088	-0.078	0.056	-0.010
RHOBTB3	0.561	-0.275	-0.170	0.148	-0.078
POLR1E	0.243	-0.075	-0.081	0.068	-0.021
AMPD3	0.213	-0.026	-0.041	0.062	-0.027
TNPO2	0.299	0.091	0.017	0.059	0.077
SMYD2	0.418	0.079	-0.009	0.065	0.046
PDLIM4	0.245	0.034	-0.029	0.017	0.001
PDZK1	0.480	-0.052	-0.135	-0.095	-0.084
OTUB2	0.352	-0.083	-0.185	-0.137	-0.149
PPP1R1A	0.345	-0.031	-0.209	-0.082	-0.132
CACNA1I	0.365	0.059	-0.159	-0.028	-0.069
GLI3	0.262	0.001	-0.127	-0.006	-0.018
CUEDC1	0.331	0.094	-0.035	0.068	0.049
MAFB	0.251	0.034	-0.119	-0.035	-0.002
RAB17	0.177	-0.062	-0.172	-0.050	-0.035
PORCN	0.245	0.069	-0.055	0.063	0.062
RIN3	0.177	0.075	0.012	0.094	0.030
ASB13	0.270	-0.019	-0.146	0.037	-0.113
IVL	0.437	0.205	0.087	0.273	0.153
FJX1	0.225	0.035	-0.048	0.095	-0.020
CYR61	0.266	0.030	-0.043	0.081	-0.010
POLR1C	0.200	0.023	-0.030	0.050	0.010
BNC2	0.447	-0.130	-0.333	-0.067	-0.139
ITPK1	0.249	0.013	-0.095	0.042	-0.019
NCOR2	0.221	0.028	-0.032	0.077	0.033
ZNF195	0.253	0.037	0.069	0.080	0.082
TSPAN5	0.320	-0.056	-0.034	0.027	0.000
DEPTOR	0.808	-0.333	-0.312	-0.124	-0.159
BCL11A	0.315	-0.242	-0.201	-0.143	-0.143
ZMIZ1	0.606	-0.043	-0.056	0.001	-0.009
MPPED2	0.510	-0.204	-0.196	-0.150	-0.122
THY1	0.251	0.004	0.012	0.009	0.027
NPY1R	0.654	-0.207	-0.224	-0.212	-0.174
NRTN	0.557	-0.237	-0.157	-0.128	-0.227
ELF3	0.261	-0.180	-0.144	-0.155	-0.164
FLG	0.434	-0.550	-0.388	-0.212	-0.368
MICAL3	0.224	-0.080	-0.039	0.034	-0.042
HIP1	0.445	-0.097	-0.014	0.040	-0.043
TMEM120B	0.623	-0.002	-0.096	0.003	-0.113
SLC7A2	0.813	-0.167	-0.322	-0.160	-0.340
RBBP8	0.493	-0.277	-0.374	-0.267	-0.376
MPHOSPH10	0.229	0.003	-0.003	0.034	-0.003
GREB1	1.960	-0.686	-0.842	-0.334	-0.777
CADM1	1.002	0.044	-0.035	0.115	-0.031

SLC9A3R1	0.242	-0.030	-0.070	-0.015	-0.045
SLC22A5	0.673	-0.162	-0.286	-0.102	-0.200
PAPSS2	0.761	0.074	-0.030	0.088	0.035
HIPK2	0.271	0.044	-0.022	0.037	-0.013
TGFA	0.290	-0.136	-0.152	-0.043	-0.158
ARHGAP26	1.084	0.017	0.022	0.217	-0.068
PLAT	0.765	-0.149	-0.269	-0.052	-0.340
E2F6	0.250	-0.064	-0.120	-0.038	-0.133
MDN1	0.301	0.018	-0.024	0.077	-0.022
LOC100505650	0.447	0.025	-0.069	0.081	-0.036
ABCC1	0.236	-0.012	-0.053	0.027	-0.037
PDGFRL	0.586	-0.042	-0.060	0.010	-0.122
CA12	1.128	0.031	-0.041	0.065	-0.123
CA12	1.406	0.041	-0.047	0.110	-0.263
ARNTL	0.777	0.026	0.029	0.111	-0.097
NRP1	0.334	-0.092	-0.089	-0.005	-0.161
ARHGAP26	0.871	0.176	0.155	0.296	-0.005
LYN	0.378	0.017	-0.014	0.009	-0.101
BCL2L11	0.416	-0.011	-0.027	0.013	-0.131
ARL4C	0.221	0.004	-0.027	0.005	-0.071
DGKI	0.435	0.116	0.071	0.143	-0.014
CBLN1	0.572	-0.337	-0.476	-0.255	-0.620
TGIF2	0.450	-0.160	0.031	-0.055	-0.168
DDX24	0.226	0.046	0.087	0.081	0.051
NOLC1	0.263	0.026	0.089	0.096	0.030
ABAT	0.302	0.007	0.097	0.111	0.026
RASGRP1	0.295	-0.124	-0.124	-0.115	-0.279
BCL2L11	0.551	0.104	0.092	0.106	-0.091
PRLR	0.422	0.184	0.200	0.215	0.095
MED13L	0.378	-0.002	0.048	0.034	-0.070
AGT	0.641	-0.083	-0.026	-0.062	-0.175
OLFM1	0.818	-0.192	-0.137	-0.227	-0.276
CA12	0.953	-0.071	-0.060	-0.109	-0.148
KDM4B	0.370	-0.055	-0.035	-0.102	-0.108
GFRA2	0.811	0.006	0.001	-0.077	-0.123
FAM134B	0.303	0.133	0.132	0.112	0.096
ZNF3	0.268	0.033	-0.034	0.065	-0.120
C10orf2	0.243	0.055	-0.002	0.039	-0.099
ULK1	0.297	0.149	0.034	0.118	0.027
POP1	0.228	0.058	-0.090	0.010	-0.100
PPRC1	0.217	0.089	-0.030	0.051	-0.055
MUC4	0.319	0.110	-0.101	0.060	-0.055
SYNJ2	0.272	0.113	0.026	0.099	0.026
CHST10	0.341	-0.037	-0.215	-0.053	-0.202

SCNN1B	0.383	0.015	-0.124	-0.040	-0.159
KAZN	0.697	-0.039	-0.214	-0.140	-0.357
NT5DC3	0.265	0.043	-0.042	0.018	-0.089
SLC7A6	0.230	0.009	-0.019	0.090	-0.105
POLR3E	0.170	0.000	0.001	0.075	-0.023
PDLIM4	0.358	0.037	0.031	0.149	0.000
PLCL2	0.448	0.102	0.106	0.216	0.019
AKAP1	0.277	-0.013	-0.083	0.124	-0.074
TLE3	0.241	0.128	-0.038	0.130	0.061
RDX	0.197	-0.363	-0.262	0.022	-0.064
NEDD9	0.225	-0.016	-0.068	0.088	0.085
GPR135	0.277	0.034	0.030	0.127	0.169
PPP1R3D	0.422	-0.036	0.125	0.083	0.146
NFAT5	0.400	0.015	0.088	0.076	0.212
MYO10	0.358	-0.002	-0.004	-0.114	0.134
EDAR	0.310	0.035	-0.136	-0.062	0.090
VNN1	0.390	0.161	0.233	0.114	-0.032
MAP3K9	0.258	0.082	0.144	0.061	-0.070
INHBA	0.540	0.245	0.298	0.179	-0.090
SLC25A36	0.207	0.103	0.083	0.063	-0.075
PPAT	0.222	0.070	0.060	0.051	-0.088
PNN	0.224	0.120	0.108	0.121	0.013
PTHLH	0.369	0.202	0.235	0.177	0.116
PTGS2	0.586	0.045	0.185	0.093	-0.162
TGIF2	0.202	-0.036	-0.029	-0.052	-0.117
ARNTL	0.676	0.158	0.148	0.068	-0.082
KIAA1199	0.406	-0.031	-0.074	-0.076	-0.192
CISH	0.621	-0.291	-0.375	-0.450	-0.607
STC2	0.424	0.043	-0.009	-0.131	-0.254
KCNF1	1.014	0.159	0.092	-0.118	-0.298
IL12A	0.899	0.006	0.099	-0.156	-0.284
SOX9	0.337	0.067	-0.010	-0.058	-0.147
C16orf45	0.384	0.109	0.040	-0.017	-0.089
PDLIM4	0.765	0.312	0.143	0.113	-0.084
MREG	0.272	0.064	-0.024	-0.010	-0.087
LYN	0.361	0.113	0.069	0.065	-0.049
TFAP2C	0.304	-0.125	-0.219	-0.199	-0.242
ST6GALNAC2	0.285	-0.066	-0.156	-0.122	-0.168
PLCG2	0.407	0.020	-0.010	-0.050	-0.037
DHRS2	0.329	0.055	-0.075	-0.043	-0.085
BDNF	0.307	0.085	0.016	0.007	0.004
SHB	0.351	0.166	0.029	0.001	-0.029
MAP3K4	0.214	0.098	0.015	-0.002	-0.008
IGF1R	0.424	0.158	-0.024	-0.016	-0.066

COBL	0.397	0.171	-0.015	-0.016	-0.075
KIAA0485	0.803	0.295	-0.066	-0.149	-0.094
PCNX	0.214	0.144	0.051	0.056	0.020
SLC7A5	0.384	0.265	0.106	0.099	-0.025
JARID2	0.624	0.463	0.311	0.323	0.085
SHB	0.342	0.163	0.102	0.027	-0.053
EDN1	0.302	0.144	0.086	0.012	-0.063
RHOF	0.282	0.170	0.093	0.061	-0.005
OSBPL3	0.770	0.442	0.247	0.175	0.053
KIAA0226L	0.627	0.428	0.210	-0.038	-0.155
BMP2	0.546	0.315	0.064	-0.190	-0.356
BMP2	0.461	0.199	-0.001	-0.172	-0.346
INHBA	0.429	0.288	0.166	-0.014	-0.153
DIRAS3	0.300	0.180	0.099	-0.038	-0.185
KIAA0226L	0.514	0.296	0.219	-0.009	-0.075
TXLNG	0.302	0.173	0.227	0.008	0.028
BCL10	0.244	0.110	0.120	-0.038	-0.020
TIPARP	0.263	0.106	0.117	-0.014	-0.034
MYC	0.235	-0.155	-0.141	-0.358	-0.477
LPIN1	0.273	0.087	0.127	-0.092	-0.116
KLF4	0.496	0.161	0.258	-0.169	-0.277
KLF4	0.604	0.230	0.238	-0.174	-0.335
SRRM2	0.270	0.118	0.107	-0.020	0.028
SLC4A7	0.281	0.154	0.168	0.040	0.146
SOWAHC	0.218	0.420	0.338	0.043	-0.119
FOS	0.351	0.609	0.561	-0.321	-0.412
EGR1	0.433	0.851	1.001	-0.144	-0.309
DNMBP	0.262	0.440	0.261	0.070	-0.060
ABTB2	0.256	0.306	0.209	0.116	0.035
BIRC3	0.412	0.491	0.411	0.018	-0.169
SF1	0.470	0.605	0.677	0.412	0.155
EGR3	0.704	0.729	1.095	0.113	-0.029
SLC19A2	0.647	0.544	0.390	-0.096	-0.305
MAPKBP1	0.385	0.323	0.223	-0.014	-0.203
PPAP2B	0.418	0.356	0.325	0.047	-0.108
LPIN1	0.263	0.152	0.175	-0.046	-0.148
EXT1	0.396	0.305	0.397	0.204	0.116
PPAP2B	0.405	0.400	0.207	-0.026	-0.079
CENPJ	0.369	0.136	0.413	0.290	0.241
ZIC1	-0.238	-0.203	-0.195	-0.098	-0.060
SMAD6	-0.286	-0.231	-0.253	-0.083	0.004
FZD7	-0.405	-0.245	-0.256	0.126	0.145
GAS1	-0.468	-0.464	-0.360	0.064	0.142
C1orf106	-0.220	-0.200	-0.229	0.096	0.087

ADM	-0.217	-0.193	-0.204	0.076	0.083
BMP4	-0.278	-0.235	-0.280	0.088	0.130
FLVCR2	-0.250	-0.297	-0.274	-0.068	-0.012
NR3C2	-0.273	-0.346	-0.413	-0.103	-0.050
PRR15L	-0.251	-0.608	-0.553	-0.146	-0.130
CCNG2	-0.296	-0.566	-0.354	-0.188	-0.126
CYP1B1	-0.268	-0.388	-0.179	-0.090	-0.117
ZBED2	-0.323	-0.054	-0.121	0.167	0.134
JAG1	-0.276	0.007	-0.069	0.173	0.228
TOX	-0.460	-0.244	-0.222	-0.043	0.067
FAM49A	-0.323	-0.084	-0.154	-0.043	0.006
TLE4	-0.418	-0.275	-0.080	-0.138	-0.141
LYST	-0.394	-0.248	-0.032	-0.112	-0.129
DDX25	-0.348	-0.245	-0.118	-0.118	-0.160
PLAU	-0.367	-0.085	0.055	0.117	0.085
NAP1L3	-0.241	-0.097	-0.048	0.062	-0.008
THEMIS2	-0.234	-0.188	-0.165	-0.068	-0.078
STYK1	-0.221	-0.089	-0.084	0.120	0.057
THEMIS2	-0.283	-0.266	-0.166	-0.086	-0.144
CLEC7A	-0.236	-0.210	-0.121	-0.116	-0.098
CCNG2	-0.387	-0.391	-0.163	-0.090	0.049
SLC39A2	-0.332	-0.095	-0.317	-0.175	-0.113
PDGFA	-0.269	0.055	-0.031	0.053	0.084
DIO2	-0.465	0.228	0.058	0.123	0.259
EPHB3	-0.299	0.023	-0.117	-0.020	0.022
GTF2IRD1	-0.202	0.005	-0.073	0.020	-0.003
LEF1	-0.429	0.056	-0.159	-0.058	-0.062
ADCY2	-0.294	-0.051	-0.147	-0.180	-0.101
TSC22D1	-0.299	0.090	0.136	0.067	0.083
ARID5B	-0.451	0.172	0.305	0.081	0.149
KLF9	-0.521	-0.008	0.286	0.075	0.097
FRMD4B	-0.357	0.077	0.224	0.159	0.144
TBX2	-0.260	-0.126	-0.072	-0.118	-0.146
BCAR3	-0.306	0.105	0.132	0.086	0.014
TNFRSF11B	-0.385	-0.061	0.000	-0.007	0.084
TNFAIP8	-0.339	0.049	0.089	0.107	0.155
TNFAIP8	-0.353	0.046	0.125	0.083	0.139
PLAU	-0.311	0.055	0.067	0.138	0.104
DLX2	-0.424	0.021	0.016	0.139	0.116
EPHB3	-0.379	-0.099	-0.108	-0.076	-0.064
EFNB2	-0.281	0.084	0.028	0.080	0.109
KIR3DL3	-0.308	-0.091	-0.067	-0.095	0.036
ACTG2	-0.240	-0.134	-0.088	-0.158	-0.089
TRIM24	-0.225	0.034	0.045	-0.087	-0.087

SPAG11B	-0.423	-0.167	-0.195	-0.281	-0.271
SAMD4A	-0.201	0.389	0.309	0.087	0.077
CYP26B1	-0.320	0.208	0.294	0.050	0.048
ACRV1	-0.243	0.032	0.085	-0.070	-0.076
CITED2	-0.268	0.224	0.261	0.107	0.060
NPTXR	-0.217	0.043	0.046	-0.109	-0.015
TP63	-0.312	0.001	-0.022	-0.269	-0.173
KCNJ3	-0.188	-0.075	-0.014	-0.048	-0.160

Table 13: Ordered gene lists from PEO4 heat maps in Fig. 3

Genes	E2	4OHT+E2	4OHT	ICI+E2	ICI
ZNF667	0.3552	-0.0769	0.0239	0.0939	0.0872
TSPAN15	0.6606	-0.0764	0.0698	0.1413	0.1682
RAB7L1	0.3069	-0.4052	-0.2600	-0.1958	-0.2313
PPP1R3D	0.2689	-0.0253	0.0037	0.0668	0.0216
MINA	0.3361	-0.1320	-0.0416	0.0362	-0.0714
PELI1	0.3748	-0.0763	0.0809	0.0580	0.0362
MYBL1	0.5997	0.1592	0.3407	0.2858	0.2496
BRIX1	0.2972	0.1473	0.1590	0.1555	0.1230
SLC7A2	0.4789	-0.0050	0.0233	0.0357	-0.1466
PPAT	0.3505	0.0451	0.0738	0.1010	-0.0208
FASTKD3	0.3043	0.0869	0.0796	0.1252	0.0582
SCNN1B	0.2544	0.1565	0.1619	0.1865	0.1431
QTRTD1	0.2739	0.0542	0.0337	0.1291	-0.0108
ID4	0.2325	0.0624	0.1078	0.1214	0.0556
WDR3	0.4131	0.1307	0.1693	0.1131	0.1540
TGIF2	0.5028	0.1411	0.1051	0.0679	0.1248
PRR5	0.3249	0.0054	-0.0272	-0.0359	0.0057
CACNA1I	0.9547	0.2536	0.2673	0.1253	0.3268
LIMS1	0.2485	0.1487	0.1641	0.1247	0.1436
RBBP8	0.6175	0.1939	0.2657	0.1518	0.1038
IL15	0.3273	0.0758	0.1492	0.1018	0.0540
TLL2	0.6063	0.0587	-0.1283	-0.0607	-0.2265
SOX17	0.3029	0.0429	-0.0318	-0.0468	-0.0923
ITSN2	0.2968	0.0800	0.0107	0.0077	-0.0305
KAZN	0.5299	0.1064	-0.0214	-0.0160	-0.0547
AKAP1	0.3471	0.1268	0.0183	0.0620	-0.0163
TIMM8A	0.1970	0.1048	0.0769	0.0557	0.0479
IL12A	1.0210	0.3535	0.1338	-0.0121	-0.1101
RASGRP1	1.9351	1.0155	0.9086	0.5433	0.5247
SHB	0.4212	0.2594	0.1746	0.1139	0.1159
PVR	0.3297	0.2089	0.1313	0.1026	0.0691
PEX5	0.2623	0.1653	0.1035	0.0788	0.0653
OSBPL3	0.7383	0.3069	-0.0119	-0.0026	-0.0039
STC2	0.4590	0.1860	0.0683	-0.0225	0.0697
E2F6	0.2543	0.1019	0.0506	-0.0140	0.0631
SLC7A5	0.3071	0.1820	0.1438	0.0600	0.1402
DHODH	0.2863	0.1705	0.1449	0.0744	0.1327
SPRY1	0.3181	0.0284	-0.0330	-0.2160	-0.1745
PLEKHF1	0.3339	0.1489	0.1395	0.0097	0.0373
SIX1	0.8042	0.4576	0.4064	0.1737	0.2887
HES1	0.5398	0.3155	0.2516	0.0911	0.1657
PPRC1	0.3750	0.2022	0.1574	0.0670	0.1111

CD3EAP	0.4827	0.2655	0.1994	0.1058	0.1645
ARL4C	0.4085	0.2329	0.1656	0.0796	0.1150
TSEN2	0.4651	0.0025	-0.0069	-0.0124	-0.0914
PLCL2	0.6375	0.0323	0.0191	0.0199	-0.0630
CEBPD	0.8994	0.1435	0.0952	-0.0053	-0.0371
PLAT	0.5546	0.1539	0.1660	0.1363	0.1505
KAZN	1.3479	0.4207	0.3601	0.2578	0.3092
HES1	0.5794	0.1329	0.0952	0.0276	0.0627
SLC22A5	0.6618	0.1217	-0.0270	0.0739	0.0685
PPYR1	0.2796	-0.0956	-0.1485	-0.0993	-0.1311
PLCL2	0.9662	0.0780	-0.0823	-0.0547	-0.1294
CA12	1.2262	0.2389	0.0827	0.1097	0.0940
ERG	0.6679	0.0642	-0.0003	0.0386	-0.0142
SYBU	0.3378	0.1655	0.1279	0.1250	0.1371
LOC100505650	0.8342	0.2002	-0.0475	0.0032	0.1073
FLG	0.5949	0.0154	-0.2486	-0.1448	-0.0576
FAM134B	0.2746	0.0077	-0.1036	-0.0536	-0.0127
TMPRSS3	0.5034	-0.0418	-0.1119	0.0036	0.0974
RPS6KA2	0.5808	-0.0847	-0.2036	-0.0452	0.0873
PIPOX	0.5089	-0.0588	-0.1474	-0.0882	0.0856
MLPH	0.3057	-0.0696	-0.1226	-0.0924	0.0334
BICD1	0.2861	0.0510	-0.0353	0.0413	0.0787
DEPTOR	1.1935	-0.1305	-0.1044	0.0664	0.0693
GREB1	1.6996	-0.1307	-0.0878	0.2120	0.0213
OLFML3	1.1165	-0.0534	-0.0886	-0.0534	0.1094
GFRA2	1.0756	0.1754	0.1944	0.2129	0.2462
PKNOX2	1.2580	0.1582	-0.0136	0.2707	0.3763
F13A1	0.2870	-0.2149	-0.2665	-0.1577	-0.1261
CASQ2	0.5071	-0.4493	-0.5533	-0.2754	-0.2099
BMP7	0.5901	-0.1642	-0.2030	-0.0862	-0.0396
TPST2	0.3431	0.0092	0.0462	0.0142	0.1293
ST6GALNAC2	0.4364	0.0252	0.0106	-0.0471	0.1183
RAB17	0.3076	0.0439	0.0488	0.0165	0.1146
CRYBG3	0.3883	0.0763	0.0593	0.0479	0.1637
SRSF7	0.3267	0.1260	0.1146	0.0740	0.1637
TBC1D16	0.4292	0.0489	-0.0406	-0.0420	0.1028
ABCC1	0.3037	0.1020	0.0518	0.0394	0.1141
PRR5	0.3717	0.0705	-0.0348	-0.0415	0.1319
RCL1	0.2766	0.1001	-0.0033	-0.0292	0.0908
RAP1GAP	0.4130	0.1158	-0.0125	-0.0645	0.1257
MPPED2	0.5915	-0.1346	-0.3624	-0.1615	-0.1355
LRRC8B	0.3537	-0.1291	-0.2264	-0.1207	-0.1072
PDGFRL	0.3488	-0.0346	-0.1136	0.0116	-0.0146
FRAT2	0.3173	0.0094	-0.1090	0.0259	-0.0049

FAM216A	0.3942	0.1249	0.0355	0.1101	0.0815
METTL21B	0.3171	0.1888	0.0991	0.1785	0.1311
ZMIZ1	0.3207	0.0047	0.0077	0.0691	0.1277
TNS1	0.2711	0.0091	0.0028	0.0512	0.1275
CHD7	0.3071	0.2028	0.2090	0.2281	0.2520
ELF3	0.4255	-0.1842	-0.3398	-0.1218	0.0678
VAX2	0.3339	-0.0904	-0.0817	-0.0152	0.1763
PDZK1	0.2566	-0.2844	-0.3013	-0.0767	0.0081
OVOL2	0.3165	-0.3349	-0.2974	-0.0897	0.0627
UGT2B28	0.4130	-0.0961	-0.1136	0.0490	0.0621
RHOBTB1	0.3337	-0.1699	-0.1966	-0.0262	-0.0375
BCL11A	0.6948	-0.0553	-0.0681	0.2210	0.1584
ABCC4	0.2140	0.0151	-0.0173	0.0715	0.0762
CEP68	0.2557	-0.1435	-0.1253	0.0490	0.0190
TMEM177	0.2114	-0.0231	0.0378	0.0700	0.1354
BNC2	0.2388	-0.3551	-0.2982	-0.0887	0.1240
DAAM1	0.3327	-0.5012	-0.3517	0.0669	0.0267
ZNF573	0.2746	0.0221	-0.2128	-0.0115	0.0998
TMEM47	0.2393	0.0659	-0.1257	0.0304	0.0898
SCAMP1	0.3004	0.1180	-0.1122	0.0416	0.1679
SV2A	0.2987	0.0027	-0.1641	-0.0605	0.0997
THY1	0.2685	0.0694	-0.0049	0.0336	0.2240
GEMIN4	0.2041	0.1222	0.0471	0.0300	0.2016
ZNF556	0.3332	0.2406	0.1861	-0.0051	0.1133
HK2	0.2740	0.1959	0.1377	-0.0144	0.1199
RGS16	0.5206	0.2805	0.3274	-0.0106	0.1475
ZNF232	0.2998	0.2536	0.1356	0.1301	0.1673
DIEXF	0.2971	0.2341	0.0288	0.0329	0.1101
JARID2	0.3921	0.3349	0.0168	-0.0049	0.1012
TSKU	0.3498	0.2734	0.1621	0.1101	0.1653
SCARB1	0.2308	0.1646	0.0220	-0.0242	0.0389
LRP8	0.2228	0.1864	0.1260	0.1036	0.1417
C10orf2	0.4579	0.2894	0.0982	-0.0442	0.0544
MID1IP1	0.2905	0.1633	0.0265	-0.0411	0.0064
NXT1	0.3052	0.2237	0.0642	-0.0284	0.0143
CHST10	0.3109	0.2166	0.0775	0.0297	0.0474
SIN3B	0.3394	0.1275	-0.1047	-0.1671	0.0091
DPH2	0.2407	0.1554	0.0615	0.0418	0.0991
TBC1D30	0.4505	0.2055	-0.1598	0.0117	0.1203
DFFB	0.3175	0.1613	0.0008	0.0608	0.1258
KIAA1199	0.6737	0.2529	-0.0752	0.0044	0.1071
CADM1	0.3000	0.1189	-0.0336	0.0073	0.0658
GPD1L	0.2100	0.0794	-0.0100	-0.0008	0.0631
TACSTD2	0.2859	0.1674	-0.0136	0.0014	0.1297

RARA	0.3176	0.2933	0.1677	0.1139	0.2887
PADI2	0.2979	0.2351	0.1027	0.0042	0.1667
YRDC	0.2179	0.3158	0.1879	0.0397	-0.0036
SLC19A2	0.4193	0.5938	0.4120	0.1962	0.1337
PDLIM4	0.4747	0.7631	0.4008	0.0824	-0.0175
PWP2	0.2646	0.3380	0.2416	0.0870	0.1103
TNFRSF10B	0.3603	0.6171	0.4044	0.1914	0.2615
COBL	0.4617	0.8233	0.5007	0.1419	0.2595
PPP1R3C	0.3386	0.7255	0.5530	0.1055	0.1291
KLHL21	0.4647	0.8082	0.6152	0.2871	0.2999
BIRC3	0.4027	1.0582	0.5856	-0.1035	-0.1818
PPAP2B	0.4248	0.7900	0.3171	0.1073	0.1157
INHBB	0.3628	0.5238	0.2232	0.0797	0.0838
MAP3K9	0.3263	0.4835	0.2487	0.0982	0.2064
CAMK2N1	0.2811	0.4417	0.1588	0.0715	0.1287
TTC9	0.3559	0.3957	0.2335	0.0793	0.1266
LHX6	0.3752	0.3501	0.2496	0.1248	0.1846
KIAA0226L	0.8586	0.8441	0.4525	0.0703	0.1300
GRPEL1	0.3289	0.2921	0.1680	0.0179	0.0275
ABTB2	0.5835	0.5265	0.3328	0.1369	0.1600
THBD	0.8094	0.9029	0.6056	0.1538	-0.0443
MAK16	0.2499	0.2714	0.1939	0.0785	0.0557
POP1	0.2618	0.2669	0.1749	0.0507	0.0211
MREG	0.3732	0.3570	0.2655	0.1051	0.0642
BMP2	0.5114	0.6059	0.3898	0.1637	0.0837
IL24	0.5889	0.6590	0.4094	0.1947	0.1315
INHBA	0.5411	0.5265	0.3686	0.0511	0.1084
DUSP2	0.7166	0.7038	0.5417	0.0762	0.0956
SOWAHC	0.5345	0.5749	0.4996	0.1875	0.1198
BDNF	0.5648	0.5257	0.4929	0.1527	0.0380
ANKRD1	0.3665	0.3089	0.2091	-0.0184	-0.1366
MNT	0.4094	0.5527	0.3960	0.1006	0.2792
CAMSAP1	0.3008	0.4309	0.3132	0.0570	0.1515
BDKRB1	0.5414	0.6045	0.4470	0.0981	0.2966
CCDC86	0.2779	0.2822	0.2250	0.0956	0.2120
MAPKBP1	0.4186	0.4033	0.1469	-0.0026	0.2110
IVL	0.6133	0.6456	0.4284	0.2898	0.4722
IFIT5	0.2377	0.2560	0.1472	0.0455	0.1607
FZD5	0.2526	0.2549	0.0777	0.0018	0.0772
ZNF239	0.4436	0.2621	0.1688	0.0530	0.0083
KLF4	0.9665	0.5092	0.4584	0.1251	0.0701
MYC	0.9676	0.5374	0.5306	0.0334	-0.1512
FJX1	0.4792	0.3343	0.3141	0.1564	0.1020
TMEM30B	0.3415	0.2058	0.1963	0.1284	0.0567

TGFA	0.3010	0.1511	0.1447	0.0994	-0.0443
RRS1	0.3913	0.1886	0.1402	0.1045	0.0042
DIEXF	0.4865	0.3124	0.2630	0.2348	0.1163
PNPLA3	0.5198	0.2601	0.1367	0.1039	-0.0407
GEMIN6	0.2397	0.0853	-0.0018	0.0022	-0.0859
EIF3M	0.4329	0.2451	0.1185	0.1365	0.0233
PPAT	0.3354	0.1533	0.1310	0.1062	0.0419
POLR1E	0.3730	0.1131	0.1176	0.0251	-0.0621
UCK2	0.2842	0.2278	0.1856	0.1058	0.0771
OTUB2	1.0120	0.7949	0.6089	0.2223	0.1990
NOP16	0.4321	0.3823	0.2616	0.1048	0.0667
POLR1C	0.4048	0.2884	0.1316	0.0233	-0.0724
HRH1	0.5150	0.3716	0.2263	0.1401	0.0424
B4GALT5	0.2813	0.2127	0.1417	0.0882	0.0700
SOX9	0.7748	0.7645	0.4565	0.2696	0.1883
PER2	0.3056	0.2766	0.1349	0.0351	-0.0466
TFAP2C	0.5288	0.3942	0.3178	0.1146	-0.2247
SLC30A1	0.2856	0.2406	0.2079	0.1642	0.1241
POLR3K	0.2145	0.1654	0.1147	0.0564	-0.0076
EHD1	0.3014	0.2181	0.1275	0.0489	-0.0687
NOP16	0.5264	0.3508	0.2873	0.2127	0.0644
ZFP36L2	0.2924	0.0985	0.2229	0.0467	-0.0698
TFB2M	0.2816	0.1024	0.1619	0.0711	-0.0409
E2F5	0.2358	-0.0351	0.0601	-0.0107	-0.3772
NIP7	0.3737	0.0568	0.1275	0.1301	-0.1374
MRPS30	0.1906	0.1170	0.0678	0.0609	-0.1084
LOC389906	0.3647	0.2441	0.1628	0.2260	0.0330
TBC1D9	0.2289	0.2070	0.0911	0.1270	0.0428
MN1	0.3772	0.3695	0.0372	0.0461	0.0124
POLR3G	0.3727	0.2493	0.0728	0.1118	0.0742
EDAR	0.4871	0.3048	0.1147	0.1741	0.1363
LYN	0.2458	0.1744	0.0255	0.1155	0.0444
FUT9	-0.2264	-0.2631	-0.3893	-0.3317	-0.3616
F3	0.4550	0.6453	0.6433	0.2152	0.0686
BAZ1A	0.2774	0.3484	0.3347	0.2292	0.1640
DUSP7	0.3288	0.4459	0.3832	0.1711	0.1081
RALA	0.2565	0.3936	0.3047	0.2430	0.0884
NDUFAF4	0.2256	0.2229	0.1872	0.1288	-0.0424
ZFP161	-0.2159	-0.2730	0.2485	0.1245	-0.4254
SCN2B	-0.3887	-0.3218	-0.3003	-0.2328	-0.4112
ITGB4	-0.2414	-0.1528	-0.2007	-0.0738	-0.3418
DNAJB4	-0.5180	-0.7041	-0.3485	-0.3306	-0.7904
C19orf6	-0.3883	-0.3998	-0.2319	-0.1975	-0.4863
TOB1	-0.2287	-0.0645	0.0240	-0.0085	-0.1282

PALLD	-0.2790	-0.0806	0.0343	0.0242	-0.2047
PAX8	-0.3546	-0.1074	0.0937	-0.0477	-0.2607
KLF9	-0.4191	0.0483	0.1937	0.0955	-0.2370
ARF6	-0.3195	-0.2144	-0.0351	-0.1164	-0.2834
RNFT1	-0.6682	-0.4867	-0.2238	-0.2865	-0.8099
PLAU	-0.4054	-0.1025	0.1237	-0.0613	-0.5188
PHACTR2	-0.2546	-0.1611	0.0276	0.0515	-0.0769
HOXB3	-0.2478	-0.1946	0.0408	0.0813	-0.1635
MLL	-0.3227	-0.2800	-0.1122	0.0709	-0.1494
CTGF	-0.4861	-0.5214	-0.3154	-0.2734	-0.3653
COL1A1	-0.2693	-0.2792	-0.2647	-0.0060	-0.1642
HEXIM1	-0.2504	-0.3087	-0.2501	-0.0813	-0.2215
LIMK2	-0.4008	-0.4585	-0.4218	-0.1905	-0.4401
IQGAP2	-0.3219	-0.3278	-0.3437	-0.2869	-0.3140
TSPAN2	-0.3278	-0.5207	-0.5113	-0.3514	-0.5287
TM4SF1	-0.4088	-0.0937	-0.0478	-0.3017	-0.4725
SERPINB2	-0.2885	0.0352	0.0285	-0.1997	-0.2880
DUSP1	-0.6017	-0.2579	-0.0765	-0.3844	-0.6249
CITED2	-0.3602	0.1175	0.2220	-0.0676	-0.3661
SLIT2	-0.2432	0.4313	0.1369	-0.0704	-0.0590
HNRNPU	-0.3214	-0.0573	-0.1859	-0.2262	-0.2057
CADM4	-0.3277	-0.1793	-0.2800	-0.2940	-0.2809
DKK1	-0.5820	0.9109	0.5376	0.3115	0.1549
ARID5B	-0.5860	0.1775	-0.0188	-0.2214	-0.1316
PCDH7	-0.2766	0.8566	0.6994	0.2109	0.2177
DUSP5	-0.3530	0.5775	0.4755	-0.0941	-0.1925
AREG	-0.4199	1.3772	1.0216	0.0958	-0.1860
SLC35G2	0.2236	0.6209	0.5146	0.2118	0.0865
DNMBP	0.2612	0.8908	0.6513	0.1501	0.1138
RSRC2	-0.2677	-0.0662	-0.1470	-0.0582	-0.2324
PPFIBP1	-0.4894	0.0399	-0.0840	0.1401	-0.2665
FZD7	-0.3318	-0.0203	-0.1931	-0.0545	-0.2449
RNF19A	-0.4274	0.0373	-0.0736	0.0806	-0.0568
PDP1	-0.4896	0.1347	0.1642	0.0230	-0.1575
EZR	-0.2830	0.2752	0.3306	0.2698	0.0744
EFNB2	-0.4112	0.4213	0.3172	0.2116	0.2719
FAM49A	-0.3242	-0.0138	-0.0531	-0.0482	-0.0751
KLF5	-0.4900	0.1356	0.0365	-0.0290	-0.1201
PTGER4	-0.2839	0.0607	-0.1772	-0.1320	-0.1168
CXCR4	-0.3084	0.0747	-0.1973	-0.1487	-0.0420
ZBED2	-0.3550	-0.1004	-0.0832	-0.1162	-0.0401
EPHB3	-0.3777	0.0134	0.0811	0.0022	0.1166
NRG1	-0.3674	-0.0370	-0.0161	-0.1202	-0.0485
ADM	-0.2855	0.0167	0.0252	-0.0096	0.1867

TSC22D1	-0.2559	-0.1319	-0.1619	-0.0434	-0.0473
PCDH9	-0.4644	-0.2752	-0.3280	-0.0589	0.0070
GPR64	-0.3369	-0.2584	-0.2204	-0.1057	0.0369
DNAJC6	-0.3696	-0.2578	-0.2995	-0.1153	0.0210
CCNG2	-0.3062	-0.2509	-0.2592	-0.0220	0.1024
SYNC	-0.4219	-0.1569	-0.1438	-0.0456	0.0025
EPHA4	-0.5011	-0.1107	-0.1015	0.0055	0.1131
FOXE1	-0.3234	-0.2023	-0.1201	-0.0620	-0.0220
NUSAP1	-0.3207	-0.1634	-0.1055	-0.0019	-0.0530
NCAPG	-0.2482	-0.1545	-0.0300	0.0560	-0.0160
KITLG	-0.2725	-0.2165	-0.0842	0.0483	-0.0705
WNT6	0.3217	-0.3095	-0.1954	-0.1677	0.0600
TLR6	-0.3320	-0.3530	-0.2925	-0.2457	-0.1459
SLC2A3	-0.4514	-0.6810	-0.7332	-0.1950	-0.0879
TMEM100	-0.3282	-0.7458	-0.7777	-0.0010	0.0479
FLVCR2	-0.2802	-0.4531	-0.5111	-0.1520	-0.1199
IGF1	-0.3663	-0.8193	-0.7820	-0.2964	-0.2050
FGF18	-0.3691	-0.4585	-0.3789	-0.1047	0.0128
BMP4	-0.2754	-0.4010	-0.3422	-0.1348	-0.0025
C1orf106	-0.2952	-0.5104	-0.3716	-0.2088	-0.0713
TXNIP	-0.3978	-0.6334	-0.4821	0.0071	-0.0823
MYCN	-0.5207	-0.9847	-0.6610	-0.1577	-0.0694
CYP1B1	-0.4264	-0.7071	-0.5211	-0.1683	-0.1196
PDZRN4	-0.4689	-0.4807	-0.4885	-0.1096	-0.0939
TRIM38	-0.2400	-0.2238	-0.1729	-0.0771	-0.0208
SEMA3A	-0.2982	-0.2980	-0.2681	-0.1752	-0.1663
C5orf54	-0.3089	-0.2928	-0.2234	-0.1178	-0.0959
NCOA3	-0.2522	-0.2755	-0.1955	-0.1078	-0.0968
ADAMTS1	-0.4051	-0.4433	-0.2441	-0.0925	-0.0930
NDC80	-0.2184	-0.3513	-0.1762	-0.0183	0.0183
STYK1	-0.2764	-0.2968	-0.3718	-0.2957	-0.1344
NOX4	-0.3271	-0.3982	-0.4322	-0.2949	-0.1359
C1orf115	-0.2507	-0.3284	-0.3698	-0.1433	0.0850
SERPINB13	0.2661	0.1919	0.2419	0.1552	0.2402
C22orf29	0.3252	0.2418	0.3300	0.2302	0.2887
OTOR	0.3295	0.2744	0.4579	0.2342	0.5747

We validated a number of the top E2-regulated genes shared between cell lines by qRT-PCR. PEO4 and PEO1 cells were treated as described in Chapter 2 for microarray studies. Gene expression instead was measured by qRT-PCR.

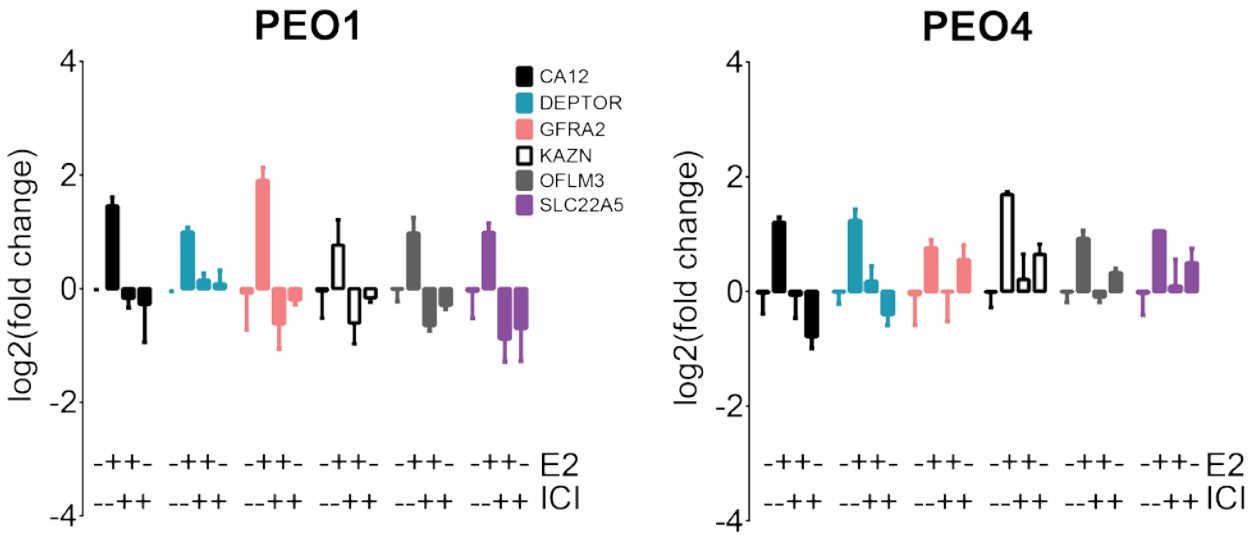

Figure 29: Validation of E2-regulated genes identified by microarray. PEO1 and PEO4 cells were hormone-deprived and treated with vhc, 1 nM E2, E2 + 1 μM ICI, or ICI alone.

APPENDIX D

BATCH EFFECT ANALYSIS OF CLINICAL SAMPLES IN CHAPTER 2

Because the samples described in Chapter 2 were procured from four different medical centers, we conducted batch comparisons to rule out variation due to differences in tissue source. These analyses were performed by Tianzhou Ma.

D.1 SURVIVAL ACROSS PATIENT COHORTS

We first compared survival between sites. As reflected in Table 6, overall survival did not differ significantly between patients at different centers. Time on endocrine therapy also did not vary significantly across sites. This is depicted in the Kaplan-Meier curves below.

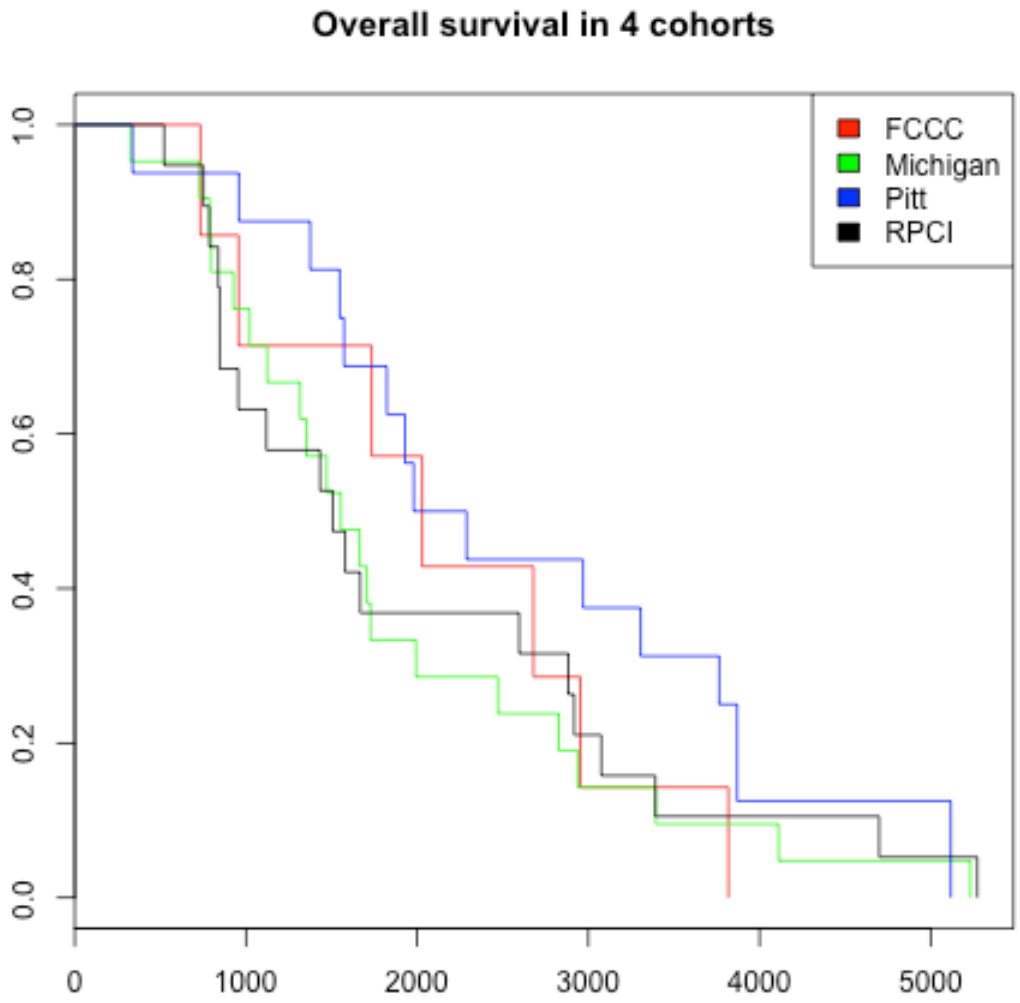

Figure 30: Kaplan-Meier analysis of overall survival in patient cohorts from Chapter 2. Y-axis shows fraction survival. X-axis shows overall survival (days).

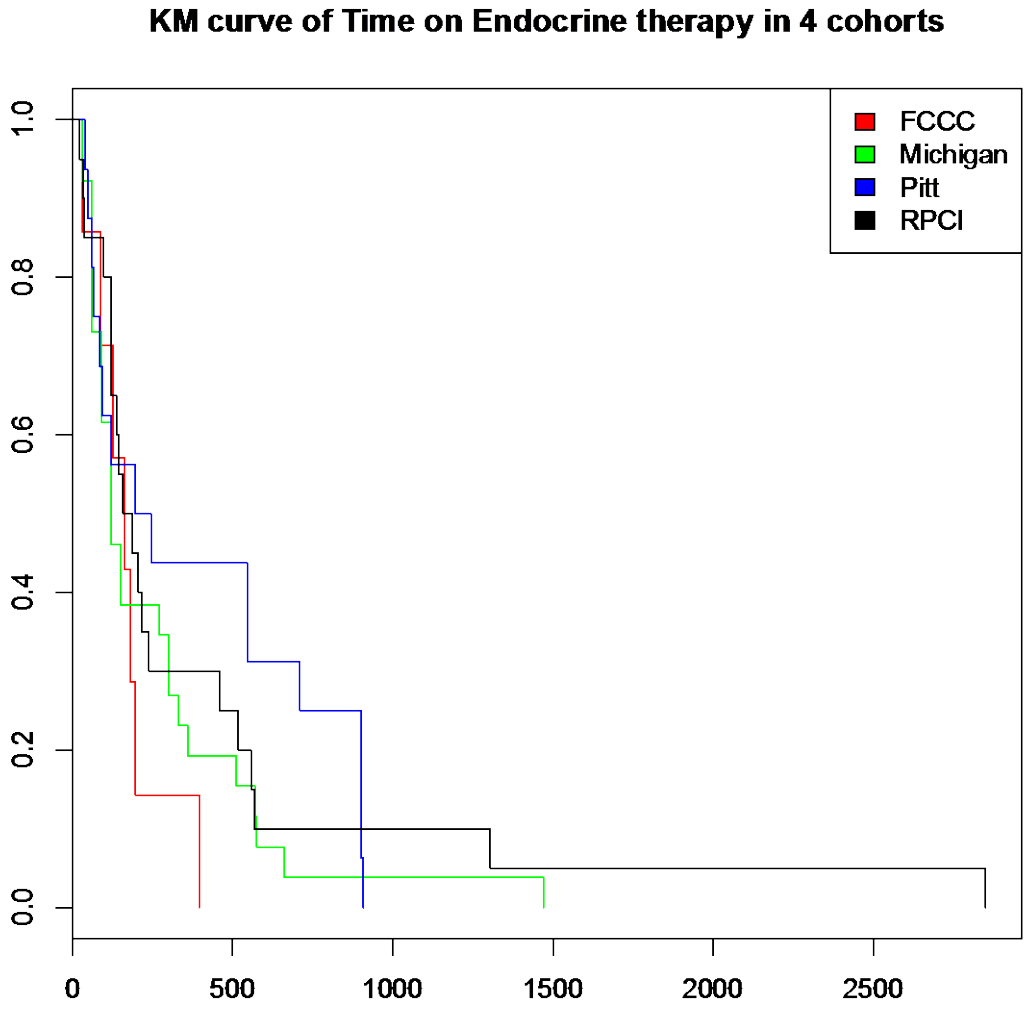

Figure 31: Kaplan-Meier analysis of time on endocrine therapy in patient cohorts in Chapter 2. Plot shows fraction survival on y-axis and time on endocrine therapy (days) on x.

D.2 NANOSTRING DATA ACROSS PATIENT COHORTS

Comparisons of NanoString data also revealed no significant sub-cohort associations with regard to either gene expression patterns (Fig. 32) or total number of counts per sample (Fig. 33).

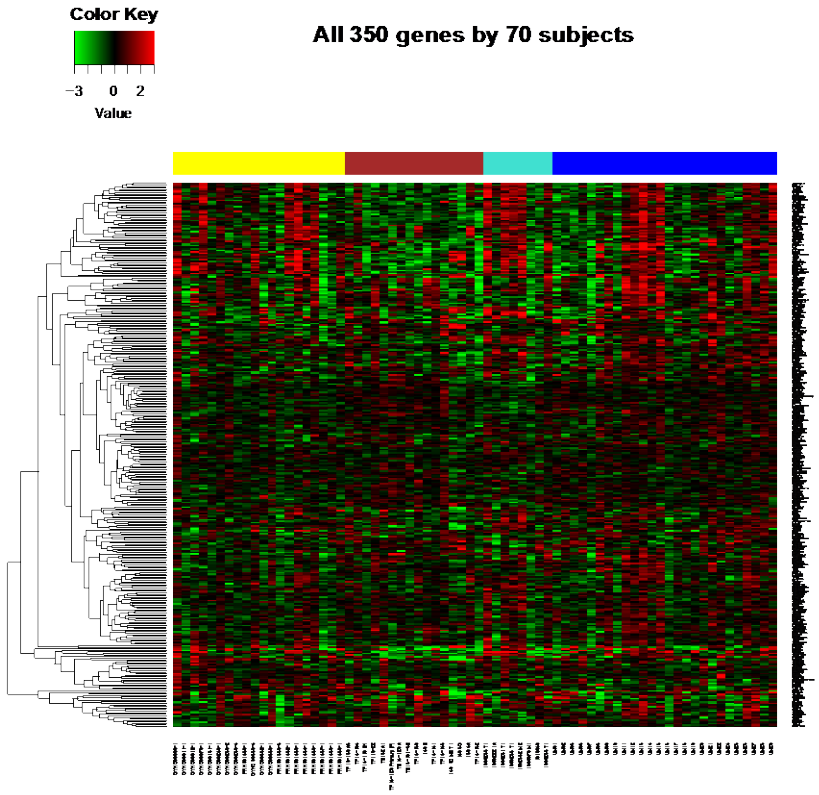

Figure 32: EndoRx gene expression by all 70 HGSOC patients. We compared expression of all 350 genes in the EndoRx code set to check for gene expression batch effects from each tissue source site.

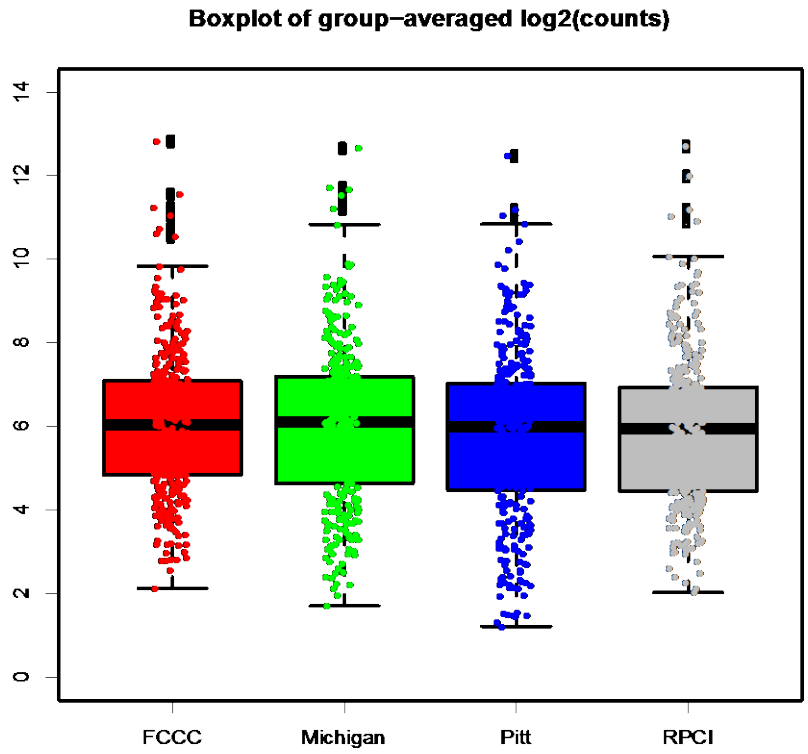

Figure 33: Comparison of total library counts from HGSOC samples across sites. As an additional batch effect test, we compared total NanoString counts across different tissue source sites.

APPENDIX E

ADDITIONAL IMMUNOBLOTS SHOWING ER TURNOVER

This appendix contains the additional blots comparing ER degradation in 2-D vs. ULA, initially described in Section 3.2. Hormone-deprived cells were plated in 2-D or ULA and treated with vhc, E2, ICI, or 4OHT as indicated. ER levels were assessed by immunoblot. No significant difference was observed in degradation between 2-D and ULA for any of the cell lines assessed.

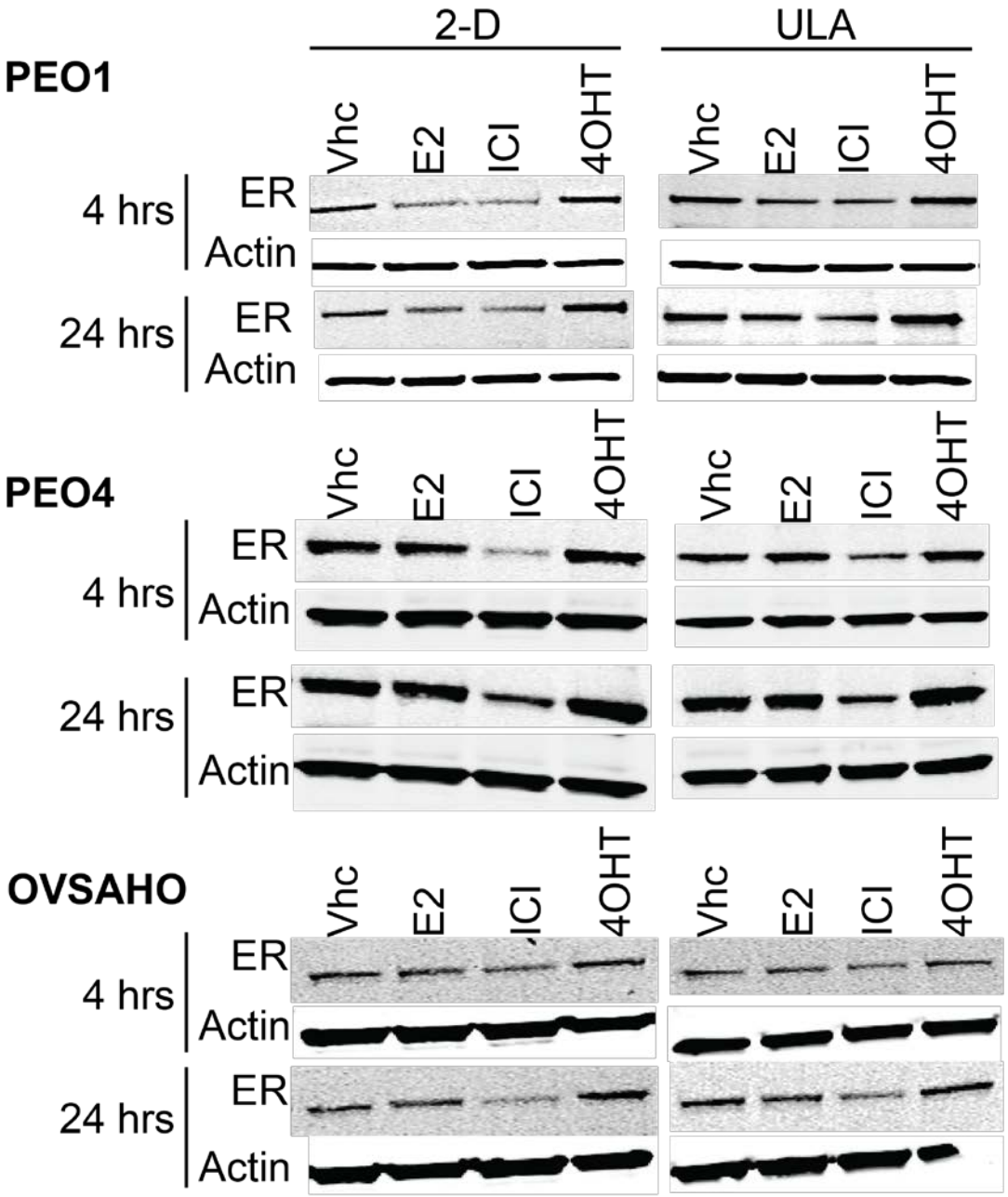

Figure 34: ER degradation in 2-D and ULA. Hormone-deprived cells were plated in 2-D or ULA and treated with vehicle, 1 nM E2, 1 μM ICI, or 1 μM 4OHT for 4 or 24 hours as indicated. Performed by M. Boisen.

APPENDIX F

SUPPLEMENTARY DATA FROM CHAPTER 4

F.1 EFFECT OF MENOPAUSAL STATUS ON E2SIG EXPRESSION

This appendix contains supplementary data for Chapter 4. We first compared gene expression between samples from pre-menopausal and post-menopausal patients. The heat map below

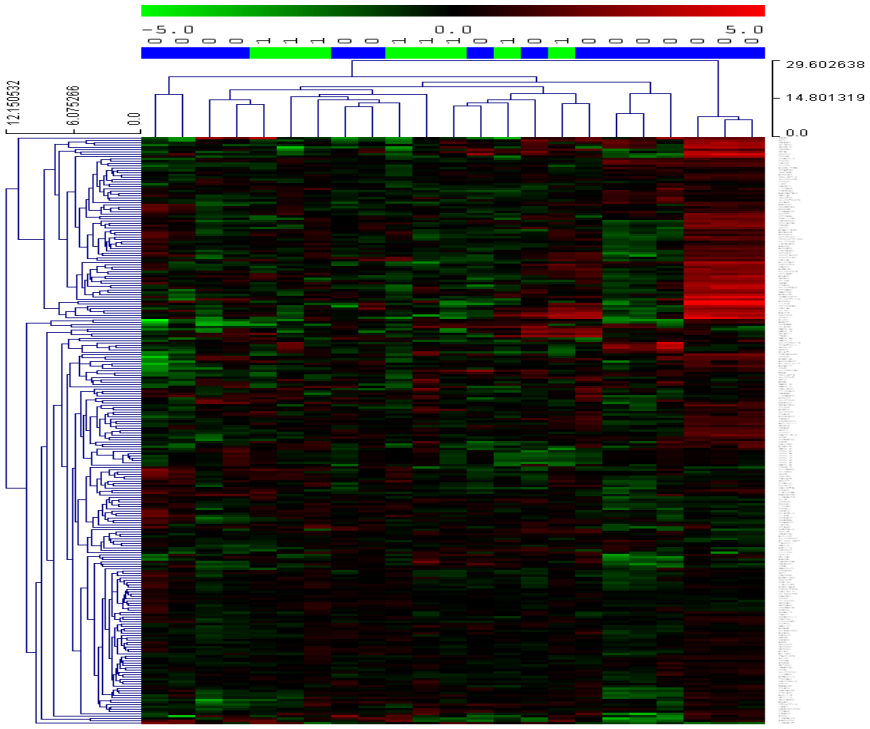

Figure 35: Changes in gene expression across normal endometrium samples by menopausal status. Heat map is colored by log2FC expression vs. median for each gene. Color bar above the heat map reflects pre- (blue) or post-menopause (green).

depicts gene expression across all normal endometrium samples. Pre- and post-menopausal cases did not cluster independently.

F.2 DIFFERENTIALLY EXPRESSED GENES BETWEEN NORMAL ENDOMETRIUM, ENDOMETRIOSIS, ATYPICAL ENDOMETRIOSIS, AND EAOC

The table below lists clusters of genes differentially expressed between normal endometrium, benign endometriosis, atypical endometriosis, and EAOC (Fig. 18). Genes were identified by ANOVA as described in Chapter 4.

Table 14: Differentially expressed genes between endometriosis and EAOC.

Cluster 1	Cluster 2	Cluster 3	Cluster 4
TGFA	EZR	FJX1	SLC22A5
C1orf116	KLF5	PSD3	CDCA7
BCAR3	MUC1	RARA	ITPK1
TLE3	CUEDC1	NFIB	MYLIP
KIAA1217	CYB561	NFIA	ZMIZ1
OSBPL3	TJP3	GSN	C5orf13
ITGB4	RAB17	GAS6	CGNL1
SLC7A5	UBE2H	DNAJB4	GREB1
BCL2L11	FZD6	FBXO32	OLFML3
PTPRE	NCOA3	IGFBP5	RNF144A
SHB	PAX8	CALD1	OLFM1
IFNAR2	SLC25A29	IGFBP4	WT1
ARL4C	SLC30A1	VIM	LONRF2
MARCKS	ENPP5	GFRA2	ZBTB38
NCF2	CPD	TIPARP	PRLR
PLAU	SCD	FOS	DAAM1
SLC39A14	PKP2	DUSP1	EGFR
ADM	MYB	THBS1	RND3
TAPBP	DEPDC6	CYR61	ESR1
PRKCD	BICD1	ARNTL	PGR
LIMK2	MCM10		MTUS1
GCLM	UHRF		ZFP36L2

LRP8	DTL	CAMK2D
RNF213	PPAT	PODXL
RHOF	GINS2	MLPH
RASGRP1	ONECUT2	ALDH3A2
FGF18	PTPRH	NCOR1
CTSC	HNF1B	ARID5B
PDGFRL	PDZK1	PPP1R3C
SLC7A2	SLC2A1	ASCL1
PDK3	MPZL2	C20orf160
PLOD2	EHF	SAMD4A
ESR2	TMPRSS2	TUBB2A
PHLDA1	CA8	RHOQ
GALNT10	FAM174B	INPP4B
RHOBTB3	TRAP1	TXNIP
TSPAN5	SLC35A3	CEP68
	TPD52L1	C6orf89
	TP53	LIFR
	HELLS	NCOA1
	AKAP1	USP25
	RBBP8	
	NCOA2	
	MDN1	
	RIF1	
	NRIP1	
	C19orf6	
	USP53	
	TGIF2	
	MPPED2	
	SPDEF	
	GALNT4	
	FAM46C	
	ATP2A3	
	SIX1	
	BMP7	
	ID2	
	EPHA4	
	IGFBP3	
	DKK1	

F.3 FGF18 IS ESTROGEN-REPRESSED IN OVARIAN CANCER.

FGF18 was one of the 207 genes identified by meta-analysis that was included in the E2sig. FGF18 is an estrogen-repressed gene. Below are data from our preclinical models (cell lines and explants) supporting this.

In PH053 explants, FGF18 expression was increased by the addition of ICI or 4OHT (Fig. 36, not significant). RNA from the explant experiments described in chapter 2 was run on the NanoString platform. Samples from three wells were pooled (n=3 explant pieces per well) to generate three replicates.

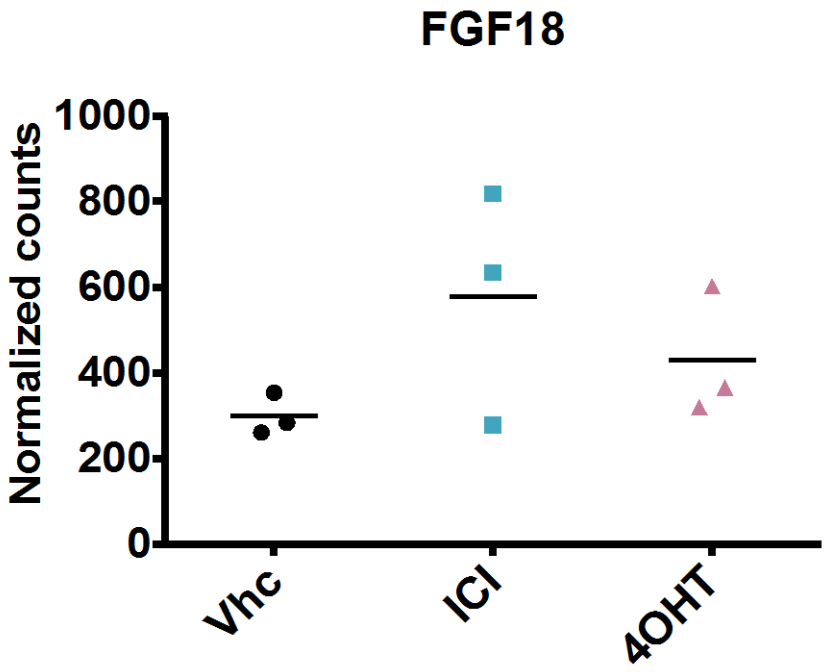

Figure 36: ER-regulated FGF18 expression in PH053 explants. Samples from three wells (n =3 explant pieces per sponge) were pooled to generate replicates. Gene expression was analyzed by NanoString. NanoString analysis was performed as described in Chapter 2. Each dot represents a pooled sample. Bars show median.

In PEO4 cells, FGF18 was significantly repressed by 8-hour treatment with E2 (p=0.001). This repression was blocked by addition of ICI (Fig. 37). The data shown below are from the NanoString experiment described in Chapter 2. Notably, FGF18 was also significantly repressed by E2 in the microarray analyses (Fig. 3, Table 13).

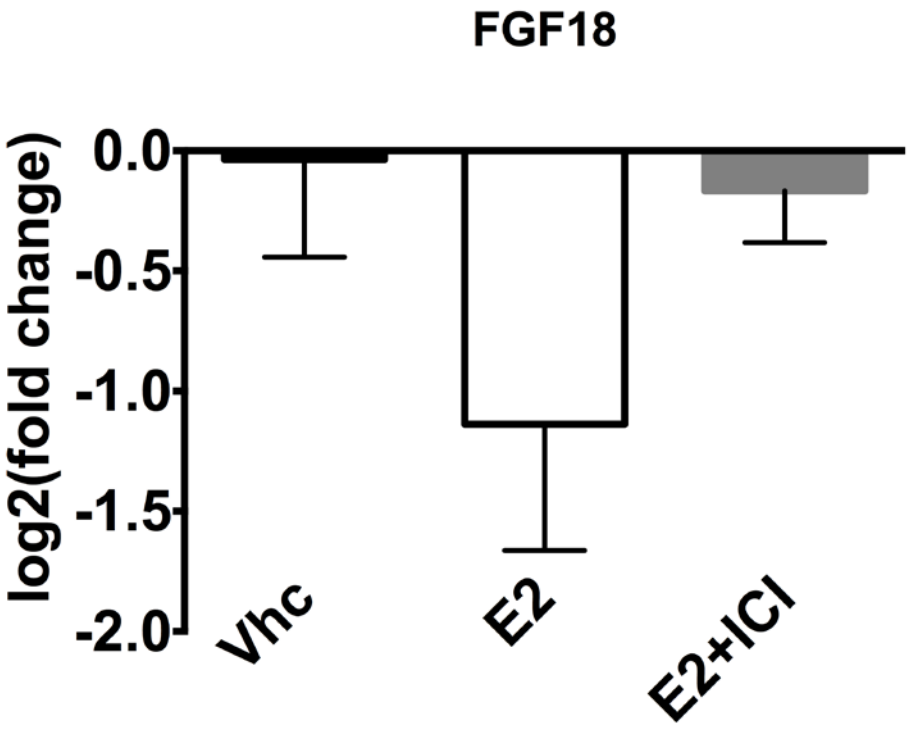

Figure 37: FGF18 is E2-repressed in PEO4 cells. PEO4 cells were treated with vhc, 1 nM E2, or 1 nM E2 + 1 μM ICI for 8 hours. Gene expression was analyzed by NanoString as described in Chapter 2. Bars represent the average of three biological replicates. Error bars show standard deviation. Significance was determined by one-way ANOVA.

BIBLIOGRAPHY

1. Siegel, R. L., Miller, K. D. & Jemal, A. Cancer statistics, 2016. *CA. Cancer J. Clin.* **66,** n/a–n/a (2015).

2. Goff, B. A. *et al.* Clear cell carcinoma of the ovary: a distinct histologic type with poor prognosis and resistance to platinum-based chemotherapy in stage III disease. *Gynecol. Oncol.* **60,** 412–7 (1996).

3. Bankhead, C. R. *et al.* Identifying symptoms of ovarian cancer: a qualitative and quantitative study. *BJOG* **115,** 1008–14 (2008).

4. Romero, I. & Bast, R. C. Minireview: human ovarian cancer: biology, current management, and paths to personalizing therapy. *Endocrinology* **153,** 1593–602 (2012).

5. Zaino, R. J. *et al.* Advanced stage mucinous adenocarcinoma of the ovary is both rare and highly lethal: a Gynecologic Oncology Group study. *Cancer* **117,** 554–62 (2011).

6. Seidman, J. D. *et al.* The histologic type and stage distribution of ovarian carcinomas of surface epithelial origin. *Int. J. Gynecol. Pathol.* **23,** 41–4 (2004).

7. Chandler, R. L. *et al.* Coexistent ARID1A–PIK3CA mutations promote ovarian clear-cell tumorigenesis through pro-tumorigenic inflammatory cytokine signalling. *Nat. Commun.* **6,** 6118 (2015).

8. Anglesio, M. S. *et al.* Molecular characterization of mucinous ovarian tumours supports a stratified treatment approach with HER2 targeting in 19% of carcinomas. *J. Pathol.* **229,** 111–20 (2013).

9. The Cancer Genome Atlas, Cancer, T. & Atlas, G. Integrated genomic analyses of ovarian carcinoma. *Nature* **474,** 609–15 (2011).

10. Bowtell, D. D. *et al.* Rethinking ovarian cancer II: reducing mortality from high-grade serous ovarian cancer. *Nat. Rev. Cancer* **15,** 668–79 (2015).

11. Tothill, R. W. *et al.* Novel molecular subtypes of serous and endometrioid ovarian cancer linked to clinical outcome. *Clin. Cancer Res.* **14,** 5198–5208 (2008).

12. Karst, A. M., Levanon, K. & Drapkin, R. Modeling high-grade serous ovarian carcinogenesis from the fallopian tube. *Proc. Natl. Acad. Sci. U. S. A.* **108,** 7547–52 (2011).

13. Levanon, K. *et al.* Primary ex vivo cultures of human fallopian tube epithelium as a model for serous ovarian carcinogenesis. *Oncogene* **29,** 1103–13 (2010).

14. Lee, A. W. *et al.* Evidence of a genetic link between endometriosis and ovarian cancer. *Fertil. Steril.* (2015). doi:10.1016/j.fertnstert.2015.09.023

15. Qiu, L. *et al.* The occurrence of endometriosis with ovarian carcinomas is not purely coincidental. *Eur. J. Obstet. Gynecol. Reprod. Biol.* (2013). doi:10.1016/j.ejogrb.2013.06.015

16. Wiegand, K. C. *et al.* ARID1A mutations in endometriosis-associated ovarian carcinomas. *N. Engl. J. Med.* **363,** 1532–43 (2010).

17. Sato, N. *et al.* Loss of heterozygosity on 10q23.3 and mutation of the tumor suppressor gene PTEN in benign endometrial cyst of the ovary: possible sequence progression from benign endometrial cyst to endometrioid carcinoma and clear cell carcinoma of the ovary. *Cancer Research* (2000). at <http://www.ncbi.nlm.nih.gov/pubmed/11156411>

18. Sainz de la Cuesta, R. *et al.* Histologic transformation of benign endometriosis to early epithelial ovarian cancer. *Gynecologic Oncology* (1995). at <http://www-ncbi-nlm-nih-gov.pitt.idm.oclc.org/pubmed/8631545>

19. Jayson, G. C., Kohn, E. C., Kitchener, H. C. & Ledermann, J. A. Ovarian cancer. *Lancet (London, England)* **384,** 1376–88 (2014).

20. McGuire, W. P. & Markman, M. Primary ovarian cancer chemotherapy: current standards of care. *Br. J. Cancer* **89,** S3–S8 (2003).

21. Wiltshaw, E. & Kroner, T. Phase II study of cis-dichlorodiammineplatinum(II) (NSC-119875) in advanced adenocarcinoma of the ovary. *Cancer Treat. Rep.* **60,** 55–60 (1976).

22. Williams, C. J. *et al.* Cisplatin combination chemotherapy versus chlorambucil in advanced ovarian carcinoma: mature results of a randomized trial. *J. Clin. Oncol.* **3,** 1455–62 (1985).

23. McGuire, W. P. & Markman, M. Primary ovarian cancer chemotherapy: current standards of care. *Br. J. Cancer* **89 Suppl 3,** S3–8 (2003).

24. Group, T. I. C. O. N. (ICON). Paclitaxel plus carboplatin versus standard chemotherapy with either single-agent carboplatin or cyclophosphamide, doxorubicin, and cisplatin in women with ovarian cancer: the ICON3 randomised trial. *Lancet (London, England)* **360,** 505–15 (2002).

25. Helm, C. W. & Edwards, R. P. Ovarian Cancer Treatment Protocols. *Medscape* (2015). at <http://emedicine.medscape.com/article/2006723-overview>

26. Davis, A., Tinker, A. V. & Friedlander, M. 'Platinum resistant' ovarian cancer: What is it, who to treat and how to measure benefit? *Gynecol. Oncol.* (2014). doi:10.1016/j.ygyno.2014.02.038

27. Bookman, M. A. Evaluation of Monoclonal Humanized Anti-HER2 Antibody, Trastuzumab, in Patients With Recurrent or Refractory Ovarian or Primary Peritoneal Carcinoma With Overexpression of HER2: A Phase II Trial of the Gynecologic Oncology Group. *J. Clin. Oncol.* **21,** 283–290 (2003).

28. Makhija, S. *et al.* Clinical activity of gemcitabine plus pertuzumab in platinum-resistant ovarian cancer, fallopian tube cancer, or primary peritoneal cancer. *J. Clin. Oncol.* **28,** 1215–23 (2010).

29. Garcia, A. A. *et al.* A phase II evaluation of lapatinib in the treatment of persistent or recurrent epithelial ovarian or primary peritoneal carcinoma: a gynecologic oncology group study. *Gynecol. Oncol.* **124,** 569–74 (2012).

30. Gordon, M. S. *et al.* Clinical activity of pertuzumab (rhuMAb 2C4), a HER dimerization inhibitor, in advanced ovarian cancer: potential predictive relationship with tumor HER2 activation status. *J. Clin. Oncol.* **24,** 4324–32 (2006).

31. Coleman, R. L. *et al.* Phase II trial of imatinib mesylate in patients with recurrent platinum- and taxane-resistant epithelial ovarian and primary peritoneal cancers. *Gynecol. Oncol.* **101,** 126–31 (2006).

32. Matei, D. *et al.* Imatinib mesylate in combination with docetaxel for the treatment of patients with advanced, platinum-resistant ovarian cancer and primary peritoneal carcinomatosis : a Hoosier Oncology Group trial. *Cancer* **113,** 723–32 (2008).

33. Schilder, R. J. *et al.* Phase II evaluation of imatinib mesylate in the treatment of recurrent or persistent epithelial ovarian or primary peritoneal carcinoma: a Gynecologic Oncology Group Study. *J. Clin. Oncol.* **26,** 3418–25 (2008).

34. Schilder, R. J. *et al.* Phase II evaluation of dasatinib in the treatment of recurrent or persistent epithelial ovarian or primary peritoneal carcinoma: a Gynecologic Oncology Group study. *Gynecol. Oncol.* **127,** 70–4 (2012).

35. Behbakht, K. *et al.* Phase II trial of the mTOR inhibitor, temsirolimus and evaluation of circulating tumor cells and tumor biomarkers in persistent and recurrent epithelial ovarian and primary peritoneal malignancies: a Gynecologic Oncology Group study. *Gynecol. Oncol.* **123,** 19–26 (2011).

36. Campos, S. M. *et al.* A phase II trial of Sunitinib malate in recurrent and refractory ovarian, fallopian tube and peritoneal carcinoma. *Gynecol. Oncol.* **128,** 215–20 (2013).

37. Rocereto, T. F., Saul, H. M., Aikins, J. A. & Paulson, J. Phase II study of mifepristone (RU486) in refractory ovarian cancer. *Gynecol. Oncol.* **77,** 429–32 (2000).

38. Rocereto, T. F. *et al.* A phase II evaluation of mifepristone in the treatment of recurrent or persistent epithelial ovarian, fallopian or primary peritoneal cancer: a gynecologic oncology group study. *Gynecol. Oncol.* **116,** 332–4 (2010).

39. Miyake, T. M., Sood, A. K. & Coleman, R. L. Contemporary use of bevacizumab in ovarian cancer. *Expert Opin. Biol. Ther.* **13,** 283–94 (2013).

40. Cohn, D. E., Kim, K. H., Resnick, K. E., O'Malley, D. M. & Straughn, J. M. At what cost does a potential survival advantage of bevacizumab make sense for the primary treatment of ovarian cancer? A cost-effectiveness analysis. *J. Clin. Oncol.* **29,** 1247–51 (2011).

41. Chan, J. K. *et al.* Bevacizumab in treatment of high-risk ovarian cancer--a cost-effectiveness analysis. *Oncologist* **19,** 523–7 (2014).

42. Kim, G. *et al.* FDA Approval Summary: Olaparib Monotherapy in Patients with Deleterious Germline BRCA-Mutated Advanced Ovarian Cancer Treated with Three or More Lines of Chemotherapy. *Clin. Cancer Res.* **21,** 4257–61 (2015).

43. Weroha, S. J. *et al.* Phase II trial of lapatinib and topotecan (LapTop) in patients with platinum-refractory/resistant ovarian and primary peritoneal carcinoma. *Gynecol. Oncol.* **122,** 116–20 (2011).

44. Baratta, M. G. *et al.* An in-tumor genetic screen reveals that the BET bromodomain protein, BRD4, is a potential therapeutic target in ovarian carcinoma. *Proc. Natl. Acad. Sci. U. S. A.* 6–11 (2014). doi:10.1073/pnas.1422165112

45. Helming, K. C. *et al.* ARID1B is a specific vulnerability in ARID1A-mutant cancers. *Nat. Med.* **20,** 251–4 (2014).

46. Delgado, E. *et al.* High expression of orphan nuclear receptor NR4A1 in a subset of ovarian tumors with worse outcome. *Under Rev.*

47. Aghmesheh, M. *et al.* Expression of steroid hormone receptors in BRCA1-associated ovarian carcinomas. *Gynecol. Oncol.* **97,** 16–25 (2005).

48. Arias-Pulido, H. *et al.* Estrogen and progesterone receptor status and outcome in epithelial ovarian cancers and low malignant potential tumors. *Gynecol. Oncol.* **114,** 480–5 (2009).

49. Sieh, W. *et al.* Hormone-receptor expression and ovarian cancer survival: an Ovarian Tumor Tissue Analysis consortium study. *Lancet Oncol.* (2013). doi:10.1016/S1470-2045(13)70253-5

50. Toft, D. & Gorski, J. A receptor molecule for estrogens: isolation from the rat uterus and preliminary characterization. *Proc. Natl. Acad. Sci. U. S. A.* **55,** 1574–81 (1966).

51. Kuiper, G. G., Enmark, E., Pelto-Huikko, M., Nilsson, S. & Gustafsson, J. A. Cloning of a novel receptor expressed in rat prostate and ovary. *Proc. Natl. Acad. Sci. U. S. A.* **93,** 5925–30 (1996).

52. Burges, A. *et al.* Prognostic significance of estrogen receptor alpha and beta expression in human serous carcinomas of the ovary. *Arch. Gynecol. Obstet.* **281,** 511–7 (2010).

53. Bossard, C. *et al.* Potential role of estrogen receptor Beta as a tumor suppressor of epithelial ovarian cancer. *PLoS One* **7,** e44787 (2012).

54. Halon, A. *et al.* Loss of estrogen receptor beta expression correlates with shorter overall survival and lack of clinical response to chemotherapy in ovarian cancer patients. *Anticancer Res.* **31,** 711–8 (2011).

55. Jordan, V. C. Effect of tamoxifen (ICI 46,474) on initiation and growth of DMBA-induced rat mammary carcinomata. *Eur. J. Cancer* **12,** 419–24 (1976).

56. Jordan, V. C., Koerner, S. & Robison, C. Inhibition of oestrogen-stimulated prolactin release by anti-oestrogens. *J. Endocrinol.* **65,** 151–2 (1975).

57. Tamoxifen for early breast cancer: an overview of the randomised trials. Early Breast Cancer Trialists' Collaborative Group. *Lancet (London, England)* **351,** 1451–67 (1998).

58. McDonnell, D. P. & Wardell, S. E. The molecular mechanisms underlying the pharmacological actions of ER modulators: implications for new drug discovery in breast cancer. *Curr. Opin. Pharmacol.* **10,** 620–8 (2010).

59. Huynh, H. T. & Pollak, M. Insulin-like growth factor I gene expression in the uterus is stimulated by tamoxifen and inhibited by the pure antiestrogen ICI 182780. *Cancer Res* **53,** 5585–5588 (1993).

60. Regan, R. M. O. *et al.* Effects of the Antiestrogens Tamoxifen , Toremifene , and ICI 182 , 780 on Endometrial Cancer Growth. **90,** (1998).

61. Wakeling, A. E. & Bowler, J. Steroidal pure antioestrogens. *J. Endocrinol.* **112,** R7–10 (1987).

62. Osborne, C. K. *et al.* Comparison of the effects of a pure steroidal antiestrogen with those of tamoxifen in a model of human breast cancer. *J. Natl. Cancer Inst.* **87,** 746–50 (1995).

63. McClelland, R. A. *et al.* Short-term effects of pure anti-oestrogen ICI 182780 treatment on oestrogen receptor, epidermal growth factor receptor and transforming growth factor-alpha protein expression in human breast cancer. *Eur. J. Cancer* **32A,** 413–6 (1996).

64. Santen, R. J., Brodie, H., Simpson, E. R., Siiteri, P. K. & Brodie, a. History of aromatase: saga of an important biological mediator and therapeutic target. *Endocr. Rev.* **30,** 343–75 (2009).

65. Grodin, J. M., Siiteri, P. K. & MacDonald, P. C. Source of estrogen production in postmenopausal women. *J. Clin. Endocrinol. Metab.* **36,** 207–14 (1973).

66. Geisler, J. Differences between the non-steroidal aromatase inhibitors anastrozole and letrozole--of clinical importance? *Br. J. Cancer* **104,** 1059–66 (2011).

67. Lu, Q. *et al.* Expression of aromatase protein and messenger ribonucleic acid in tumor epithelial cells and evidence of functional significance of locally produced estrogen in human breast cancers. *Endocrinology* **137,** 3061–8 (1996).

68. Tilson-Mallett, N., Santner, S. J., Feil, P. D. & Santen, R. J. Biological significance of aromatase activity in human breast tumors. *J. Clin. Endocrinol. Metab.* **57,** 1125–8 (1983).

69. Modugno, F., Ness, R. B. & Wheeler, J. E. Reproductive risk factors for epithelial ovarian cancer according to histologic type and invasiveness. *Ann. Epidemiol.* **11,** 568–74 (2001).

70. Tsilidis, K. K. *et al.* Oral contraceptive use and reproductive factors and risk of ovarian cancer in the European Prospective Investigation into Cancer and Nutrition. *Br. J. Cancer* **105,** 1436–42 (2011).

71. Tung, K.-H. Reproductive Factors and Epithelial Ovarian Cancer Risk by Histologic Type:A Multiethnic Case-Control Study. *Am. J. Epidemiol.* **158,** 629–638 (2003).

72. Gong, T.-T., Wu, Q.-J., Vogtmann, E., Lin, B. & Wang, Y.-L. Age at menarche and risk of ovarian cancer: a meta-analysis of epidemiological studies. *Int. J. Cancer* **132,** 2894–900 (2013).

73. Greer, J. B., Modugno, F., Allen, G. O. & Ness, R. B. Androgenic progestins in oral contraceptives and the risk of epithelial ovarian cancer. *Obstet. Gynecol.* **105,** 731–40 (2005).

74. Beral, V., Doll, R., Hermon, C., Peto, R. & Reeves, G. Ovarian cancer and oral contraceptives: collaborative reanalysis of data from 45 epidemiological studies including 23,257 women with ovarian cancer and 87,303 controls. *Lancet (London, England)* **371,** 303–14 (2008).

75. Goodman, M. T., Lurie, G., Thompson, P. J., McDuffie, K. E. & Carney, M. E. Association of two common single-nucleotide polymorphisms in the CYP19A1 locus and ovarian cancer risk. *Endocr. Relat. Cancer* **15,** 1055–60 (2008).

76. Forbes, J. F. *et al.* Anastrozole versus tamoxifen for the prevention of locoregional and contralateral breast cancer in postmenopausal women with locally excised ductal carcinoma in situ (IBIS-II DCIS): a double-blind, randomised controlled trial. *Lancet (London, England)* (2015). doi:10.1016/S0140-6736(15)01129-0

77. Group, C. *et al.* Menopausal hormone use and ovarian cancer risk: individual participant meta-analysis of 52 epidemiological studies. *Lancet* **6736,** 1835–42 (2015).

78. Zhou, B. *et al.* Hormone replacement therapy and ovarian cancer risk: a meta-analysis. *Gynecol. Oncol.* **108,** 641–51 (2008).

79. Mørch, L. S., Løkkegaard, E., Andreasen, A. H., Kjaer, S. K. & Lidegaard, O. Hormone therapy and different ovarian cancers: a national cohort study. *Am. J. Epidemiol.* **175,** 1234–42 (2012).

80. Yang, H. P. *et al.* Ovarian cancer incidence trends in relation to changing patterns of menopausal hormone therapy use in the United States. *J. Clin. Oncol.* **31,** 2146–51 (2013).

81. Modugno, F. *et al.* Hormone response in ovarian cancer: time to reconsider as a clinical target? *Endocr. Relat. Cancer* **19,** R255–79 (2012).

82. Simpkins, F., Garcia-Soto, A. & Slingerland, J. New insights on the role of hormonal therapy in ovarian cancer. *Steroids* (2013).

83. Boisen, M. M., Andersen, C. L., Sreekumar, S., Stern, A. M. & Oesterreich, S. Treating gynecologic malignancies with selective estrogen receptor downregulators (SERDs): promise and challenges. *Mol. Cell. Endocrinol.* **418 Pt 3,** 322–33 (2015).

84. Hurteau, J. a *et al.* Randomized phase III trial of tamoxifen versus thalidomide in women with biochemical-recurrent-only epithelial ovarian, fallopian tube or primary peritoneal carcinoma after a complete response to first-line platinum/taxane chemotherapy with an evaluation . *Gynecol. Oncol.* **119,** 444–50 (2010).

85. Tevaarwerk, A. J. *et al.* Phase III Comparison of Tamoxifen Versus Tamoxifen Plus Ovarian Function Suppression in Premenopausal Women With Node-Negative, Hormone Receptor-Positive Breast Cancer (E-3193, INT-0142): A Trial of the Eastern Cooperative Oncology Group. *J. Clin. Oncol.* (2014). doi:10.1200/JCO.2014.55.6993

86. Hatch, K. D., Beecham, J. B., Blessing, J. A. & Creasman, W. T. Responsiveness of patients with advanced ovarian carcinoma to tamoxifen. A Gynecologic Oncology Group study of second-line therapy in 105 patients. *Cancer* **68,** 269–71 (1991).

87. Shirey, D. R. *et al.* Tamoxifen therapy of epithelial ovarian cancer. *Obstet. Gynecol.* **66,** 575–8 (1985).

88. Slevin, M. L. *et al.* A phase II study of tamoxifen in ovarian cancer. *Eur. J. Cancer Clin. Oncol.* **22,** 309–12 (1986).

89. Belinson, J. L., McClure, M. & Badger, G. Randomized trial of megestrol acetate vs. megestrol acetate/tamoxifen for the management of progressive or recurrent epithelial ovarian carcinoma. *Gynecol. Oncol.* **28,** 151–5 (1987).

90. Benedetti Panici, P. *et al.* A combination of platinum and tamoxifen in advanced ovarian cancer failing platinum-based chemotherapy: results of a Phase II study. *Int. J. Gynecol. Cancer* **11,** 438–44

91. Hofstra, L. S., Mourits, M. J., de Vries, E. G., Mulder, N. H. & Willemse, P. H. Combined treatment with goserelin and tamoxifen in patients with advanced chemotherapy resistant ovarian cancer. *Anticancer Res.* **19,** 3627–30

92. Hasan, J. *et al.* Phase II trial of tamoxifen and goserelin in recurrent epithelial ovarian cancer. *Br. J. Cancer* **93,** 647–51 (2005).

93. Tropé, C., Marth, C. & Kaern, J. Tamoxifen in the treatment of recurrent ovarian carcinoma. *Eur. J. Cancer* **36 Suppl 4,** S59–61 (2000).

94. Weiner, S. A., Alberts, D. S., Surwit, E. A., Davis, J. & Grosso, D. Tamoxifen therapy in recurrent epithelial ovarian carcinoma. *Gynecol. Oncol.* **27,** 208–13 (1987).

95. Ramirez, P. T. *et al.* Efficacy of letrozole in the treatment of recurrent platinum- and taxane-resistant high-grade cancer of the ovary or peritoneum. *Gynecol. Oncol.* **110,** 56–9 (2008).

96. Smyth, J. F. *et al.* Antiestrogen therapy is active in selected ovarian cancer cases: the use of letrozole in estrogen receptor-positive patients. *Clin. Cancer Res.* **13,** 3617–22 (2007).

97. Del Carmen, M. G. *et al.* Phase II trial of anastrozole in women with asymptomatic müllerian cancer. *Gynecol. Oncol.* **91,** 596–602 (2003).

98. Ahlgren, J. D. *et al.* Hormonal palliation of chemoresistant ovarian cancer: three consecutive phase II trials of the Mid-Atlantic Oncology Program. *J. Clin. Oncol.* **11,** 1957–68 (1993).

99. Argenta, P. A. *et al.* A phase II study of fulvestrant in the treatment of multiply-recurrent epithelial ovarian cancer. *Gynecol. Oncol.* **113,** 205–9 (2009).

100. Group, C. & Cancer, O. Menopausal hormone use and ovarian cancer risk: individual participant meta-analysis of 52 epidemiological studies. *Lancet* **385,** 1835–1842 (2015).

101. Hammond, M. E. H. *et al.* American Society of Clinical Oncology/College of American Pathologists guideline recommendations for immunohistochemical testing of estrogen and progesterone receptors in breast cancer (unabridged version). *Arch. Pathol. Lab. Med.* **134,** e48–72 (2010).

102. Deyarmin, B. *et al.* Effect of ASCO/CAP guidelines for determining ER status on molecular subtype. *Ann. Surg. Oncol.* **20,** 87–93 (2013).

103. Harbeck, N. & Rody, A. Lost in translation? Estrogen receptor status and endocrine responsiveness in breast cancer. *J. Clin. Oncol.* **30,** 686–9 (2012).

104. Prabhu, J. S. *et al.* A Majority of Low (1-10%) ER Positive Breast Cancers Behave Like Hormone Receptor Negative Tumors. *J. Cancer* **5,** 156–65 (2014).

105. Argenta, P. a *et al.* Predicting response to the anti-estrogen fulvestrant in recurrent ovarian cancer. *Gynecol. Oncol.* (2013). doi:10.1016/j.ygyno.2013.07.099

106. Walker, G. *et al.* Estrogen-regulated gene expression predicts response to endocrine therapy in patients with ovarian cancer. *Gynecol. Oncol.* **106,** 461–8 (2007).

107. Stasenko, M., Plegue, M., Sciallis, A. P. & McLean, K. Clinical Response to Antiestrogen Therapy in Platinum-Resistant Ovarian Cancer Patients and the Role of Tumor Estrogen Receptor Expression Status. *Int. J. Gynecol. Cancer* **00,** 1–7 (2014).

108. Papadimitriou, C. A. *et al.* Hormonal therapy with letrozole for relapsed epithelial ovarian cancer. Long-term results of a phase II study. *Oncology* **66,** 112–7 (2004).

109. Carroll, J. S. *et al.* Genome-wide analysis of estrogen receptor binding sites. *Nat. Genet.* **38,** 1289–97 (2006).

110. Stossi, F. *et al.* Transcriptional profiling of estrogen-regulated gene expression via estrogen receptor (ER) alpha or ERbeta in human osteosarcoma cells: distinct and common target genes for these receptors. *Endocrinology* **145,** 3473–86 (2004).

111. Madak-Erdogan, Z. *et al.* Integrative genomics of gene and metabolic regulation by estrogen receptors α and β, and their coregulators. *Mol. Syst. Biol.* **9,** 676 (2013).

112. Oñate, S. A., Tsai, S. Y., Tsai, M. J. & O'Malley, B. W. Sequence and characterization of a coactivator for the steroid hormone receptor superfamily. *Science* **270,** 1354–7 (1995).

113. Johnson, A. B. & O'Malley, B. W. Steroid receptor coactivators 1, 2, and 3: critical regulators of nuclear receptor activity and steroid receptor modulator (SRM)-based cancer therapy. *Mol. Cell. Endocrinol.* **348,** 430–9 (2012).

114. Yi, P. *et al.* Structure of a biologically active estrogen receptor-coactivator complex on DNA. *Mol. Cell* **57,** 1047–58 (2015).

115. Katzenellenbogen, B. S. *et al.* Estrogen receptors: selective ligands, partners, and distinctive pharmacology. *Recent Prog. Horm. Res.* **55,** 163–93; discussion 194–5 (2000).

116. Smith, C. L., Nawaz, Z. & O'Malley, B. W. Coactivator and corepressor regulation of the agonist/antagonist activity of the mixed antiestrogen, 4-hydroxytamoxifen. *Mol. Endocrinol.* **11,** 657–66 (1997).

117. Shang, Y. & Brown, M. Molecular determinants for the tissue specificity of SERMs. *Science* **295,** 2465–8 (2002).

118. Romano, A. *et al.* Identification of novel ER-alpha target genes in breast cancer cells: gene- and cell-selective co-regulator recruitment at target promoters determines the response to 17beta-estradiol and tamoxifen. *Mol. Cell. Endocrinol.* **314,** 90–100 (2010).

119. Britton, D. J. *et al.* Bidirectional cross talk between ERalpha and EGFR signalling pathways regulates tamoxifen-resistant growth. *Breast Cancer Res. Treat.* **96,** 131–46 (2006).

120. Scully, M. M., Palacios-Helgeson, L. K., Wah, L. S. & Jackson, T. A. Rapid Estrogen Signaling Negatively Regulates PTEN Activity Through Phosphorylation in Endometrial Cancer Cells. *Horm. Cancer* (2014). doi:10.1007/s12672-014-0184-z

121. Le Romancer, M. *et al.* Regulation of estrogen rapid signaling through arginine methylation by PRMT1. *Mol. Cell* **31,** 212–21 (2008).

122. Kahlert, S. *et al.* Estrogen receptor alpha rapidly activates the IGF-1 receptor pathway. *J. Biol. Chem.* **275,** 18447–53 (2000).

123. Bonomi, P. *et al.* Quantitative estrogen and progesterone receptor levels related to progression-free interval in advanced breast cancer patients treated with megestrol acetate or tamoxifen. *Semin. Oncol.* **15,** 26–33 (1988).

124. Allegra, J. C. *et al.* Relationship between the progesterone, androgen, and glucocorticoid receptor and response rate to endocrine therapy in metastatic breast cancer. *Cancer Res.* **39,** 1973–9 (1979).

125. Mohammed, H. *et al.* Progesterone receptor modulates ERα action in breast cancer. *Nature* **523,** 313–317 (2015).

126. Lee, P., Rosen, D. G., Zhu, C., Silva, E. G. & Liu, J. Expression of progesterone receptor is a favorable prognostic marker in ovarian cancer. *Gynecol. Oncol.* **96,** 671–7 (2005).

127. Diep, C. H. *et al.* Progesterone receptors induce FOXO1-dependent senescence in ovarian cancer cells. *Cell Cycle* **12,** 1433–49 (2013).

128. Diep, C. H., Knutson, T. P. & Lange, C. A. Active FOXO1 is a Key Determinant of Isoform-Specific Progesterone Receptor Transactivation and Senescence Programming. *Mol. Cancer Res.* (2015). doi:10.1158/1541-7786.MCR-15-0431

129. Geisler, H. E. The use of high-dose megestrol acetate in the treatment of ovarian adenocarcinoma. *Semin. Oncol.* **12,** 20–2 (1985).

130. Tropé, C., Johnsson, J. E., Sigurdsson, K. & Simonsen, E. High-dose medroxyprogesterone acetate for the treatment of advanced ovarian carcinoma. *Cancer Treat. Rep.* **66,** 1441–3 (1982).

131. Mangioni, C., Franceschi, S., La Vecchia, C. & D'Incalci, M. High-dose medroxyprogesterone acetate (MPA) in advanced epithelial ovarian cancer resistant to first- or second-line chemotherapy. *Gynecol. Oncol.* **12,** 314–8 (1981).

132. Spillman, M. a *et al.* Tissue-specific pathways for estrogen regulation of ovarian cancer growth and metastasis. *Cancer Res.* **70,** 8927–36 (2010).

133. Nash, J. D., Ozols, R. F., Smyth, J. F. & Hamilton, T. C. Estrogen and anti-estrogen effects on the growth of human epithelial ovarian cancer in vitro. *Obstet. Gynecol.* **73,** 1009–16 (1989).

134. Romero, I. L. *et al.* The effects of 17β-estradiol and a selective estrogen receptor modulator, bazedoxifene, on ovarian carcinogenesis. *Gynecol. Oncol.* **124,** 134–41 (2012).

135. Docquier, A. *et al.* Negative regulation of estrogen signaling by ERβ and RIP140 in ovarian cancer cells. *Mol. Endocrinol.* (2013). doi:10.1210/me.2012-1351

136. Hua, W., Christianson, T., Rougeot, C., Rochefort, H. & Clinton, G. M. SKOV3 ovarian carcinoma cells have functional estrogen receptor but are growth-resistant to estrogen and antiestrogens. *J. Seroid Biochem. Mol. Biol.* **55,** 279–89 (1995).

137. Runge, H. M., Teufel, G., Neulen, J., Geyer, H. & Pfleiderer, A. In vitro responsiveness of ovarian epithelial carcinomas to endocrine therapy. *Cancer Chemother. Pharmacol.* **16,** 58–63 (1986).

138. Korch, C. *et al.* DNA profiling analysis of endometrial and ovarian cell lines reveals misidentification, redundancy and contamination. *Gynecol. Oncol.* **127,** 241–8 (2012).

139. Domcke, S., Sinha, R., Levine, D. a, Sander, C. & Schultz, N. Evaluating cell lines as tumour models by comparison of genomic profiles. *Nat. Commun.* **4,** 2126 (2013).

140. Anglesio, M. S. *et al.* Type-specific cell line models for type-specific ovarian cancer research. *PLoS One* **8,** e72162 (2013).

141. Simpkins, F. a *et al.* Src inhibition with saracatinib reverses fulvestrant resistance in ER-positive ovarian cancer models in vitro and in vivo. *Clin. Cancer Res.* (2012). doi:10.1158/1078-0432.CCR-12-1257

142. Hirakawa, H., Yokoyama, Y., Yoshida, H. & Mizunuma, H. Inhibitory effects of aromatase inhibitor on estrogen receptor-alpha positive ovarian cancer in mice. *J. Ovarian Res.* **7,** 4 (2014).

143. Laviolette, L. a *et al.* 17Beta-Estradiol Accelerates Tumor Onset and Decreases Survival in a Transgenic Mouse Model of Ovarian Cancer. *Endocrinology* **151,** 929–38 (2010).

144. Laviolette, L. A., Hodgkinson, K. M., Minhas, N., Perez-Iratxeta, C. & Vanderhyden, B. C. 17beta-estradiol upregulates GREB1 and accelerates tumor progression in vivo. *Int. J. Cancer* (2013).

145. Treviño, L. S., Buckles, E. L. & Johnson, P. A. Oral contraceptives decrease the prevalence of ovarian cancer in the hen. *Cancer Prev. Res. (Phila).* **5,** 343–9 (2012).

146. Tkalia, I. G., Vorobyova, L. I., Grabovoy, A. N., Svintsitsky, V. S. & Tarasova, T. O. The antitumor efficacy of cisplatin in combination with triptorelin and exemestane therapy for an ovarian cancer ascites model in Wistar rats. *Exp. Oncol.* **37,** 30–5 (2015).

147. Clinton, G. M. *et al.* Estrogens increase the expression of fibulin-1, an extracellular matrix protein secreted by human ovarian cancer cells. *Proc. Natl. Acad. Sci. U. S. A.* **93,** 316–20 (1996).

148. Langdon, S. P. *et al.* The regulation of growth and protein expression by estrogen in vitro: A study of 8 human ovarian carcinoma cell lines. *J. Steroid Biochem. Mol. Biol.* **50,** 131–135 (1994).

149. O'Donnell, A. J. M., Macleod, K. G., Burns, D. J., Smyth, J. F. & Langdon, S. P. Estrogen receptor-alpha mediates gene expression changes and growth response in ovarian cancer cells exposed to estrogen. *Endocr. Relat. Cancer* **12,** 851–66 (2005).

150. Lengyel, E. *et al.* Epithelial ovarian cancer experimental models. *Oncogene* **33,** 3619–33 (2014).

151. Howell, V. M. Genetically engineered mouse models for epithelial ovarian cancer: are we there yet? *Semin. Cell Dev. Biol.* **27,** 106–17 (2014).

152. Perets, R. *et al.* Transformation of the Fallopian Tube Secretory Epithelium Leads to High-Grade Serous Ovarian Cancer in Brca;Tp53;Pten Models. *Cancer Cell* **24,** 751–765 (2013).

153. Wu, R. *et al.* Mouse model of human ovarian endometrioid adenocarcinoma based on somatic defects in the Wnt/beta-catenin and PI3K/Pten signaling pathways. *Cancer Cell* **11,** 321–33 (2007).

154. Dinulescu, D. M. *et al.* Role of K-ras and Pten in the development of mouse models of endometriosis and endometrioid ovarian cancer. *Nat. Med.* **11,** 63–70 (2005).

155. Scott, C. L., Becker, M. a, Haluska, P. & Samimi, G. Patient-Derived Xenograft Models to Improve Targeted Therapy in Epithelial Ovarian Cancer Treatment. *Front. Oncol.* **3,** 295 (2013).

156. Tentler, J. J. *et al.* Patient-derived tumour xenografts as models for oncology drug development. *Nat. Rev. Clin. Oncol.* **9,** 338–50 (2012).

157. Weroha, S. J. *et al.* Tumorgrafts as in vivo surrogates for women with ovarian cancer. *Clin. Cancer Res.* **20,** 1288–97 (2014).

158. Ricci, F. *et al.* Patient-derived ovarian tumor xenografts recapitulate human clinicopathology and genetic alterations. *Cancer Res.* (2014). doi:10.1158/0008-5472.CAN-14-0274

159. Centenera, M. M., Raj, G. V, Knudsen, K. E., Tilley, W. D. & Butler, L. M. Ex vivo culture of human prostate tissue and drug development. *Nat. Rev. Urol.* **10,** 483–7 (2013).

160. Goodwin, J. F. *et al.* A hormone-DNA repair circuit governs the response to genotoxic insult. *Cancer Discov.* **3,** 1254–71 (2013).

161. Schiewer, M. J. *et al.* Dual roles of PARP-1 promote cancer growth and progression. *Cancer Discov.* **2,** 1134–49 (2012).

162. Centenera, M. M. *et al.* Evidence for efficacy of new Hsp90 inhibitors revealed by ex vivo culture of human prostate tumors. *Clin. Cancer Res.* **18,** 3562–70 (2012).

163. Crystal, a. S. *et al.* Patient-derived models of acquired resistance can identify effective drug combinations for cancer. *Science (80-.).* **8,** 1–50 (2014).

164. Narod, S. A. *et al.* Oral contraceptives and risk of hereidtary ovarian cancer. *N. Engl. J. Med.* **389,** 424–428 (1998).

165. Sikora, M. J. *et al.* Invasive lobular carcinoma cell lines are characterized by unique estrogen-mediated gene expression patterns and altered tamoxifen response. *Cancer Res.* (2014). doi:10.1158/0008-5472.CAN-13-2779

166. Kandoth, C. *et al.* Integrated genomic characterization of endometrial carcinoma. *Nature* **497,** 67–73 (2013).

167. Comprehensive molecular portraits of human breast tumours. *Nature* **490,** 61–70 (2012).

168. Walker, G. *et al.* Insulin-like growth factor binding proteins IGFBP3, IGFBP4, and IGFBP5 predict endocrine responsiveness in patients with ovarian cancer. *Clin. Cancer Res.* **13,** 1438–44 (2007).

169. Langdon, S. P. *et al.* Oestrogen receptor expression and effects of oestrogen and tamoxifen on the growth of human ovarian carcinoma cell lines. *Br. J. Cancer* **1,** 213–216 (1990).

170. Laviolette, L. A., Hodgkinson, K. M., Minhas, N., Perez-Iratxeta, C. & Vanderhyden, B. C. 17β-estradiol upregulates GREB1 and accelerates ovarian tumor progression in vivo. *Int. J. Cancer* (2014). doi:10.1002/ijc.28741

171. Ochsner, S. a *et al.* GEMS (Gene Expression MetaSignatures), a Web resource for querying meta-analysis of expression microarray datasets: 17beta-estradiol in MCF-7 cells. *Cancer Res.* **69,** 23–6 (2009).

172. Goodwin, J. F. *et al.* DNA-PKcs-Mediated Transcriptional Regulation Drives Prostate Cancer Progression and Metastasis. *Cancer Cell* **28,** 97–113 (2015).

173. Augello, M. A. *et al.* Convergence of oncogenic and hormone receptor pathways promotes metastatic phenotypes. *J. Clin. Invest.* **123,** 493–508 (2013).

174. Brown, A. P., Morrissey, R. L., Crowell, J. A. & Levine, B. S. Thirteen-week oral toxicity study of difluoromethylornithine in combination with tamoxifen citrate in female dogs. *Cancer Chemother. Pharmacol.* **43,** 479–88 (1999).

175. Hou, J. Y. *et al.* Exploiting MEK inhibitor-mediated activation of ERα for therapeutic intervention in ER-positive ovarian carcinoma. *PLoS One* **8,** e54103 (2013).

176. Yamnik, R. L. & Holz, M. K. mTOR/S6K1 and MAPK/RSK signaling pathways coordinately regulate estrogen receptor alpha serine 167 phosphorylation. *FEBS Lett.* **584,** 124–8 (2010).

177. Bostner, J. *et al.* Activation of Akt, mTOR, and the estrogen receptor as a signature to predict tamoxifen treatment benefit. *Breast Cancer Res. Treat.* **137,** 397–406 (2013).

178. Beck, J. T. *et al.* Everolimus plus exemestane as first-line therapy in HR^+, $HER2^-$ advanced breast cancer in BOLERO-2. *Breast Cancer Res. Treat.* **143,** 459–67 (2014).

179. Wheler, J. J. *et al.* Anastrozole and everolimus in advanced gynecologic and breast malignancies: activity and molecular alterations in the PI3K/AKT/mTOR pathway. *Oncotarget* **5,** 3029–38 (2014).

180. Sun, X. *et al.* IL-6 secreted by cancer-associated fibroblasts induces tamoxifen resistance in luminal breast cancer. *Oncogene* (2014). doi:10.1038/onc.2014.158

181. Wang, Y. *et al.* Autocrine production of interleukin-6 confers ovarian cancer cells resistance to tamoxifen via ER isoforms and SRC-1. *Mol. Cell. Endocrinol.* (2013). doi:10.1016/j.mce.2013.10.029

182. Peterson, T. R. *et al.* DEPTOR is an mTOR inhibitor frequently overexpressed in multiple myeloma cells and required for their survival. *Cell* **137,** 873–86 (2009).

183. Wang, Z. *et al.* An evolving role for DEPTOR in tumor development and progression. *Neoplasia* **14,** 368–75 (2012).

184. Schust, J., Sperl, B., Hollis, A., Mayer, T. U. & Berg, T. Stattic: a small-molecule inhibitor of STAT3 activation and dimerization. *Chem. Biol.* **13,** 1235–42 (2006).

185. Dijkgraaf, E. M., Welters, M. J. P., Nortier, J. W. R., van der Burg, S. H. & Kroep, J. R. Interleukin-6/interleukin-6 receptor pathway as a new therapy target in epithelial ovarian cancer. *Curr. Pharm. Des.* **18,** 3816–27 (2012).

186. Selvendiran, K. *et al.* Anticancer efficacy of a difluorodiarylidenyl piperidone (HO-3867) in human ovarian cancer cells and tumor xenografts. *Mol. Cancer Ther.* **9,** 1169–79 (2010).

187. Yamamoto, T. *et al.* Cross-talk between signal transducer and activator of transcription 3 and estrogen receptor signaling. *FEBS Lett.* **486,** 143–8 (2000).

188. Liu, M., Wang, G., Gomez-Fernandez, C. R. & Guo, S. GREB1 Functions as a Growth Promoter and Is Modulated by IL6/STAT3 in Breast Cancer. *PLoS One* **7,** e46410 (2012).

189. Ghosh, M. G., Thompson, D. a & Weigel, R. J. PDZK1 and GREB1 are estrogen-regulated genes expressed in hormone-responsive breast cancer. *Cancer Res.* **60,** 6367–75 (2000).

190. Mohammed, H. *et al.* Endogenous Purification Reveals GREB1 as a Key Estrogen Receptor Regulatory Factor. *Cell Rep.* (2013). doi:10.1016/j.celrep.2013.01.010

191. Jong, N. N. & McKeage, M. J. Emerging roles of metal solute carriers in cancer mechanisms and treatment. *Biopharm. Drug Dispos.* **35,** 450–62 (2014).

192. Angelini, S. *et al.* Polymorphisms in OCTN1 and OCTN2 transporters genes are associated with prolonged time to progression in unresectable gastrointestinal stromal tumours treated with imatinib therapy. *Pharmacol. Res.* **68,** 1–6 (2013).

193. Ren, X. *et al.* Local estrogen metabolism in epithelial ovarian cancer suggests novel targets for therapy. *J. Steroid Biochem. Mol. Biol.* **150,** 54–63 (2015).

194. Cunat, S. *et al.* Aromatase expression in ovarian epithelial cancers. *J. Steroid Biochem. Mol. Biol.* **93,** 15–24 (2005).

195. MacLusky, N. J. *et al.* Aromatase activity in human ovarian cancer. *Steroids* **50,** 423–33

196. Voitp, R. *et al.* Aromatase activity in human ovarian cancer. *Steroids* **50,** (1987).

197. Chura, J. C., Blomquist, C. H., Ryu, H. S. & Argenta, P. a. Estrone sulfatase activity in patients with advanced ovarian cancer. *Gynecol. Oncol.* **112,** 205–9 (2009).

198. Eskenazi, B. & Warner, M. L. Epidemiology of endometriosis. *Obstet. Gynecol. Clin. North Am.* **24,** 235–58 (1997).

199. Giudice, L. C. Endometriosis. *N. Engl. J. Med.* **362,** 2389–2398 (2010).

200. Van Gorp, T., Amant, F., Neven, P., Vergote, I. & Moerman, P. Endometriosis and the development of malignant tumours of the pelvis. A review of literature. *Best Pract. Res. Clin. Obstet. Gynaecol.* **18,** 349–71 (2004).

201. Pearce, C. L. *et al.* Association between endometriosis and risk of histological subtypes of ovarian cancer: a pooled analysis of case-control studies. *Lancet Oncol.* **13,** 385–94 (2012).

202. Suryawanshi, S. M. *et al.* Plasma microRNAs as novel biomarkers for endometriosis and endometriosis-associated ovarian cancer. *Clin. Cancer Res.* **19,** 1213–24 (2013).

203. Suryawanshi, S. *et al.* Complement pathway is frequently altered in endometriosis and endometriosis-associated ovarian cancer. *Clin. Cancer Res.* **20,** 6163–74 (2014).

204. Zhao, Y. *et al.* Dual suppression of estrogenic and inflammatory activities for targeting of endometriosis. *Sci. Transl. Med.* **7,** 271ra9 (2015).

205. Rae, J. M. *et al.* GREB 1 is a critical regulator of hormone dependent breast cancer growth. *Breast Cancer Res. Treat.* **92,** 141–9 (2005).

206. Gertz, J., Reddy, T. E., Varley, K. E., Garabedian, M. J. & Myers, R. M. Genistein and bisphenol A exposure cause estrogen receptor 1 to bind thousands of sites in a cell type-specific manner. *Genome Res.* **22,** 2153–62 (2012).

207. Dressing, G. E. *et al.* Progesterone receptor-cyclin D1 complexes induce cell cycle-dependent transcriptional programs in breast cancer cells. *Mol. Endocrinol.* **28,** 442–57 (2014).

208. Wei, W. *et al.* FGF18 as a prognostic and therapeutic biomarker in ovarian cancer. *J. Clin. Invest.* **123,** 4435–48 (2013).

209. Han, S. J. *et al.* Estrogen Receptor β Modulates Apoptosis Complexes and the Inflammasome to Drive the Pathogenesis of Endometriosis. *Cell* **163,** 960–74 (2015).

210. Han, S. J. *et al.* A new isoform of steroid receptor coactivator-1 is crucial for pathogenic progression of endometriosis. *Nat. Med.* **18,** 1102–11 (2012).

211. Trukhacheva, E. *et al.* Estrogen receptor (ER) beta regulates ERalpha expression in stromal cells derived from ovarian endometriosis. *J. Clin. Endocrinol. Metab.* **94,** 615–22 (2009).

212. Matthews, J. *et al.* Estrogen receptor (ER) beta modulates ERalpha-mediated transcriptional activation by altering the recruitment of c-Fos and c-Jun to estrogen-responsive promoters. *Mol. Endocrinol.* **20,** 534–43 (2006).

213. Williams, C., Edvardsson, K., Lewandowski, S. A., Ström, A. & Gustafsson, J.-A. A genome-wide study of the repressive effects of estrogen receptor beta on estrogen receptor alpha signaling in breast cancer cells. *Oncogene* **27,** 1019–32 (2008).

214. Paruthiyil, S. *et al.* Estrogen receptor beta inhibits human breast cancer cell proliferation and tumor formation by causing a G2 cell cycle arrest. *Cancer Res.* **64,** 423–8 (2004).

215. Zhu, J. *et al.* Re-expression of estrogen receptor β inhibits the proliferation and migration of ovarian clear cell adenocarcinoma cells. *Oncol. Rep.* **26,** 1497–503 (2011).

216. Tomlinson, D. C., Knowles, M. A. & Speirs, V. Mechanisms of FGFR3 actions in endocrine resistant breast cancer. *Int. J. Cancer* **130,** 2857–66 (2012).

217. Turner, N. *et al.* FGFR1 amplification drives endocrine therapy resistance and is a therapeutic target in breast cancer. *Cancer Res.* **70,** 2085–94 (2010).

218. Aguilar, H. *et al.* Biological reprogramming in acquired resistance to endocrine therapy of breast cancer. *Oncogene* **29,** 6071–83 (2010).

219. Meijer, D. *et al.* Fibroblast growth factor receptor 4 predicts failure on tamoxifen therapy in patients with recurrent breast cancer. *Endocr. Relat. Cancer* **15,** 101–11 (2008).

220. Worley, M. J. *et al.* Molecular changes in endometriosis-associated ovarian clear cell carcinoma. *Eur. J. Cancer* (2015). doi:10.1016/j.ejca.2015.05.011

221. Fujimura, M. *et al.* Absence of estrogen receptor-alpha expression in human ovarian clear cell adenocarcinoma compared with ovarian serous, endometrioid, and mucinous adenocarcinoma. *Am. J. Surg. Pathol.* **25,** 667–72 (2001).

222. Skírnisdóttir, I., Garmo, H., Wilander, E. & Holmberg, L. Borderline ovarian tumors in Sweden 1960-2005: trends in incidence and age at diagnosis compared to ovarian cancer. *Int. J. Cancer* **123,** 1897–901 (2008).

223. Trimble, C. L., Kosary, C. & Trimble, E. L. Long-term survival and patterns of care in women with ovarian tumors of low malignant potential. *Gynecol. Oncol.* **86,** 34–7 (2002).

224. Boran, N. *et al.* Fertility and recurrence results of conservative surgery for borderline ovarian tumors. *Gynecol. Oncol.* **97,** 845–51 (2005).

225. Morice, P. *et al.* Borderline ovarian tumour: pathological diagnostic dilemma and risk factors for invasive or lethal recurrence. *Lancet. Oncol.* **13,** e103–15 (2012).

226. Suh-Burgmann, E. Long-term outcomes following conservative surgery for borderline tumor of the ovary: a large population-based study. *Gynecol. Oncol.* **103,** 841–7 (2006).

227. Buttin, B. M., Herzog, T. J., Powell, M. A., Rader, J. S. & Mutch, D. G. Epithelial ovarian tumors of low malignant potential: the role of microinvasion. *Obstet. Gynecol.* **99,** 11–7 (2002).

228. Crispens, M. A. *et al.* Response and survival in patients with progressive or recurrent serous ovarian tumors of low malignant potential. *Obstet. Gynecol.* **99,** 3–10 (2002).

229. Sutton, G. P. *et al.* Stage III ovarian tumors of low malignant potential treated with cisplatin combination therapy (a Gynecologic Oncology Group study). *Gynecol. Oncol.* **41,** 230–3 (1991).

230. Riman, T. *et al.* Risk factors for epithelial borderline ovarian tumors: results of a Swedish case-control study. *Gynecol. Oncol.* **83,** 575–85 (2001).

231. Stabile, L. P. *et al.* Combined analysis of estrogen receptor beta-1 and progesterone receptor expression identifies lung cancer patients with poor outcome. *Clin. Cancer Res.* **17,** 154–64 (2011).

232. Kavanagh, J. J. *et al.* Anti-tumor activity of letrozole in patients with recurrent advanced low malignant potential or low-grade serous ovarian tumors. *ASCO Meet. Abstr.* **25,** 5582 (2007).

233. Lee, M.-T., Ouyang, B., Ho, S.-M. & Leung, Y.-K. Differential expression of estrogen receptor beta isoforms in prostate cancer through interplay between transcriptional and translational regulation. *Mol. Cell. Endocrinol.* **376,** 125–35 (2013).

234. Smith, L. *et al.* Differential regulation of oestrogen receptor β isoforms by 5' untranslated regions in cancer. *J. Cell. Mol. Med.* **14,** 2172–84 (2010).

235. Vaughan, S. *et al.* Rethinking ovarian cancer: recommendations for improving clinical outcomes. *Nat. Rev. Cancer* **11,** (2011).

236. Jemal, A. *et al.* Global cancer statistics. *CA. Cancer J. Clin.* **61,** 69–90

237. Sonnendecker, H. E., Cooper, K. & Kalian, K. N. Primary fallopian tube adenocarcinoma in situ associated with adjuvant tamoxifen therapy for breast carcinoma. *Gynecol. Oncol.* **52,** 402–7 (1994).

238. Ma, C. X., Reinert, T., Chmielewska, I. & Ellis, M. J. Mechanisms of aromatase inhibitor resistance. *Nat. Rev. Cancer* **15,** 261–275 (2015).

239. Ariazi, E. A. *et al.* Emerging principles for the development of resistance to antihormonal therapy: Implications for the clinical utility of fulvestrant. *J. Steroid Biochem. Mol. Biol.* **102,** 128–138 (2006).

240. Van ’t Veer, L. J. *et al.* Gene expression profiling predicts clinical outcome of breast cancer. *Nature* **415,** 530–6 (2002).